

Université de Montréal

**EVALUATING DNA DAMAGE RESPONSE (DDR)
ACTIVATION IN HUMAN PROSTATE CANCER**

By

Guila Delouya

Programme de Sciences Biomédicales

Faculté de Médecine

Memoir presented to the Faculty of Medicine to obtain the degree of Masters
(M.Sc) in Biomedical Sciences, General option.

APRIL 2014

© Guila Delouya, 2014

Université de Montréal

This memoir entitled:
EVALUATING DNA DAMAGE RESPONSE (DDR) ACTIVATION IN
HUMAN PROSTATE CANCER

Presented by:

Guila Delouya

Was evaluated by a jury composed of the following people:

Dr Elliot Drobetsky

Reporting President

Dr Francis Rodier

Research Director

Dre Anne-Marie Mes-Masson

Research Co-director

Dr Thierry Muanza

Jury Member

Summary

Background: Prostate cancer is the most frequently diagnosed cancer in Canadian men and is the third deadliest after lung and colon cancers. Currently, prostate cancer treatments are based on results obtained of digital rectal exam, Gleason scores from biopsy specimens and serum PSA (Prostatic Specific Antigen) levels. The identification of specific biomarkers for diagnosis and prognosis, as well as new therapeutic targets, is quickly paving the way for personalized medicine. Ideally, in the future, patient care will include molecular signature of a patient's disease to guide for a more efficient treatment.

In this thesis, we evaluated the DNA damage response (DDR) as a potential biomarker in prostate cancer. DNA lesions in mammalian cells trigger the DDR signalling cascade that orchestrates DNA repair and activate cell cycle checkpoints to preserve genome integrity. Loss of genome stability is usually associated with cancer development, and activated DDR signalling in cells with genomic instability act as a cancer barrier in several pre-neoplastic human lesions, including prostate cancer. Thus, the DDR is an important cancer suppression mechanism. The DDR is also activated in response to anti-cancer agents including radiation therapy (RT) and DNA-damaging chemotherapies. Pre-existing DDR levels in prostate cancer cells may influence the outcome of these cancer treatments. DDR signalling has been detected during human prostate cancer progression from low levels in normal prostate cells to high levels in high-grade prostatic intraepithelial neoplasia (HG-PIN). However, DDR signalling variations detected from HG-PIN to adenocarcinoma remain unclear, and no correlations were performed with

patient clinical outcome data. Our hypothesis is that the levels of persistent DDR signalling activity will be variable with different grades and aggressiveness of prostate cancer. The levels of this activity could be correlated with the clinical responses to treatments and could even predict this process. We believe that having new biomarkers will help personalizing cancer treatment and certainly increase treatments' efficiency.

Our objectives are to characterize the occurrence of DDR activation in prostate carcinoma and to correlate it with patients' survival and responsiveness to treatment.

Methods: We used tissue microarrays (TMAs) from human radical prostatectomy specimens of 300 men with prostate cancer and estimated the level of DDR protein expression in the stromal and epithelial compartments of normal and aggressive cancer tissues. The expression level of the DDR markers p53 binding protein-1 (53BP1), phosphorylated H2AX (p-H2AX), p65 (p65 subunit of Nuclear Factor (NF- κ B) and phosphorylated checkpoint kinase-2 (p-CHK2) was quantified using immunofluorescence (IF) coupled to high-content automated imaging. The quantification of our DDR markers was first validated on an experimental TMA (TMA-cell) including normal and irradiated (to induce DDR signalling) cultured human fibroblasts. The data was quantified using binary layers commonly used to classify pixels in an image so areas could be analysed independently allowing the segregation of specific compartments including nuclei, epithelia and stroma. Arithmetic operations were performed to render values corresponding to DDR activation that were then correlated with clinical outcomes such as biochemical recurrence and occurrence of bone metastasis.

Results: We found that low levels of p65 protein expression in the nuclear epithelial compartments of normal prostate tissue were associated with a reduced probability of biochemical failure (which corresponds to a rise in the serum level of PSA in prostate cancer patients following treatment, surgery in this cohort of patients). Moreover, we also observed that low levels of 53BP1 protein expression in the nuclear epithelial compartments of normal and cancerous prostate tissue were associated with a lower incidence of bone metastasis.

Conclusion: These results confirm that p65 has prognostic value in patients with prostate adenocarcinoma. Based on our results, we suggest that 53BP1 marker may have a prognostic value as well. The validation of other markers and particularly DDR markers may correlate with patients' outcome. With longer follow-up, it may translate into correlation with survival. Levels of DDR activity in cancer tissue could be used in daily clinic as part of the patient's diagnostic profile as much as his prostatic specific antigen (PSA) or Gleason score in order to predict response and personalize the treatment in order to guide the patients towards the most appropriate treatment amongst all those available for their prostate cancer.

Keywords: DNA damage response (DDR), prostate cancer, DDR marker, biomarker.

Résumé

Introduction: Au Canada, le cancer de la prostate est le cancer le plus fréquemment diagnostiqué chez les hommes et le plus mortel après les cancers du poumon et du côlon. Il y a place à optimiser le traitement du cancer de la prostate de manière à mettre en œuvre une médecine personnalisée qui s'adapte aux caractéristiques de la maladie de chaque patient de façon individuelle.

Dans ce mémoire, nous avons évalué la réponse aux dommages de l'ADN (RDA) comme biomarqueur potentiel du cancer de la prostate. Les lésions potentiellement oncogènes de l'ADN déclenche une cascade de signalisation favorisant la réparation de l'ADN et l'activation des points de contrôle du cycle cellulaire pour préserver l'intégrité du génome. La RDA est un mécanisme central de suppression tumorale chez l'homme. La RDA joue un rôle important dans l'arrêt de la prolifération des cellules dont les génomes sont compromis, et donc, prévient la progression du cancer en agissant comme une barrière. Cette réponse cellulaire détermine également comment les cellules normales et cancéreuses réagissent aux agents utilisés pour endommager l'ADN lors du traitement du cancer comme la radiothérapie ou la chimiothérapie, en plus la présence d'un certain niveau de RDA dans les cellules du cancer de la prostate peuvent également influencer sur l'issue de ces traitements. L'activation des signaux de la RDA peut agir comme un frein au cancer dans plusieurs lésions pré-néoplasiques de l'homme, y compris le cancer de la prostate. Il a été démontré que la RDA est augmentée dans les cellules de néoplasie intra-épithéliale (PIN) comparativement aux cellules prostatiques normales. Toutefois, le devenir de la RDA entre le PIN et l'adénocarcinome est encore mal documenté et aucune corrélation n'a été réalisée avec les données cliniques des patients. Notre hypothèse est que les niveaux d'activation de la RDA seront variables selon les différents grades et

agressivité du cancer de la prostate. Ces niveaux pourront être corrélés et possiblement prédire les réponses cliniques aux traitements des patients et aider à définir une stratégie plus efficace et de nouveaux biomarqueurs pour prédire les résultats du traitement et personnaliser les traitements en conséquence. Nos objectifs sont de caractériser l'activation de la RDA dans le carcinome de la prostate et corréler ses données avec les résultats cliniques.

Méthodes : Nous avons utilisé des micro-étalages de tissus (tissu microarrays-TMAs) de 300 patients ayant subi une prostatectomie radicale pour un cancer de la prostate et déterminé le niveau d'expression de protéines de RDA dans le compartiment stromal et épithélial des tissus normaux et cancéreux. Les niveaux d'expression de 53BP1, p-H2AX, p65 et p-CHK2 ont été quantifiés par immunofluorescence (IF) et par un logiciel automatisé. Ces marqueurs de RDA ont d'abord été validés sur des TMAs-cellule constitués de cellules de fibroblastes normales ou irradiées (pour induire une activation du RDA). Les données ont été quantifiées à l'aide de couches binaires couramment utilisées pour classer les pixels d'une image pour que l'analyse se fasse de manière indépendante permettant la détection de plusieurs régions morphologiques tels que le noyau, l'épithélium et le stroma. Des opérations arithmétiques ont ensuite été réalisées pour obtenir des valeurs correspondant à l'activation de la RDA qui ont ensuite été corrélées à la récurrence biochimique et l'apparition de métastases osseuses.

Résultats : De faibles niveaux d'expression de la protéine p65 dans le compartiment nucléaire épithélial du tissu normal de la prostate sont associés à un faible risque de récurrence biochimique. Par ailleurs, nous avons aussi observé que de faibles niveaux d'expression de la protéine 53BP1 dans le compartiment nucléaire épithéliale du tissu prostatique normal et cancéreux ont été associés à une plus faible incidence de métastases

osseuses.

Conclusion: Ces résultats confirment que p65 a une valeur pronostique chez les patients présentant un adénocarcinome de la prostate. Ces résultats suggèrent également que le marqueur 53BP1 peut aussi avoir une valeur pronostique chez les patients avec le cancer de la prostate. La validation d'autres marqueurs de RDA pourront également être corrélés aux résultats cliniques. De plus, avec un suivi des patients plus long, il se peut que ces résultats se traduisent par une corrélation avec la survie. Les niveaux d'activité de la RDA pourront éventuellement être utilisés en clinique dans le cadre du profil du patient comme le sont actuellement l'antigène prostatique spécifique (APS) ou le Gleason afin de personnaliser le traitement.

Mots clés: Réponse aux dommages de l'ADN (RDA), Cancer de la prostate, Marqueur de RDA, Biomarqueur

TABLE OF CONTENTS

Summary	i
Keywords	iii
Résumé	iv
Mots-Clés	vi
List of figures	x
List of tables	xi
List of Acronyms and Abbreviations.....	xii
Acknowledgements	xvii

<u>CHAPTER 1: INTRODUCTION</u>	1
1.0 Prostate Cancer	1
1.1 Overview of prostate Cancer	1
1.2 Cellular effects of radiation therapy.....	6
2.0 The DNA damage response (DDR)	8
2.1 DNA damage	8
2.2 Cellular detection of DNA damage	11
2.2.1 ATM-MRN	12
2.2.2 DNA-PKcs-KU	13
2.2.3 ATR-ATRIP	13

2.3 Signalling to effector pathways.....	14
2.4 DDR and ionizing radiation	17
2.5 DNA repair	19
2.6 Nuclear factor-kappa B (NF- κ B) transcription factors	20
2.7 DDR as a barrier to cancer progression	26
3.0 Biomarkers	31
3.1 Prognostic vs. Predictive markers	31
3.2 DDR as a tissue marker	32
4.0 The Tissue Microarrays (TMAs)	34
HYPOTHESIS AND OBJECTIVES	38
1. Premiss	38
2. Hypothesis and objectives	38
<u>CHAPTER 2: EXPERIMENTAL RESULTS</u>	<u>41</u>
Novel streamlined DNA damage response signalling quantification in human prostate cancer tissue samples reveals a prognostic role 53BP1	41
Abstract	42
1.0 Introduction	44
2.0 Materials and methods.....	48
3.0 Results	54
4.0 Discussion	59
5.0 Conclusion	67
References	68

Figure Legends	72
Tables Legends	78
Figures	80
Tables	92
<u>CHAPTER 3: DISCUSSION</u>	96
1.0 The DDR as a cancer barrier	96
1.1 DDR activity: a cancer barrier in prostate cancer	97
2.0 Repair Mechanisms	98
2.1 53BP1 and homologous recombination	100
3.0 Why do we need biomarkers?	101
3.1 DDR activity as a biomarker	102
4.0 DDR activity in our cohort of patients	104
5.0 Limitations of our study	106
5.1 Validation study on TMA-cell and TMA-tissue	106
5.2 Data quality control	106
5.3 Immunofluorescence technique	107
Conclusion	109
Perspectives	110
<u>CHAPTER 4: REFERENCES</u>	112

LIST OF FIGURES

CHAPTER 1:

Figure 1: Gleason grading system diagram	6
Figure 2: Major DDR Activation pathways	16
Figure 3: A model depicting distinct and common steps between NF- κ B signaling induced by TNF α and DNA damaging agents.....	25
Figure 4: ATM activation in normal prostatic gland, PIN, and carcinoma	27
Figure 5: Tissue Micro Arrays (TMAs)	36
Figure 6: Hypothesis	39

CHAPTER 2:

Figure 1: Detection of DDR activity and DDR foci in paraffin embedded cells using multicolour immunofluorescence	80
Figure 2: Multicolor immunofluorescence and mask segmentation analysis in prostate cancer TMA core	81
Figure 3: Software-based quantification of immunofluorescence-detected DDR activity in paraffin embedded cells	82
Figure 4: Quality Control of DDR data on duplicate samples for prostate cancer TMA.....	83
Figure 5: Kaplan–Meier PSA recurrence-free survival and bone metastasis free curves in patients with prostate cancer for specific DDR signals	86

Figure S1: A-Schematic representation of the TMA-cell approach for irradiated cells	89
B-Map of the TMA-cell and representative full-core immunofluorescence images	89
C- Software mediated entire core detection and nucleus identification.....	89
Figure S2: Multicolor immunofluorescence staining in whole prostate cancer TMA	90
Figure S3: Software quantification of immunofluorescence-detected DDR activity in paraffin embedded cells	91

LIST OF TABLES

CHAPTER 1:

Table 1: D’Amico risk stratification for clinically localized prostate cancer	3
---	---

CHAPTER 2:

Table 1: Terry Fox Research Institute TMA (TMA-TFRI) of prostate cancer patient cohort	92
Table 2: Univariate and multivariate cox regression analysis for A) Biochemical failure and B) Bone metastasis	93
Table 3: Pearson Correlation (2-tailed) between DDR activity and clinico- pathological parameters	94
Table 4: Paired Sample T test for DDR markers	95

LIST OF ACRONYMS AND ABBREVIATIONS

53BP1	p53 binding protein-1
ADT	Androgen deprivation therapy
ATM	Ataxia Telangiectasia Mutated
ATR	ATM and Rad 3-related
ATRIP	ATR interacting protein
Bax	Bcl-2-associated x protein
Bcl-2	B-cell lymphoma 2
BCR	Biochemical recurrence
BMI-1	Polycomb complex protein B lymphoma Mo-MLV insertion region 1 homolog
BPH	Benign prostatic hyperplasia
BRCA1	Breast cancer 1
BRCT	Breast cancer 1 (BRCA1) carboxy-terminal
CAG	Cytosine, adenine, and guanine
CAK	CDK activating kinase
CDC25	Cell division cycle 25
CDK1	Cyclin-dependent kinase 1
Cox-2	Cyclooxygenase-2
CRPC	Castrate resistant prostate cancer
Cy5	Rhodamine cyanine dyes
CYP3A4	Androgen receptor cytochrome P450 3A4

DAPI	4',6-diamidino-2-phenylindole
DDR	DNA damage response
DNA	Deoxyribonucleic acid
DRE	Digital rectal exam
DSBs	Double strand breaks
EBRT	External beam radiation
ECE	Extra-capsular extension
FFPE	Formalin fixed paraffin embedded
FISH	Fluorescence hybridization
FIT-C	Fluorescein isothiocyanate
GS	Gleason score
GUROC	Genito-Urinary Radiation Oncologists of Canada
Gy	Gray
H/E	Hematoxylin/eosin
HDR	High dose rate
HG-PIN	High-grade prostatic intraepithelial neoplasia
HMCK	High molecular cytokeratin
HR	Homologous recombination
IF	Immunofluorescence
IHC	Immunohistochemistry
IMRT	Intensity modulated radiation therapy

LDR	Low dose rate
LNI	Lymph node invasion
MDC1	Mediator of DNA damage checkpoint 1
MDM2	Mouse double minute 2 homolog
MFI	Mean fluorescent intensity
MRN	Mre11-Rad50-Nbs1
NCCN	National Comprehensive Cancer Network
NHEJ	Non-homologous end-joining
p-CHK2	Phosphorylated checkpoint kinase-2
p-H2AX	Phosphorylated H2AX
p65	p65 subunit of Nuclear Factor kappa B (NF- κ B)
PARPs	Poly ADP ribose polymerase
PCa	Prostate cancer
PIKK	Phosphoinositide 3-kinase related kinase
PIN	Prostatic intraepithelial neoplasia
PKA	Protein kinase A RI-alpha
PML	Promyelocytic leukemia protein
ProCaRS	Prostate Cancer Risk Stratification
PSA	Prostate specific antigen
pTNM	Pathological TNM staging (Tumor Nodes Metastasis)
Rb	Retinoblastoma

RNF2	Ring finger protein 2
ROC	Receiver operative characteristic
ROS	Reactive oxygen species
RP	Radical prostatectomy
RT	Radiation therapy
RTOG	Radiation Therapy Oncology Group
S/T-Q	Ser/Thr-Gln
SSB	Single strand break
Stat-3	Signal transducer and activator of transcription 3
SVI	Seminal vesicles invasion
TFRI	Terry Fox Research Institute
TMA _s	Tissue microarrays
TRIT-C	Tetramethyl rhodamine isothiocyanate
UV	Ultraviolet

To my husband Yohann

To my 4 beautiful sons: Noah, Nathan, David, Liam

To my mother Ida

To my father watching me over the sky

Thank you for your support over the long years,

I know I can always count on you

Acknowledgements

My interest in fundamental research began in 2008 during my second year of residency in radiation oncology when I was first introduced to Dre Anne-Marie Mes-Masson, now my co-director. It is through her welcome in her laboratory during an entire summer where I was paired to Véronique Barrès, my dear friend and now co-worker that I had the desire to continue in fundamental research and do my Master's degree in this big family of our laboratory. I was later introduced to Dr Francis Rodier, my director who had a particular interest in radiobiology and accepted to supervise me during those past three years. The confidence you have always given me has allowed me to evolve throughout my exciting project and grown out of this experience. You are always available and a pleasure to talk to. I am looking forward to our future collaborations.

Thank you to all the wonderful members of both laboratories, without which my experience would not have been so pleasant. Thank you all for your support, your smiles, your help and for all the discussions that have helped me to advance my project. I sincerely thank you all very much. In particular, I thank Véronique Barrès, Guillaume Chouinard and Véronique Ouellet for their valuable advice, their precious time and for answering all of my emails 24/7. Thank you to Guillaume Cardin who helped me find my way in the lab during the first months and guiding me through my first experiments. Thank you to Ingrid Labouba for her insight and experience on immunofluorescence. Thank you to Audrey Carrier-Leclerc, with whom I attended courses and conferences and whose great heart is always open to discussions and for giving piano lessons to my children after our day at the

lab. I would also like to thank Nawel Mechtouf, Amel Derdour, Stéphanie Nadeau, Shuofei Cheng, Sabrina Ghadaouia, Nicolas Malaquin, Aurélie Martinez, Lilians Calvo Gonzalez, Katia Caceres and all those that have passed through our lab throughout the years for their support, in all its forms. In particular, I wish to emphasize the friendship of Véronique, which was, is and always will be very precious. Our discussions helped me over the years. Thank you to professor A. Zini for reviewing this thesis.

I cannot help say a big thank you to all the other members of the ICM, the CR-CHUM and mostly to my great and special department of radiation-oncology that made my project possible. My colleagues have allowed me to spend many hours, days, weeks in the laboratory while they would see patients and particularly my patients when I was not around. I cannot thank you enough.

Finally, I wish to conclude this section by thanking with all my heart the people who have been supporting me throughout my 20 years at l'Université de Montréal. My husband, my children, my mother, my brothers and sisters, my amazing cousins, my in laws, my friends who were always around especially when I wasn't. You always pushed me to challenge myself, and encourage me to pursue my dreams. You have always believed in me and knew how to be there to encourage me. You were all always there to support me in difficult times and to congratulate me in happier ones.

CHAPTER 1: INTRODUCTION

1.0 Prostate Cancer

1.1 Overview of prostate cancer

Prostate cancer is the most frequently diagnosed cancer in Canadian men and is the third deadliest cancer in males after lung and colon cancer ¹.

According to the Canadian Cancer Society, Canadian males are most likely to develop prostate cancer, with one in eight males expected to be diagnosed with prostate cancer in their lifetime (statistics Canada website: <http://www.cancer.ca/en/cancer-information/cancer-101/canadian-cancer-statistics-publication/?region=qc>).

More than 23 000 new cases of prostate cancer were diagnosed in Canada in 2013 with almost 5000 of these being in the province of Quebec. High-grade prostatic intraepithelial neoplasia (HG-PIN) is considered the precursor of prostate carcinoma. It is associated with progressive abnormalities of phenotype and genotype, which are midway between normal epithelial cells and cancer cells. This indicates impairment of cell differentiation and regulatory control with advancing stages of prostatic carcinogenesis ².

Management of localized non-metastatic prostate cancer remains very complex because there are multiple issues to consider including risk stratification, efficacy and

toxicity of the different treatments, relative risk of death from diseases other than the cancer itself and lastly, patient preferences ³. The National Comprehensive Cancer Network (NCCN), an alliance of the world's leading cancer centers, is an authoritative source of comprehensive cancer, which develops guidelines to improve the quality, effectiveness and efficiency of cancer care. Both the National Comprehensive Cancer Network (NCCN) risk classification and the D'Amico classification, which are very similar, are the most commonly used categorical strategies for pre-treatment risk estimation in prostate cancer. Originally developed in 1998 by a medical researcher named D'amico, this classification system is designed to evaluate the risk of recurrence following localized treatment of prostate cancer. It stratifies patients in three categories based on three parameters:

a) Patient's diagnostic serum prostatic specific antigen (PSA): The PSA is a protein made by the cells of the prostate gland. It is mostly found in semen, but it is also normal to find small amounts of PSA in the blood of healthy men. In case of prostate cancer, PSA levels are often above normal as it is secreted in excess by the prostate cancer cells.

b) Patient's highest biopsy Gleason score: The Gleason score is given to prostate cancer based upon its microscopic appearance. Lower grades are associated with small, closely packed glands. Cells spread out and lose glandular architecture as grade increases. Gleason score usually varies between 6-10 with 10 being the highest

possible grade.

c) Patient's clinical stage: The clinical stage varies from T1 to T4 and is determined by the physician's digital rectal exam of the prostate gland. Indeed, the prostate can be palpated through the rectum. T1 represents the absence of a palpable tumor whereas T4 represents a tumor invading the bladder or rectum.

<u>Low Risk</u>	Diagnostic PSA < 10.0 ng/mL <i>and</i> Highest biopsy Gleason score ≤ 6 <i>and</i> Clinical stage T1c or T2a
<u>Intermediate Risk</u>	Diagnostic PSA ≥ 10 but < 20 ng/mL <i>or</i> Highest biopsy Gleason score = 7 <i>or</i> Clinical stage T2b
<u>High Risk</u>	Diagnostic PSA ≥ 20 ng/mL <i>or</i> Highest biopsy Gleason score ≥ 8 <i>or</i> Clinical stage T2c/T3

Table 1: D'Amico risk stratification for clinically localized prostate cancer

This risk stratification is based on clinical characteristics such as the diagnostic serum PSA, the Gleason score as determined by the pathologist from prostate biopsy and the clinical stage as determined by the physician's digital rectal exam.

Nomograms are online tools that have been developed to guide and help clinicians decide which treatment approach (ie: surgery, radiation therapy (RT) or androgen deprivation therapy - ADT) can be offered to a patient. The nomogram analysis is based on multiple factors such as PSA values and number of positive biopsy cores.

Nomograms are often complex, time-consuming (making routine use difficult), and are not necessarily applicable to individual treating centers ⁴. An important advantage of risk grouping systems (ie: D'Amico or NCCN classifications) compared to nomograms is their simplicity ⁵. On the other hand, risk groups have the disadvantage of assuming that patients within the same group are homogeneous. Moreover, risk groups do not consider factors such as the number of positive biopsies or whether there are single or multiple intermediate-risk or high-risk factors present when considering the treatment decisions. Nomograms do incorporate this information, but more time is required to calculate the score and this information may not be applicable for use in daily clinical practice. Regardless of the scoring system, which is used by the clinician in his/her practice, neither the risk classification nor the nomograms incorporate the tumor's biology. The most important criterion for a prediction tool is its ability to discriminate between patients with or without a given outcome with high accuracy ⁶. Predictive models for patients treated by RT for localized prostate cancer have been established ⁷. Recently, the Genito-Urinary Radiation Oncologists of Canada (GUROC) developed a pan-Canadian Prostate Cancer Risk Stratification (ProCaRS) database based on 7974 patients and this group of experts suggests that the definition of additional risk

categories (i.e., very low risk and very high risk) may further improve patient risk categorization⁸. A recent trial (PIVOT trial) where patients with clinically localized prostate cancer were randomized between radical prostatectomy and active surveillance (ie: no treatment) showed that active surveillance remains an excellent option for 70% of patients diagnosed with low risk prostate cancer⁹. However, 90% of diagnosed patients still favour treatment because of the anxiety associated with an untreated cancer. Prostate cancer treatments include surgery to remove the prostate gland (radical prostatectomy (RP)), external beam radiation (EBRT), interstitial brachytherapy (low dose rate - LDR and high dose rate - HDR), ADT or a combination of these therapies. Each treatment comes with its own set of side effects, which are not negligible. Nevertheless, to date, clinicians do not have the necessary tools (markers) to identify men with slow growing cancers (that can be managed by active surveillance) from men with aggressive cancers (that require treatment). As such, until we establish better predictive models, clinicians will continue to rely on basic risk classification systems that typically incorporate information on DRE (digital rectal exam), serum PSA and pathology from biopsy specimens (Gleason score-GS).

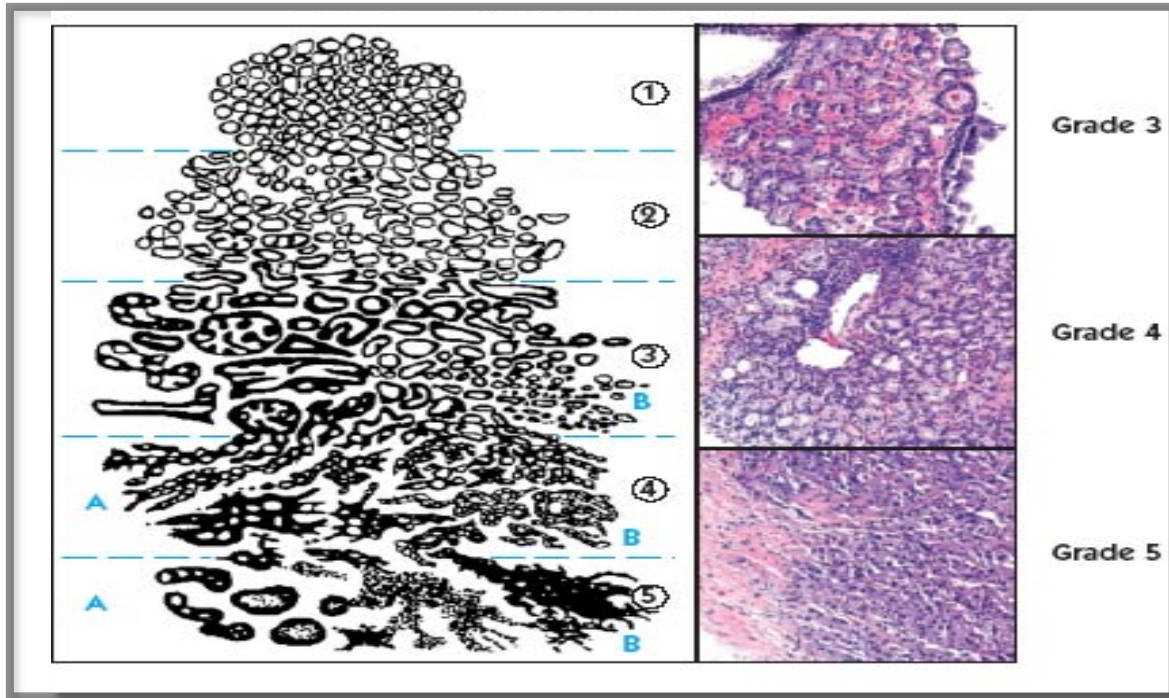


Figure 1: Gleason grading system diagram

This figure illustrates a cartoon (left panel) as well as histological (right panel) representation of cells according to the Gleason grade (1-5). The number is assigned to two of the areas of the prostate that have the most cancer on the biopsy cores taken. Those two numbers are added together to come up with the Gleason score, which ranges from 2 to 10.

1.2 Cellular effects of radiation therapy

Radiation therapy (RT) is administered by one of several methods. It can be given via an external source using a linear accelerator, which is directed toward the tumor (almost always by intensity modulated radiation therapy (IMRT) in order to protect healthy tissues). Alternatively, RT can be given by an internal source (e.g. brachytherapy where radioactive sources such as Iodine 125 are placed and decay

within the tumor). Radiation interacts with matter by the photoelectric effect, the coherent scattering effect, the pair production effect, the photodisintegration or the Compton effect. The latter is the most relevant for the range of energies used in clinical RT. In the Compton effect, the observed biologic effect results from photons creating multiple ionizations by ejection of electrons from the target biomolecule¹⁰. In this regard, the extent of biologic effects in cells after exposure to ionized radiation is largely due to oxygen with the subsequent production of free radicals. These free radicals can break cellular deoxyribonucleic acid (DNA), which is the critical target for the biologic effects of ionizing radiation. The extent of DNA damage will eventually determine cell death^{11; 12}. Cells that cannot effectively repair their DNA damage are therefore more sensitive to ionizing radiation¹³. It is also known that when radiation is focused on the nucleus rather than on the cytoplasm, cell death occurs at a higher rate¹⁴. Interference to DNA can occur directly or indirectly, but mostly via indirect means in that photons of radiation being more likely to ionize the molecules surrounding the DNA creating free radicals, which subsequently destabilize nucleic acids^{15; 16}. Cells that are unable to generate free radicals (cells under hypoxic conditions) are much less sensitive to ionizing radiation compared to those that are well oxygenated. This explains why the effect of radiation is related with blood flow and oxygen concentration of the target tissue¹⁷.

2.0 The DNA damage response (DDR)

2.1 DNA damage

In human cells, both normal metabolic activities and environmental factors such as ultraviolet (UV) light and radiation can cause DNA damage, resulting in as many as 1 million individual molecular lesions per cell per day. Many of these lesions cause structural damage to the DNA molecule and can alter or eliminate the cell's ability to transcribe the gene that the affected DNA encodes. Other lesions induce potentially harmful mutations in the cell's genome, which affect the survival of its daughter cells after it undergoes mitosis. Therefore, if these lesions are not or are incorrectly repaired, they lead to mutations or aberrations that threaten viability. DNA damage leading to either single strand break (SSB), impair base pairing and/or DNA replication or transcription errors may be produced by ¹⁸:

- a) Physiological processes (ex: DNA mismatches introduced during DNA replication)
- b) Hydrolytic reactions and non-enzymatic methylations
- c) Abortive topoisomerase I and II activity
- d) Reactive-oxygen compounds (ex: arising either from oxidative respiration or produced by macrophages and neutrophils at sites of infections and inflammation).

Double-strand breaks (DSB), although not as frequent as SSB, impair base pairing and DNA replication or transcription errors, are difficult to repair and are very lethal. DSBs can arise from a) two single strand breaks that are in close proximity b) ionizing radiation or c) from treatment using chemical drugs such as certain chemotherapy agents. Because of the importance of DNA, cells have developed a complex series of processes and pathways to ensure that the DNA remains undamaged and unaltered despite the continuous attack from the inside (ex: oxidation and alkylation owing to metabolism) as well as from the outside (ex: ingested chemicals, ultraviolet (UV) and ionizing radiation) ¹⁹. These include multiple types of DNA repair aimed at repairing various types of DNA damage caused by a variety of agents.

Specialized repair systems have therefore evolved for detecting and repairing damage: a) to bases: The Base Excision Repair (BER), where most of the damaged bases in the DNA will be detected and removed by specialized proteins called glycosylases. They cut out the damaged base without cutting the DNA backbone, resulting in an abasic site. Another class of enzyme (endonucleases) will recognize this and will cut the DNA backbone leaving a SSB. The resulting SSB can then be processed by either short-patch (where a single nucleotide is replaced) or long-patch BER (where 2-10 new nucleotides are synthesized) ²⁰. Ligases will then seal the break.

b) To single-strand breaks: The Single strand break repair (SSBR) which is similar to BER but since radiation itself causes the break rather than being a repair intermediate,

the ends are not recognized by ligases. There is therefore an extra end-processing step, mainly by the enzyme polynucleotide kinase (PNK). Once a clean nick is produced, short or long patch repair can then follow as for BER.

c) To double-strand breaks (Homologous recombination (HR) and Non-homologous end joining (NHEJ)). These two repair mechanisms are quite different in the genes involved, the position in the cell cycle where they primarily act and in the speed and accuracy of repair. These processes are described in more detail below.

All these lesions are produced by ionizing radiation. There are also other DNA repair pathways, such as those for correcting mismatches of bases in DNA which can occur during replication, such as mismatch repair (MMR), and for repairing bulky lesions or DNA adducts such as those formed by UV light and some drugs such as the chemotherapeutic agent cisplatin (NER-Nucleotide Excision Repair).

The DNA damage response (DDR) is a highly complex and coordinated system that determines the cellular outcome of DNA damage. This system can be divided in two parts, the sensors of DNA damage and the effectors of the damage response. The sensors consist of a group of proteins that actively examine the genome for the presence of the damage. These proteins then signal this damage to three main effector pathways that together determine the outcome for the cell. These effector pathways include (1) programmed cell death pathways that destroy damaged cells, (2) DNA repair pathways that physically repair DNA breaks and (3) pathways that cause

temporary or permanent halts in the progress of cells through the cell cycle--the damage checkpoints.

Failure of the DDR or associated events causes genomic instability, an underlying cause of several human syndromes and diseases, particularly cancer.

2.2 Cellular detection of DNA damage

Shortly after exposure to ionizing radiation, a signal is transmitted to the regulators of the cell cycle machinery and the sensors of DNA damage. Cells with damaged DNA mostly undergo G1 or G2/M cell cycle arrest. During this cell cycle arrest, normal cells can either 1) repair and continue through the cell cycle, 2) not repair and stay arrested, or 3) not repair and undergo apoptosis²¹. Cells have developed mechanisms that sense the presence of the DSBs and initiate the DDR. The DDR is essential to stop the proliferation of cells with genomic instability, and therefore, prevent events that can contribute to cancer initiation and progression.

The first cellular response to DSBs is characterized by the recruitment of many different proteins to the sites of DNA damage. This clustering (known as foci) can be observed microscopically as small regions or dots in the nucleus following staining with antibodies to these proteins (See Chapter 2, figure 1). One of the earliest events to occur in the DDR (occurring within 5-30 minutes after induction of a DSB) is the phosphorylation of the protein called histone H2AX²². This phosphorylated form

(known as γ -H2AX or p-H2AX) is required for the recruitment of many of the other proteins involved in the DDR. The early phosphorylation of H2AX indicates that one or more kinases are activated at the sites of DSBs. Three related kinases have been shown to be able to phosphorylate H2AX at sites of DSBs ²³:

- (1) ATM-MRN
- (2) DNA-PKcs-KU
- (3) ATR-ATRIP

2.2.1 ATM-MRN

The phosphorylation of H2AX occurs primarily by the protein ATM (Ataxia Telangiectasia Mutated). ATM is normally present in the cell, but in an inactive form. Activation of ATM occurs once it becomes associated with a DSB resulting in phosphorylation of H2AX at the site of the DSB. However, in order to detect and locate the DSB and be activated, ATM requires at least one additional protein complex.

This complex is known as MRN. The MRN complex consists of the proteins Mre11, Rad50, and Nbs1 ^{24, 25, 26}. This MRN complex is able to recognize damaged DNA and bind to or near the site and transmit DDR signals downstream to the transducers, which is important for the ‘processing’ of the DSB. These transducers are members of the phosphoinositide 3-kinase related kinase (PIKK) family such as ATM and ATR (ATM and Rad 3-related) ²⁴, respectively. Moreover, one of the key functions of Nbs1 is to

directly bind to ATM, and bring it to the site of damage and Rad50 directly binds to DNA.

2.2.2 DNA-PKcs-KU

DNA-dependent protein kinase (DNA-PKcs) is a kinase that is structurally related to ATM and which is very important in the NHEJ DNA repair. The mechanism through which it finds DSBs is very similar to that of ATM. Like ATM, DNA-PKcs is unable to act as a sensor of damage itself. This sensor function is carried out by the Ku70-Ku80 complex, which directly binds to the ends of DSBs. This binding then recruits DNA-PKcs allowing phosphorylation of H2AX.

2.2.3 ATR-ATRIP

AT-related kinase (ATR) does not a prominent role in the initial recognition of the DSBs but is important for the types of damage that occur during normal DNA replication. ATR phosphorylates H2AX in response to other types of DNA damage and abnormalities such as stalled or broken replication forks and single-stranded DNA. Just like ATM and DNA-PKcs, ATR is recruited to sites of damage by ATRIP (ATR interacting protein) that acts as the sensor of the damage. As described above, the ATM-MRN complex leads to processing of the DNA at sites of DSBs. This can create

stretches of single-stranded DNA, which will then activate ATR. Thus, ATR can be activated downstream of ATM which then phosphorylates a distinct set of proteins that participate in the DDR.

ATM and ATR are key components of these initial sensors of DNA damage^{27; 28}. While ATR is only activated when DNA is being replicated in S phase, ATM can be activated throughout the cell cycle.

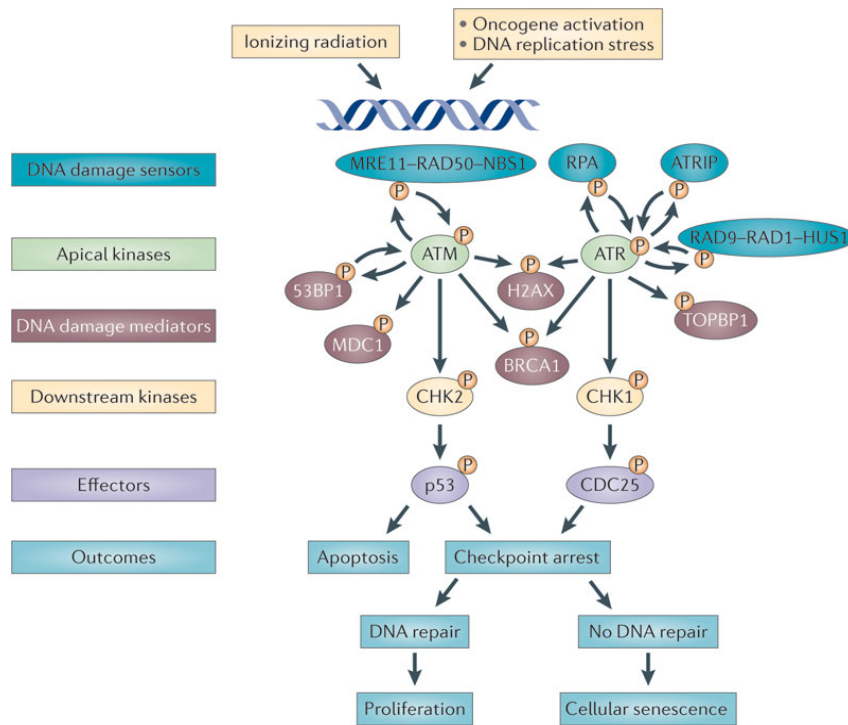
Finally, although ATM and ATR have some overlapping activities, they are activated by separate signals and by different types of DNA damage^{29; 30}.

2.3 Signalling to effector pathways

Activation of ATM, DNA-PKcs and ATR leads to the phosphorylation not only of H2AX, but also of many other cellular proteins. It has been shown that as many as 700 proteins are substrates for the ATM and ATR kinases in response to DNA damage³¹. They relay the signal to various downstream effectors that mediate cell cycle arrest, DNA repair, and apoptosis.

ATM substrates include H2AX and 53BP1, which facilitates checkpoint activation and repair, both essential for their efficient repair of DNA damage. Phosphorylated H2AX and 53BP1 rapidly localize to DSBs, forming characteristic foci. ATM also phosphorylates the kinase CHK2 (p-CHK2), which promotes growth arrest and p53, a

tumor suppressor and transcriptional regulator that coordinates repair and cell cycle arrest³². This DDR leads to transient cell cycle arrest and DNA repair, cell death, or permanent cell cycle arrest (cellular senescence) preventing cells to replicate with accumulated mutations thereby protecting cellular integrity and avoiding the development of cancers^{33; 34}. Figure 2³⁵ illustrates in a cartoon fashion the major DDR activation pathways. DNA damage sensors (MRN and ATRIP complexes) detect DNA damage and then recruit ATM and ATR, respectively. These, in turn, phosphorylate (P) the histone variant H2AX on Serine 139 (γ -H2AX) in the region proximal to the DNA lesion.



Sulli G, Di Micco R, d'Adda di Fagagna F. Crosstalk between chromatin state and DNA damage response in cellular senescence and cancer. *Nature reviews. Cancer*. Oct 2012;12(10):709-720. Written authorization obtained by Dr Fabrizio d'Adda di Fagagna, Principal Investigator IFOM Foundation – The FIRC Institute of Molecular Oncology Foundation on April 10th 2014.

Figure 2: Major DDR Activation pathways

MRN and ATRIP complexes detect DNA damage, which then recruit ATM and ATR, respectively. These in turn phosphorylate (P) the histone variant H2AX on Serine 139 (γ -H2AX) in the region proximal to the DNA lesion. γ -H2AX is required to recruit mediator of DNA damage checkpoint 1 (MDC1) that further maintains and amplifies DDR signalling by enforcing additional accumulation of the MRN complex and activation of ATM.

As mentioned previously, 53BP1 is also involved in sustaining DDR signalling by enhancing ATM activation. DDR signalling relies on additional mechanisms that are based on ubiquitination (a post-translational modification where ubiquitin is attached to a substrate protein). This post-translational modification affects proteins in many ways. It can be a signal for (1) protein degradation (via the proteasome), (2) change in cellular location, (3) change in protein activity and (4) change in protein-protein interactions. In DDR, γ -H2AX is ubiquitylated by ring finger protein 2 (RNF2), which causes the recruitment of Polycomb complex protein BMI-1 (B lymphoma Mo-MLV insertion region 1 homolog) to sites of DNA lesions. BMI1 is an oncogene which blocks transcriptional elongation at the DNA damage site and promotes DNA repair^{35; 36}.

Eventually, DDR signalling spreads away from the region of the damaged DNA and triggers the diffusible kinases CHK2 (which is mainly phosphorylated by ATM) and CHK1 (which is mainly phosphorylated by ATR) with signalling converging on downstream effectors such as p53 and the cell division cycle 25 (CDC25) phosphatases.

2.4 DDR and ionizing radiation

In order for a cell to synthesize its DNA and go through division, it needs to pass by the multiple cell cycle checkpoints. Blocks at these checkpoints can prevent important cell cycle transitions to ensure the integrity of the DNA^{37; 38; 39; 40}. All movement

through the cell cycle, be it in the G1, S, G2 or M phases, is driven by cyclin-dependent kinases (CDKs). The CDKs phosphorylate other proteins to initiate the processes required for progression through the cell cycle.

Depending on when the cell is exposed to radiation in its cell cycle, it may respond differently. Cells are extremely sensitive to radiation during mitosis (during which there is little DNA repair)^{41; 42; 43; 44}. DNA damage can activate multiple pathways that eventually lead to G1 arrest. When ATM is activated, it stabilizes p53 by phosphorylating its serine-15 and also adds a phosphate group on serine 395 of mouse double minute 2 homolog (MDM2). Phosphorylation of MDM2 prevents p53-MDM2 nuclear export and degradation of p53⁴⁵. As mentioned in the previous section, ATM is also known to phosphorylate Chk2, which subsequently phosphorylates p53 on serine 20⁴⁶. This further prevents interaction of p53 and MDM2 and hence increases levels of available nuclear p53, which is free to transcriptionally activate p21, a major inhibitor of the cyclin E- Cyclin-dependent kinase 2 (CDK2) complex⁴⁷.

ATM also controls a p53/p21 independent G1 arrest pathway. When ATM activates Chk2, it phosphorylates cdc25A, which is primed for ubiquitination and subsequent degradation⁴⁸. Cdc25A is a phosphatase that removes inhibitory phosphates from CDK2 and CDK4, both of which are important G1 phase progression molecules²⁴. Cells have been shown to be radioresistant during the G1 phase, but their radiosensitivity increases at the end of this phase⁴⁹. Most commonly, irradiated cells can be blocked in the G2/M phase, which is the next most sensitive phase in the cell

cycle post replication. Although the G2/M checkpoint remains complex and is not fully understood, there are multiple known pathways involved in this arrest²⁴. The final step in this pathway is deactivation of the cyclin B- Cyclin-dependent kinase 1 (CDK1) complex, which orchestrates the G2/M transition⁵⁰. The specific site of phosphorylation determines activation or deactivation of the CDK1 complex. The ATM/CDC25A pathway is also important because cdc25A is an activator of the cyclin B-CDK1 complex. ATM activates p21 (through p53), which is an inhibitor of an activator of CDK1, namely CAK (CDK activating kinase)⁵¹.

2.5 DNA repair

As seen above, once cells are irradiated, they sense the DNA damage and eventually activate the mechanism for DNA repair. Various repair processes are activated according to the lesion types, with DSBs being the most lethal lesion to the cell compared to single-strand breaks. These lesions can be repaired either through homologous recombination (HR) or non-homologous end-joining (NHEJ)⁵². In the former, either the intact chromosome or the sister chromatid serve as a template to reconstruct the missing DNA. HR is most effective in late S or G2 phase, when the sister chromatids have replicated but are still attached⁵³. NHEJ is more important in G1 and early S phase, but can essentially occur throughout the cell cycle⁵². Once cells are irradiated, ATM phosphorylates histone H2AX resulting in quick localized

accumulation of the protein 53BP1. This protein is involved in enhancing phosphorylation of the tumor suppressor molecule p53, activating proteins essential for DNA repair, and inducing G2 checkpoint block^{54; 55; 56}. Thus, G2 checkpoint induced by radiation, possibly via 53BP1, provide more time for repair and increases the probability of escaping cell death.

2.6 Nuclear factor-kappa B (NF-κB) transcription factors

Our group has already addressed the prognostic value of the p65 subunit of NF-κB in prostate cancer (p65) where it was observed that elevated amounts of nuclear p65 in tumors is associated with more aggressive prostate cancer^{57; 58; 59}.

The NF-κB family is composed of five transcription factors characterized by their Rel-homology domain responsible for DNA binding, dimerization and interaction with inhibitor of κB (IκB) proteins. The family is subdivided into two groups, members of the first group named RelA (p65), RelB, and c-Rel, carry a transactivation domain responsible for NF-κB potent activity as a transcription factor. The second group contain NFκB1 (p50 and its precursor p105) and NFκB2 (p52 and its precursor p100). The carboxy-terminal domain of p105 and p100 contains ankyrin repeats that must be degraded to create transcriptionally active p50 and p52 proteins respectively. All these transcription factors function as homo and heterodimers, the dimer most known and studied is composed of subunits p50 and RelA (p65). In most normal cells, the dimer

p50-p65 is kept inactive in the cytoplasm by association with I κ B family of inhibitors (α and β)^{60;61}.

Research from the past 20 years has revealed that there are three major NF- κ B pathways can be distinguished^{62;63;64}. The first is the classical or canonical pathway in which p65/p50, the main active dimer, is rendered inactive by I κ B inhibitors (I κ B α and I κ B β). This pathway may be activated by signals such as the proinflammatory cytokine tumor necrosis factor α (TNF α). The activation of NF- κ B also often requires the activation of the I κ B-Kinase complex (IKK α , IKK β and IKK γ) via multiple signals including (but not limited to) cytokine binding to cell surface receptors, DNA damage, hypoxic conditions, and oxidative stress⁶⁵. Canonical NF- κ B signaling is induced rapidly within minutes of stimulation without the need for *de novo* protein synthesis. The alternative or non-canonical pathway is activated by a smaller number of inducers, such as lymphotoxin β and B cell activating factor, and plays an important role in B-cell maturation and the formation of secondary lymphoid tissues^{66;67}. This pathway uses RelB/p52 as the active dimer.

In the canonical pathway (IKK β -dependent), the IKK complex phosphorylates I κ Bs that are then ubiquitinated and degraded by proteasomes. In the non-canonical pathway (IKK α -dependent), the IKK complex regulates the processing of the p100 precursor. Subsequently, the NF- κ B complex translocates to the nucleus and activates the expression of specific target genes^{68;69}. Although p65/p50 represents the main functional unit of the classical NF- κ B pathway, p65 also forms transcriptionally active

dimers with p52. In the same way, RelB/p52 constitutes the main alternative functional unit, however, RelB can also dimerize with p50 resulting in another alternative NF- κ B functional unit ⁷⁰.

Finally, and particularly relevant to our study, the third NF- κ B pathway, the so-called ‘atypical pathways’, refer to those pathways that do not fall in the abovementioned categories. Originally, all signaling cascades activated by atypical stimuli, such as DNA damage or oxygen stress, were classified as ‘atypical’ NF- κ B activators, as they all induce a slow and weak NF- κ B signal (with peak activities reached after 2–4 h). Later studies revealed that these stimuli could not be categorized in one class as they induced completely unrelated pathways. Thus, ultraviolet (UV)-induced NF- κ B signaling appears to occur in an IKK-independent way, while most other genotoxic stress agents activate a pathway that follows more or less the classical NF- κ B activation scheme. For example, ionizing radiation (IR)-induced NF- κ B activation has been reported following both low and high doses of irradiation ^{71;72}. This NF- κ B activation results in the induction of anti-apoptotic genes, inhibiting apoptosis induced by many chemotherapeutic drugs and irradiation ^{73;74;75;76}. Similarly, NF- κ B activation impact numerous other molecular and biological functions that could be relevant for responses to chemo-radiation such as inflammation ^{77;78}, angiogenesis ⁷⁹, survival, migration, and invasion ⁸⁰ are associated with the activity of NF- κ B nuclear factors.

ATM and NF- κ B

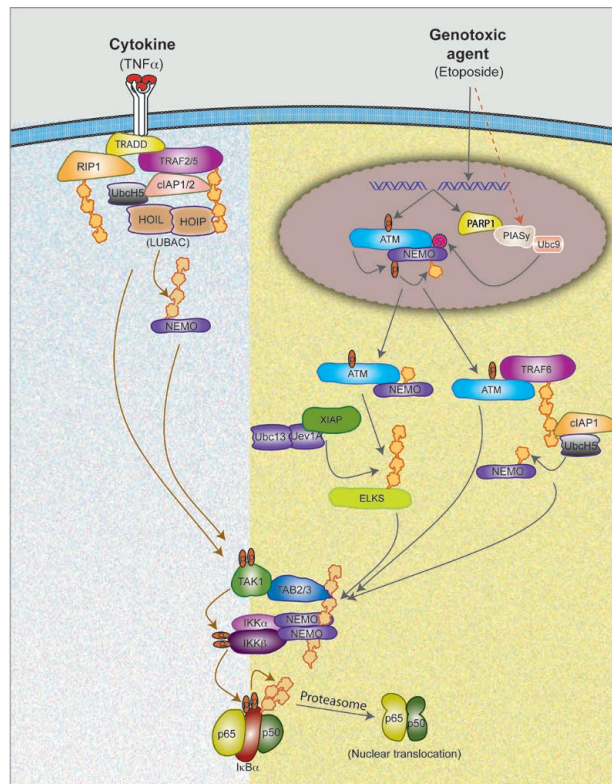
Given the nature of the biological processes modulated by NF- κ B, it is not surprising to see an overactivation of NF- κ B in many cancers⁸¹. Regarding solid tumors, aberrant nuclear localization of subunits of NF- κ B has been observed in various cancers, including pancreatic⁸², breast⁸³, endometrium⁸⁴, renal⁸⁵ and melanoma⁸⁶. Moreover, a large number of cell lines exhibiting high activity of the dimer p50-p65 are resistant to various chemotherapeutic agents^{76; 87}.

Furthermore, genotoxic agents used in cancer treatment (ex: IR, chemotherapy such as topoisomerase inhibitors, replication stress inducers such as hydroxyurea or DNA photolesions induced by UV-C) can activate p50/RelA NF- κ B complexes through the atypical pathway or through activation of CK2 (formally known as casein kinase II). CK2 is a highly conserved and ubiquitous serine/threonine kinase that may participate in the transduction of survival signals^{88;89} and CK2-mediated I κ B α phosphorylation has an important UV-protective function⁹⁰. Recently, several studies have shown that ATM is essential for NF- κ B activation following DNA damage^{91;92;93;94;95}.

The ATM-NEMO (Nf- κ B essential modulator) pathway activates p50/RELA Nf- κ B complexes via the induction of IKK β following DNA damage^{96;95}. Following cellular stresses, the nuclear translocation of the RIP1/NEMO death domain complex occurs. This nuclear NEMO is then post-transcriptionally modified by the small ubiquitin-like

modifier (SUMO)1, and phosphorylated by ATM, which is simultaneously activated in case of DNA damage. Ubiquitination of the ATM–NEMO complex targets these proteins for nuclear export, enabling the complex to interact with and activate the IKK- β subunit and initiate I κ B- α phosphorylation^{97;95;91}. This is substantiated by the discovery that the ATM inhibitor KU55933 block both constitutive and DNA damage-activated NF- κ B in breast cancer cell lines with mutant p53 and the downstream inhibition of NF- κ B activation is a major mechanism accounting for the radio-sensitizing effect of this ATM inhibitor⁹⁸.

Unlike NF- κ B signaling induced by cell surface receptors where the signal initiation event can be precisely defined, the necessary and sufficient molecular signal initiation events induced by various genotoxic agents are still being addressed. Highlighting the complexity of this issue, ultraviolet (UV) irradiation-induced NF- κ B activation led to the conceptualization of nuclear-to-cytoplasmic signalling⁹⁹. Accumulated evidence over the last two decades demonstrates that nuclear DNA damage is probably not the signal initiation event for immediate activation of NF- κ B in this case^{100;101;102}. Importantly, several lines of evidence support the requirement of nuclear DSB in initiating the canonical IKK-NF- κ B signaling pathway in response to many different genotoxic agents^{96;103}.



Miyamoto S., Nuclear initiated NF- κ B signaling: NEMO and ATM take center stage, *Cell Res*, 21, 116-30, 2011. Written authorization obtained by Dr Miyamoto and the journal through Copyright Clearance Center's RightsLink service

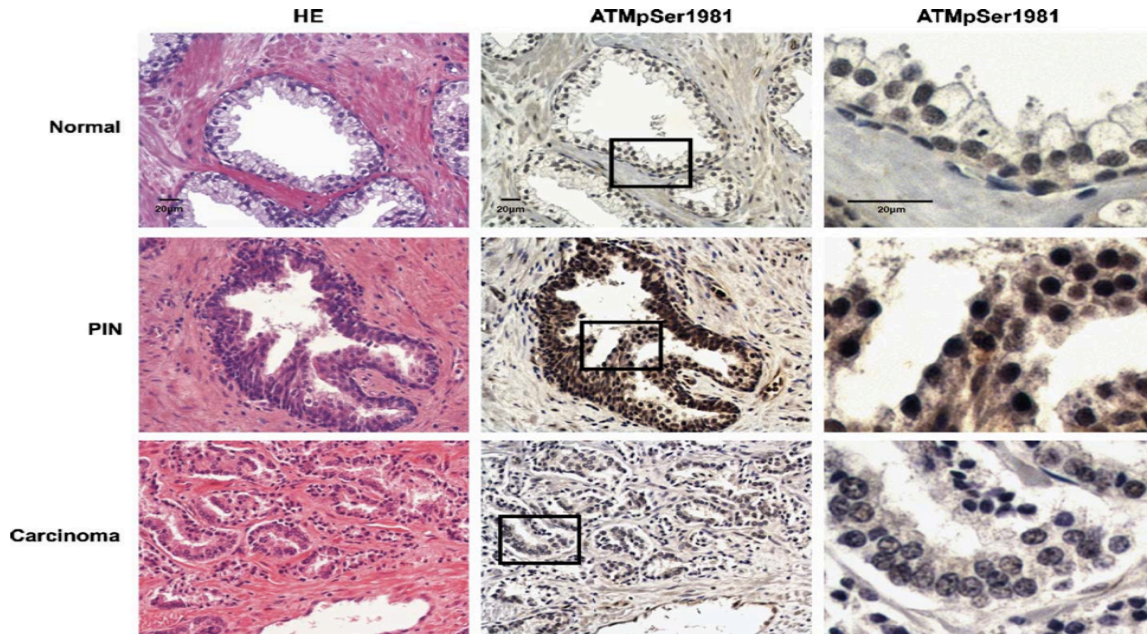
Figure 3: A model depicting distinct and common steps between NF- κ B signalling induced by TNF α and DNA damaging agents

In this figure 3, one can see that TNF α stimulation of TNFR1 engages receptor adaptor proteins (TRADD and RIP1) and results in the recruitment of ubiquitinating enzymes (Ubc13/Uev1A and UbcH5) and E3 ligases (cIAP1/2, TRAF2/5 and HOIL/HOIP) to promote K63-linked, mixed and linear polyubiquitination of multiple target proteins. These polyubiquitin chains form the scaffold on which TAK1/TAB2/3 and IKK/NEMO complexes are formed and TAK1-dependent activation of IKK β is induced. DNA damaging agents, such as etoposide, a widely used chemotherapeutic drug, cause ATM activation via induction of DSB and SUMOylation of NEMO through a mechanism dependent on PARP1, PIASy and Ubc9. PIASy dependent SUMOylation of NEMO may also be induced by additional stress conditions. ATM then phosphorylates NEMO, which results in cIAP1-dependent monoubiquitination of NEMO. ATM and NEMO are exported to the cytoplasm where K63-linked polyubiquitination of ELKS and TRAF6 via ATM-dependent mechanism, as well as monoubiquitination of NEMO on lysine 285 via cIAP1, are induced. The polyubiquitin scaffolds then activate IKK via TAK1, similar to the mechanism induced by TNF α . Active IKK then phosphorylates I κ B α , which then causes K48-linked polyubiquitination and degradation of I κ B α by the proteasome to liberate active NF- κ B (p50/p65) dimer. Polyubiquitin is represented in repeated yellow units, phosphate is shown in orange oval with "P" and SUMOylation is shown in purple circle with "S". (LUBAC, linear ubiquitin assembling complex).

2.7 DDR as a barrier to cancer progression

The DDR acts as a barrier against the progression of cancer beyond its early stages. Previous research in animal models has shown that activation of numerous oncogenes or loss of tumor suppressors result in DNA replication stress or DNA damage. DNA damage triggers the DDR, which leads to cellular senescence or death of oncogene-transformed cells and results in delay or prevention of tumor formation. Recent discoveries reinforce this dogma and demonstrate that activated DDR signalling act as a cancer barrier in several pre-neoplastic human lesions, including prostate cancer^{104; 105}.

A Canadian group has analyzed 35 primary prostate cancer specimens for ATM activation, p-CHK2, p-H2AX and p53 by immunohistochemistry in normal prostate glands, PINs (the precursors to carcinomas) and carcinomas¹⁰⁴. They had showed an increased intensity of p-ATM, p-CHK2 and p-H2AX in PINs, compared to normal prostatic glands or carcinomas. Figure 4 depicts representative images of the detected levels of ATM activation in normal prostatic glands and carcinoma compared to PINs.



Fan C, Quan R, Feng X, et al. ATM activation is accompanied with earlier stages of prostate tumorigenesis.. *Biochimica et biophysica acta*. Oct 2006;1763(10):1090-1097. Written authorisation obtained by Dr D. Tang on April 26th, 2014

Figure 4: ATM activation in normal prostatic gland, PIN, and carcinoma

ATM activation in normal prostatic gland, PIN, and carcinoma: Morphologically normal prostatic gland, PIN, and carcinoma from the same patient (or slide) were H&E stained and immunohistochemically stained for Ser1981 phosphorylated ATM using an anti-pSer1981-ATM antibody. The inset areas are enlarged (right column).

These findings suggest that early oncogenic events result in ATM activation, that are attenuated by events occurring in the later stages of prostate tumorigenesis, perhaps via genome re-stabilization in advanced cancer cells. The authors mention that the activation of ATM at the early stages of prostate tumorigenesis prevents tumor progression and its desensitization to oncogenic signals promotes tumor development. However, little is known about DDR activity beyond the PIN stage. Of note this study

did not detect any significant DDR signaling differences between normal and adenocarcinoma prostate tissues.

Separately, and in support of a DDR cancer barrier in prostate cancer, investigators have established that a DDR-mediated tumor suppression activity restricts early-stage prostate cancer progression in mouse models^{104; 105}. This senescence-mediated DDR barrier occurs at a stage associated with persistent DDR signalling and is analogous to human high-grade prostatic intraepithelial neoplasia (HG-PIN)^{106;107}. Further supporting this DDR-mediated cancer barrier, short telomeres (known to directly trigger the DDR) have been observed in human HG-PIN¹⁰⁸. Together, these lines of evidence strongly suggest that the DDR-mediated cancer barrier during HG-PIN is at least partially driven by DDR signalling. However, at the same time, the fact that DDR is persistently activated favours the outgrowth of malignant cells having defects in the DDR such as aberrations in the ATM cascade. Cancer cells, including prostate cancer cells, acquire an intrinsic capacity to tolerate DNA damage during cancer progression. This can happen through the loss of redundant DDR signalling pathways such as the p53 pathway, allowing HG-PIN to move to invasive carcinoma in mouse models. DDR and DNA repair are essential for genome stability and prolonged cell survival, therefore, cancer cells must maintain other redundant DDR pathways functional.

It is thus proposed that inactivation of these remaining DDR pathways could greatly sensitize cancer cells to DNA damage^{109; 110}. The identification of these remaining pathways in prostate cancer could represent new therapeutic opportunities. On their

own, these potential therapeutic avenues warrant a better characterization of active DDR pathways during prostate cancer progression^{104; 111}.

As described above, the DDR acts as a barrier against cancer progression. Moreover in prostate cancer, it has also been shown that promyelocytic leukemia protein (PML) body formation is defective in prostate tumor cells but is active in benign prostatic hyperplasia (BPH)¹¹². PML was identified in the early 90's as a gene target for translocations with the retinoic acid receptor gene in acute promyelocytic leukemia¹¹³. The expression of this protein in primary cells leads to cellular senescence. PML acts as a tumor suppressor and is often lost in human cancers¹¹⁴. It has been shown that PML represses genes involved in DNA replication, repair and checkpoints. Indeed, PML represses E2F target genes and induces p53 and the DDR. The decrease in the expression of genes required for DNA repair and checkpoints promptly after PML expression suggests a mechanism by which PML could contribute to the senescence cell cycle arrest, which we know involves DNA damage signals^{115; 116; 117}. Vernier and colleagues investigated whether the PML/senescence pathway is important in human cancers, and to do so, they measured PML expression by immunohistochemistry in TMAs with samples from patients with benign or malignant prostate tumors¹¹². BPH is a benign prostate lesion characterized by the presence of senescence markers¹¹⁸ and low E2F target gene expression¹¹⁹. In their study, PML staining in the normal prostate was very weak, but a few PML bodies could be distinguished. In contrast, PML staining was stronger in BPH samples where many PML bodies were easily

distinguished. Inversely, PML bodies were rarely distinguished in prostate cancer samples, including PIN, although they did detect some homogenous expression in the nucleus or cytoplasm. Their results indicate that cells from BPH contain more PML bodies than cells from normal tissues or cells from the few cases of prostate carcinomas in their TMAs where PML bodies were visualized. Taken together, they suggest that PML bodies may suppress malignant transformation in the prostate by promoting senescence, and that PML staining could be used to distinguish benign from malignant lesions.

It is known that the retinoblastoma (Rb) pathway controls the cell cycle at the transcriptional level via repression of E2F target genes^{120; 121; 122}. Many E2F target genes mediate DNA repair and checkpoints, and, in their absence, cells accumulate DNA damage signals that are essential for activation of p53 and the senescence process^{115;116; 117}. According to this same group, the lack of PML bodies in tumor cells can explain why prostate tumors exhibit high levels of expression of E2F target genes such as EZH2¹²³ and BRCA1^{124; 125} which is also one of the genes most efficiently downregulated in PML–senescent fibroblasts.

Furthermore, DDR determines how normal and cancer cells react to cancer therapy such as DNA damaging RT or chemotherapies. Indeed, DDR activity has been detected in prostate cancer tumors following chemotherapy¹²⁶.

The identification of biomarkers that predict the kind of DDR responses particular

cells/tumors would mount against therapy could highly improve treatment selection and successes. Currently, the exact regulation and outcomes of DDR signalling in cancer cells, particularly in prostate cancer, remain relatively unknown.

3.0 Biomarkers

3.1 Prognostic vs. Predictive markers

Prognostic markers may help clinicians guide their patients in their decision-making and avoid treatment and toxicities for men with slow growing cancer while promoting the initiation of treatment in the others. Although “predictive” and “prognostic” markers are often used interchangeably, they are different¹²⁷. Prognosis refers to the ability to distinguish clinically important variation and reliably project the course, the progression, the pattern and the end of disease. Prognostic markers are associated with prognosis, unrelated to the treatment received. They predict the “natural” outcome of the disease before a treatment is given or regardless of it. As such, the treatment can change the prognosis in addition to the end point (local control, PSA control, overall survival or preservation of the prostate). As for “predictive” factors, they are those that foretell the response to a treatment. In summary, predictive markers suggest the outcome of a treatment, thus allowing the identification of patients who will benefit from particular therapies, whereas a prognostic factor is a marker for gravity of a disease and outcome that is independent of treatment.

3.2 DDR as a tissue marker

To our knowledge, the protein expression of DDR factors in tissues has not been studied as biomarkers for cancer biology. Few studies have looked at tissue markers predictive of radiosensitivity in prostate cancer because the analyses are done on very small specimens obtained during prostate biopsies. Moreover, there are no studies on post radiation prostatectomy specimens. The Radiation Therapy Oncology Group (RTOG) has identified several biomarkers, from patients treated by RT under phase 3 randomized trials. Those markers are mainly involved in the cell cycle or apoptosis. The first biomarker studied by the RTOG was p53. They found a statistically significant correlation between abnormal p53 protein expression and an increased risk of distant metastases ($p=0.04$), a decreased probability of progression-free survival ($p=0.03$), and a reduction in overall survival ($p=0.02$). Furthermore, patients with tumors exhibiting abnormal p53 expression who received RT with androgen deprivation therapy (ADT) who had tumors that exhibited abnormal p53 expression developed metastases faster ($p=0.001$) but this was not observed in patients treated by RT alone without ADT¹²⁸. The RTOG also evaluated patients in a different randomized phase 3 study. Of the 777 patient cohort, 22% had abnormal p53 expression defined as $\geq 20\%$ cells with positive nuclear staining by immunohistochemistry (IHC) and this was associated with a decreased survival ($p=0.014$) and an increased risk of distant metastasis ($p=0.013$). For patients treated with ADT, there was a correlation between the p53 status and cause-specific survival

($p=0.004$). When these patients were divided into subgroups based on p53 status, only the subgroup of patients with abnormal p53 was found to have a significant association between the assigned treatment and cause-specific survival ($p<0.01$). Unfortunately, because all patients had received ADT, the question of a possible unfavourable interaction between abnormal p53 expression and the use of ADT compared with RT alone could not be resolved¹²⁹. Other markers that have been studied include DNA ploidy¹³⁰, loss of p16 expression^{131; 132}, Ki-67^{133; 134}, mouse double-minute p53 binding protein homolog (MDM2) expression (an oncoprotein that promotes p53 degradation)¹³⁵, B-cell lymphoma 2 (Bcl-2) and Bcl-2-associated x protein (Bax) expression levels^{136; 137}, a quantitative assessment of cytosine, adenine, and guanine (CAG) base pair repeats on the androgen receptor gene¹³⁸, Cyclooxygenase-2 (Cox-2) expression¹³⁹, Signal transducer and activator of transcription 3 (Stat-3) expression¹⁴⁰, Polymorphisms in the androgen receptor cytochrome P450 3A4 (CYP3A4)¹⁴¹ and protein kinase A RI-alpha (PKA) expression¹⁴². Despite these numerous studies, an adequate biomarker is still not available for routine use within the clinic.

4.0 The Tissue Microarrays (TMAs)

Tissue microarrays (TMAs) consists of paraffin blocks in which up to 1000 separate tissue cores are assembled in array fashion to allow multiple analysis such as immunofluorescence (IF), immunohistochemistry and in situ fluorescence hybridization (FISH). Kononen and colleagues, in the laboratory of Ollie Kallioniemi, developed this technique in 1998¹⁴³. Since tissue have been preserved in formalin and embedded in paraffin for sectioning before microscopic examination as a standard of care for over a century, this group defined a method for examining several histologic sections at one time by arraying them in a paraffin block. TMAs are produced by a method of relocating tissue from conventional histologic paraffin blocks such that tissue from multiple patients or blocks can be seen on the same slide. To do this, a hollow needle is used to remove tissue cores as small as 0.6 mm in diameter from regions of interest in pre-existing paraffin-embedded tissues such as biopsies taken from patients or tumor samples following patients' surgery. These tissue cores are then inserted in a recipient paraffin block in a precisely spaced, array pattern. Sections from this block are cut using a microtome and mounted on a microscope slide. The number of spots on a single slide is variable depending on the array design. Currently, up to 600 cores can fit on a standard glass slide. In this way, tissue from hundreds of archived pathologic specimens (one specimen per patient) can be represented on a single paraffin block that can be analyzed by any method of standard histological analysis, using a variety of techniques. Figure 5 illustrates the creation of a TMA¹⁴⁴.

The two major advantages of this technique are the fact that an entire cohort of patients can be studied by analyzing just a few slides and that all specimens are processed at once using identical conditions. Nevertheless, a disadvantage of this technique is that it reduces the amount of tumor analyzed since each core represents a minuscule portion of the tumor. In order to address this, a validation study determined how many tissue cores are required to adequately represent the expression of a particular antigen by a tumor¹⁴⁵.

It was determined that the analysis of two cores is comparable to analysis of a whole tissue section in more than 95% of cases. To ensure adequate representation of the whole-section staining pattern, at least two, and in most cases three, punches are available for evaluation. One must also consider a few important aspects such as the technical expertise of the individual constructing the array blocks and slides as well as the fact that each tumor block is punched three times in various regions of the tumor mass, including both the leading edge and the tumor center. It is also important to carefully outline areas of invasive carcinoma distinct from the non-invasive or in situ component and this process is performed by a technician and verified by a pathologist¹⁴⁵.

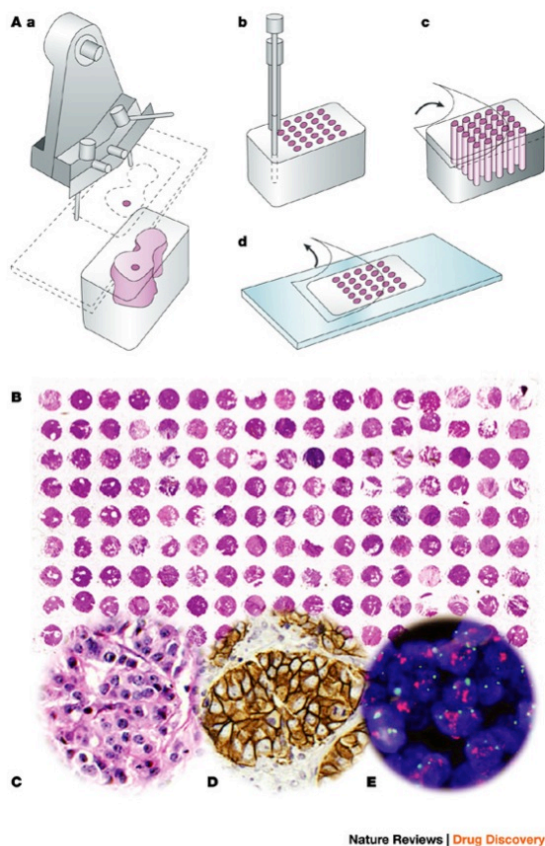


Figure 5: TMA

A | Cylindric tissue cores (usually 0.6 mm in diameter) are removed from a conventional ('donor') paraffin block using a tissue microarrayer; these are released into premade holes of an empty ('recipient') paraffin block. Regular microtomes can be used to cut tissue microarray sections. The use of an adhesive-coated slide system (Instrumedics) facilitates the transfer of tissue microarray (TMA) sections on the slide and minimizes tissue loss, thereby increasing the number of sections that can be taken from each TMA block. **B** | Overview of a haematoxylin-eosin (H&E) stained TMA section. Each tissue spot measures 0.6 mm in diameter. **C–E** | Magnifications of sectors from tissue spots from different experiments. **C** | H&E staining of breast cancer tissue. **D** | Immunohistochemistry of breast cancer tissue using the HercepTest (DAKO). Brown membranous staining indicates strong ERBB2 expression. **E** | FISH analysis of the same case showing ERBB2 gene amplification (red signals) but normal copy numbers of centromere 17 (green signals)

Sauter G, Simon R, Hillan K. Tissue microarrays in drug discovery. *Nature reviews. Drug discovery*. Dec 2003;2(12):962-972.
 Written authorization obtained by Dr Sauter on April 24th, 2014

This technique permits dramatic advancement of research based on the use of materials from biobanks. Many institutions have developed TMAs that can then be shared for research. For example, through a collaborative effort of the specialized programs of research excellence (SPORE) in skin cancer, a group¹⁴⁶ has developed a melanocytic

tumor progression TMA to serve as a template for the examination of candidate biomarkers generated at a meeting in Gaithersburg¹⁴⁷. Similarly, OriGene Technologies is a corporation founded as a research tool company. They provide TMAs that are created from high-quality tissue samples from the OriGene Tissue Biorepository, a growing collection of over >140,000 tissue samples, molecular derivatives, and associated clinical data that represent hundreds of pathology diagnoses.

Our academic institution developed the TMA used herein (TMA-TFRI-Terry Fox Research Institute) starting in 2009 and by 2011, the TMA of the cohort of 300 patients was completed. This TMA has allowed many researchers from our institution to make great advancements in cancer research resulting with the first publication in 2012¹⁴⁸.

Our laboratory has developed great interest and expertise in the development of TMAs whether in prostate or ovarian cancer. Our team of assistants regularly updates the clinical data of the patients represented in the TMAs. Furthermore, this technology has greatly encouraged the bench to bedside research where clinicians and basic researchers have come together to collaborate on research projects¹⁴⁹.

Hypothesis and objectives

1. Premiss:

The DDR acts as a barrier against the progression of cancer beyond its early stages.

This was shown in several pre-neoplastic human lesions, including prostate cancer.

Activation of DDR signalling is detected during human prostate cancer progression¹⁰⁴;

¹⁰⁵, or following chemotherapy¹⁵⁰ and warrants the investigation of the DDR pathways

involved. Moreover, clinical correlations between DDR signalling and individual

patients' clinical outcomes have never been done. This could allow us to identify

novel biomarkers that can predict treatment outcomes and that can be used to develop

better treatment strategies. We have characterized DDR protein expression in prostate

cancer, which is particularly promising with respect to potential treatment

improvement based on DDR manipulation since DNA damaging agents such as RT are

part of the first line of treatment.

2. Hypothesis and objectives

DDR activity is detected increasingly during cancer progression with a peak at the pre-

neoplastic state (HG-PIN) illustrating the DDR-mediated barrier to cancer

progression. Much less is known about the state of the DDR once the cancer

progresses beyond pre-neoplasia to adenocarcinoma. Will DDR remain stable,

increase or decrease (Figure 6)? One hypothesis is that an increase in DDR may

indicate a defect in DNA repair and, hence, the relative radiosensitivity of those cells. Notably, DNA damaging agents are also used in cancer therapy and drugs targeting DNA damage response enzymes are exhibiting an exciting potential as new anti-cancer agents. Our hypothesis is that the levels of DDR protein expression in prostate tissue will vary with the grade and behaviour of the prostate cancer. Moreover, we expect that the levels of DDR protein expression are related to treatment response for individual patients.

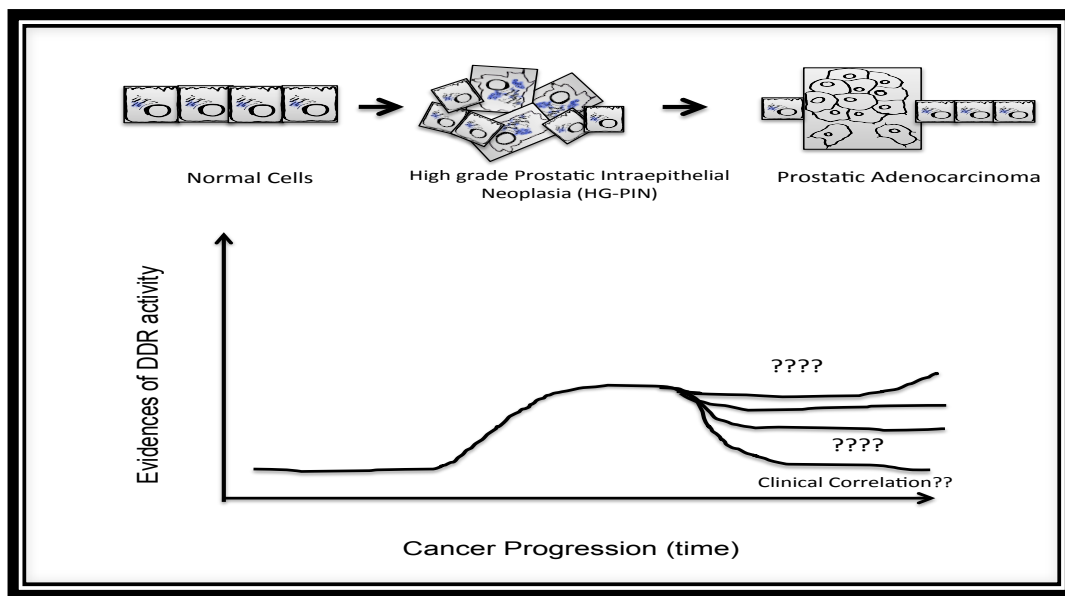


Figure 6: Hypothesis

Activation of DDR signalling has been shown in PIN. Less is known about the state of the DDR once the cancer progresses beyond pre-neoplasia, from HG-PIN to adenocarcinoma. Clinical correlations between DDR signalling and individual patients' clinical outcomes have never been done, but we predict that they may provide clues to treatment response, especially where therapy targets DNA integrity.

Our objectives are to:

- 1) Use human prostate cancer tissue TMAs to characterize the occurrence of DDR expression.
- 2) Correlate the activation of specific DDR markers with patient survival and responsiveness to treatment (biochemical recurrence free survival as measured by PSA and bone metastasis free survival).
- 3) Determine the difference between DDR expression in epithelial cells and stromal cells using a specific epithelial mask to differentiate epithelial and stromal compartments when analyzing DDR activation signals. This epithelial-stromal specific DDR data will also be correlated to prostate cancer stages and clinical histories as in objectives 1 and 2 above.

Our long-term goal is to identify new prognostic markers based on DDR activity in prostate cancer tissues that would allow better characterization of patients (i.e. low risk, high risk). Eventually, we hope to find a predictive marker to determine which patients should be counselled towards surgery or RT.

CHAPITRE 2: EXPERIMENTAL RESULTS

Novel streamlined DNA damage response signalling quantification in human prostate cancer tissue samples reveals a prognostic role for 53BP1

**Guila Delouya MD ^{1,2}, Guillaume Chouinard MSc ¹, Véronique Barrès MSc ¹,
Véronique Ouellet PhD ¹, Guillaume Cardin MSc¹, Fred Saad MD ^{1,3}, Anne-Marie
Mes-Masson PhD ¹ and Francis Rodier PhD ¹**

¹ Centre de recherche du Centre hospitalier de l'Université de Montréal (CR-CHUM)/Institut du Cancer de Montréal, Montreal, Canada;

² Department of Radiation Oncology, Centre hospitalier de l'Université de Montréal (CHUM), Hôpital Notre-Dame, Montreal, Canada;

³ Department of Urology, Centre hospitalier de l'Université de Montréal (CHUM), Hôpital Notre-Dame, Montreal, Canada;

Article in preparation

Keywords : Prostate Cancer, DNA Damage response (DDR), Biomarker

ABSTRACT

Background: DNA lesions trigger a DNA damage response (DDR) that acts as a cancer barrier in several pre-neoplastic human lesions, including prostate cancer. DDR signalling is based on a cascade of phosphorylation events that regulate DNA repair, cell cycle checkpoints and extracellular communications. As such, the DDR also heavily influences the outcome of DNA damage based cancer treatments. Here, we quantified the levels of selected DDR components and DDR activity proxy in archived human prostate cancer tissues and correlated their levels with patient clinical outcomes.

Methods: We used tissue microarrays (TMAs) built from archived human radical prostatectomy specimens of 300 men with prostate cancer and estimated the levels of DDR protein expression or activity in the nuclear stromal and epithelial compartments of normal and cancer tissues. The protein expression of the DDR markers 53BP1, phosphorylated-H2AX, RELA and phosphorylated-CHK2 was quantified using immunofluorescence (IF) coupled to high-content automated imaging. The quantification of our DDR markers was first validated on a small scale TMA of normal and irradiated (to induce DDR signalling) cultured human fibroblasts before final analysis on patient TMAs. The validated markers were then used to quantify DDR signals on prostate cancer patients TMAs. The data were quantified using binary layers commonly used to classify pixels in an image so areas can be analysed independently allowing detection of many morphological regions such as nuclei, epithelium and stroma. Arithmetic operations were then performed to render values

corresponding to DDR activation. Finally, the results were correlated with clinical outcome such as biochemical recurrence (BCR) and occurrence of bone metastasis.

Results: We found that low levels of RELA protein expression in the nuclear epithelial compartments of normal prostate tissue were associated with a reduced probability of biochemical failure. Moreover, we also observed that low levels of 53BP1 protein expression in the nuclear epithelial compartments of normal and cancerous prostate tissue were associated with a lower incidence of bone metastasis ($p=0.005$).

Conclusion: This study confirms previous findings of p65 detectability in prostate cancer tissue and its usefulness as a prognostic factor. All together, our study points out the presence of the DDR marker 53BP1 in prostate cancer tissues and its uses as prognostic value in patients with prostate adenocarcinoma.

1.0 Introduction

Prostate cancer is the most frequently diagnosed cancer in Canadian men and is the third deadliest cancer in males after lung and colon cancers ¹. Some patients do not receive treatment while others will have prostatectomy, external beam radiation, brachytherapy, androgen deprivation therapy (ADT) or a combination of these therapies. Currently, the decision to treat (e.g. surgery or radiation) or not (e.g. active surveillance) is based on the clinical and histologic features of the prostate cancer ². To better stratify prostate cancer patients by prognosis, the identification of specific molecular biomarkers able to predict outcome would represent an important advancement over existing clinical tools. Several research points out the importance of DDR responses in prostate cancer prognosis. DDR activity is detected in prostate cancer tumors following chemotherapy ³ and during prostate cancer progression with a peak at the pre-neoplastic state illustrating the DDR-mediated barrier to cancer progression ⁴. Specifically, increased intensities of p-ATM, p-CHK2 and p-H2AX were observed in prostatic intra-epithelial neoplasia (PINs) compared to normal prostatic glands and carcinomas. However, much less is known about the state of the DDR once the cancer progresses beyond PIN to adenocarcinoma, in addition the regulation and outcome of DDR signalling in cancer cells remains poorly understood. To preserve genomic integrity, and allow homeostasis state, cells require constant protection against the most lethal type of DNA damage; DNA double strand breaks (DSBs). DSBs results from exogenous stresses, such as ionizing radiation, ultraviolet

light and chemical compounds (i.e. chemotherapy), as well as endogenous insults such as reactive oxygen species (ROS) production and DNA replication errors ⁵.

To counteract DNA damage, cells have developed a mechanism that sense DSBs and initiate the DNA damage response (DDR). The DDR is a signal transduction implicated in the inhibition of cell proliferation and therefore act to prevent cancer progression. DDR act as a sensor to detect DSBs and initiate the activation of phosphoinositide-3 kinase-like kinase (PIKK) family. PIKK is a apical transducers kinases including ATM (Ataxia Telangiectasia Mutated) which initiate a complex cascade orchestrated around phosphorylation events. Signal mediators activated via phosphorylation by ATM/PIKK can amplify and expand the DNA damage signal from the source (DSBs) to downstream cellular mediators such as Chk2 and p53 DDR effectors leading to DNA repair, cell cycle arrest, apoptosis, senescence and even activating Nuclear Factor (NF)- κ B inflammatory extracellular signals ^{6; 7}. ATM induces the activation of the nucleosomal histone variant H2AX, which in turn enhances the local recruitment of DDR factors on the chromatin including the tudor-domain p53 binding protein-1 (53BP1). Phosphorylated H2AX (p-H2AX) and 53BP1 rapidly co-localize to DSBs forming characteristic structures termed DNA damage foci. ATM also phosphorylates the kinase CHK2 (checkpoint kinase-2), which promotes growth arrest and p53, a tumor suppressor and transcriptional regulator that coordinates repair and cell cycle arrest ⁸.

The DDR acts as a barrier against the progression of cancer beyond its early stages. Indeed, the DDR cascade leads to transient cell cycle arrest and DNA repair, cell death, or permanent cell cycle arrest (cellular senescence) preventing the accumulation of cells containing mutations and cancer development ^{9; 10}. Previous research using animal models shows that the activation of numerous oncogenes or the loss of tumor suppressors result in DNA replication stress and DNA damage that triggers the DDR leading to cellular senescence or death of oncogene-transformed cells preventing tumor formation. Similarly, a DDR-mediated tumor suppression barrier restricts early-stage prostate cancer progression in mouse models ^{11; 12}. This senescence barrier occurs simultaneously with the detection of persistent DDR signalling and at a cancer progression stage analogous to human high-grade prostatic intraepithelial neoplasia (HG-PIN) ^{13; 14}. Further supporting this DDR-mediated cancer barrier, short telomeres (known to directly trigger the DDR) have been observed in human HG-PIN ¹⁵. All together, these observations strongly support that the DDR-mediated cancer barrier restricting progression during HG-PIN is at least partially driven by DDR signalling. However, the fact that DDR is persistently activated could promote the outgrowth of malignant cells bearing a defect in the DDR as an aberration in the ATM cascade. Cancer cells, including prostate cancer cells, are known to acquire an intrinsic capacity to tolerate DNA damage during cancer progression. In mouse carcinoma cells, this can happen through the loss of redundant DDR signalling pathways such as the p53 pathway, allowing HG-PIN to progress to invasive carcinoma cells ^{11; 12}. However, in

general, the DDR and DNA repair functions are absolutely essential for cell survival; thus cancer cells must maintain other redundant DDR pathways functional. It is therefore proposed that inactivation of these remaining DDR pathways could greatly sensitize cancer cells to DNA damage^{16; 17}. The identification of these remaining pathways in prostate cancer could represent a new therapeutic opportunities in combination with current RT. On their own, these potential therapeutic avenues warrant a better characterization of active DDR pathways during prostate cancer progression^{4; 18}.

In the present study, we investigated the effect of DDR signalling in DNA repair because our group has already addressed the prognostic value of the p65 subunit of (NF)- κ B in prostate cancer (p65) where it was observed that a high level of nuclear p65 in tumors is associated with more aggressive prostate cancer¹⁹. In addition, we examined the possibility that DDR activity could be correlated with patients' clinical outcomes.

2.0 Materials and Methods

2.1 Tissue Microarrays (TMAs) Construction

The tissue microarrays (TMAs) used in this study were paraffin blocks in which up to 300 separate paraffin-embedded tissue cores were arrayed. Briefly, a hollow needle is used to remove tissue cores as small as 0.6 mm in diameter from regions of interest in a paraffin-embedded tissue block made from patient's biopsies, tumor samples or cultured cells. The samples were then embedded in a recipient paraffin block in a precisely spaced, arrayed pattern. Sections were made using a microtome, mounted on a microscope slide, and processed/analyzed by any method of standard histological analysis^{19; 20; 21}.

2.2 DDR markers validation study: TMA-cell and TMA-tissue

We established a specific procedure to measure DDR activity in formalin fixed paraffin embedded (FFPE) samples (TMA-cell). Briefly, the TMA-cell consisted of BJ-u cells (normal fibroblasts) exposed to a 10 Gy dose and different times of recovery following irradiation (30 minutes, 2h, 8h, and 24h) to induce DDR signalling. The negative control consisted of non-irradiated BJ-u cells. Figure S1 illustrates the construction and map of the TMA-cell. The selected DDR antibodies were optimized using the TMA-cell and validated on TMA-tissue consisting of tissue cores from patients having had transurethral resection of the prostate (TURP), prostatectomy or ovariectomy.

Once all antibodies were validated on the first two TMAs, they were then used on our cohort of patients, TMA-TFRI (Terry Fox Research Institute).

2.3 TMA- Terry Fox Research Institute (TFRI) / Cohort of patients

The TMA-*TFRI* consists of 300 patients treated by surgery for their prostate cancer. From the FFPE tissue samples, tumor areas were selected based on the hematoxylin/eosin (H/E) - stained slides analysed by a pathologist. FFPE tumor blocks were then cored using a 0.6 mm diameter tissue arrayer and resultant cores were arrayed into a grid in a recipient paraffin block. All patients were distributed on three TMAs, a total of 100 patients per TMA. Each TMA consisted of one core of tumor sample and one core of normal prostatic glandular tissue per patient (one set per patient). Every TMA was also duplicated so that two different sets per patient was represented on two different TMA slides. These TMAs were then sectioned, stained by H/E and immunohistochemistry (IHC) of high molecular cytokeratin (HMCK) and underwent an independent pathology review to confirm the histology of each core.

The current study was based on a cohort of 300 prostate cancer patients whose paraffin-embedded primary prostate cancer specimens were used to construct TMA-TFRI. All patients had radical prostatectomy between 1992-2006. All patients with the exception of 12 (these cases were excluded) had no prior treatment. The median patient follow-up was 100.5 months. Biochemical recurrence (BCR) was defined as a prostate specific antigen (PSA) above 0.3ng.ml^{-1} after date of surgery (RP).

Recurrence-free interval was defined as the time between RP and the date of first PSA increase above 0.3ng/mL. The final staging, grading and histological diagnosis was based on the clinical pathology report from the patients' file. The main clinical parameters of the cohort are listed in Table 1. All patients provided informed consent and the institutional review board approved this retrospective analysis.

2.4 Immunofluorescence technique (IF)

We optimized the immunofluorescence (IF) protocol to detect total nuclear signal of specific proteins that are part of DDR pathway.

To ensure coverage of all prostate cancer cells, even in their most undifferentiated state, a combination of cytokeratin 18 (CK18), cytokeratin 19 (CK19) and PSA was used (epithelial mask). They were all labeled to emit in the orange channel, tetramethyl rhodamine isothiocyanate (TRIT-C). Slides were also stained with 4',6-diamidino-2-phenylindole (DAPI - blue) to identify nuclei (nuclear mask). Selected DDR antibodies were labeled with Cy-5 (red cyanine dyes) or with FITC (green fluorescein isothiocyanate). This allowed us to define epithelial-stromal specific staining of the DDR antibodies, and to define whether this staining was nuclear or cytoplasmic.

The IF protocol consisted of a two steps procedure. The first part using an autostainer and the second part directly on the bench. The slides were first deparaffinized and then washed in toluene. The 4µm tissue sections from TMAs were then stained with the Benchmark XT autostainer (Ventana Medical

System Inc.). Antigen retrieval was obtained using Cell Conditioning 1 (Ventana Medical System Inc., #760-501) for 60 minutes. Pre-diluted primary antibodies (anti 53BP1 (rabbit, Clone 304, lot #A3 1:1000), anti-p-H2AX (mouse, JBW 301,1:2000), RELA / NfKB-p65 (mouse, F-6, Santa Cruz 1:25), pCHK2 (rabbit, Thr68, Lot 11, #2661, 1:500)) were manually added to the slides and incubated at 37°C for 60 minutes. All following steps were manually done at room temperature under conditions to protect slides from light. The specimens were then blocked with a protein-blocking serum-free reagent (Dako) at room temperature for 20 minutes followed by a 60 minutes simultaneous incubation in the dark with secondary antibodies: anti-mouse Cy-5 (#A10524, Life Technologies Inc., ON, CANADA) for mouse primary antibodies and anti-rabbit Alexa Fluor488 (A488) (#A11008, Life Technologies Inc., ON, CANADA) to detect rabbit primary antibodies, both diluted at 1:250 in 1X PBS. Between incubations, specimens were washed in PBS for 10 min. Because epithelial mask-specific mouse antibodies are used in addition to the DDR-specific antibodies above, TMAs slides were blocked 60 minutes with Mouse-On-Mouse blocking reagent (MKB-2213, Vector Laboratories, CA, USA) (1 drop in 250 µL PBS) and then incubated for 90 min at RT with anti-PSA (1:100 in PBS). After two successive washes, TMAs slides were incubated for 45 minutes at RT with secondary fluorescent anti-goat Cy3 (#705-165-003, Jackson ImmunoResearch Laboratories Inc., PA, USA) diluted at 1:250 in PBS.

After two more successive rinses, TMAs slides were blocked once again with Mouse-On-Mouse blocking reagent overnight at 4°C. Subsequently, they were incubated for 90 minutes at RT with a mix of anti-CK18 and anti-CK19, both at 1:100 in PBS. After two rinses, TMAs slides were incubated 45 minutes at RT with secondary fluorescent antibody anti-mouse Alexa Fluor546 (A546) (#A10036, Life Technologies Inc., ON, CANADA). TMAs slides were then rinsed three times and incubated 15 minutes at RT with a 0.1% (w/v) solution of Sudan Black in 70% ethanol, to quench tissue auto-fluorescence. Finally, TMAs slides were mounted with anti-fade mounting medium containing DAPI for nuclei staining. Slides were stored at 4°C and scanned the next day. A negative TMA slide was used in parallel where PBS replaced all the primary antibodies.

2.5 Image Analysis

The immunofluorescence results were analysed and quantified using the ViosiomorphDP software (Visiopharm, Denmark) following whole slide mosaic digital images acquisition using the Olympus software linked to our automated microscope. The 4 different colour channels were DAPI, FITC, TRIT-C and Cy-5 each associated to a particular mask. DAPI stains nucleus, TRIT-C the epithelium whereas FITC and Cy-5 were associated to the DDR antibodies of interest. The means fluorescent

intensities (MFI) were evaluated based on dye used. Hence, the image content is « Segmented ». Binary Layers are commonly used to classify pixels in an image so areas can be analysed independently. The use of many binary layers allowed the detection of the morphological regions. Arithmetic operations (AND, NAND, OR, NOR, etc.) were performed on those binary layers allowing even more segmentation and measurements options. This allows a quality control in order to reject cores from our analysis showing less than a certain percentage of epithelia or simply to reject damaged cores.

MFI was calculated based on the sum of the intensities of each pixel (every nucleus being divided in many pixels) divided by the number of pixels in the nucleus, assuming that MFI is proportional to the number of nucleus.

2.6 Statistic analysis

Statistical program SPSS was used for all data analysis (SPSS 16.0 statistical software package, SPSS Inc, Chicago, IL, USA). The correlation with clinico-pathological variables was estimated with a Pearson correlation coefficient test. BCR-free survival and bone metastasis free curves were plotted using the Kaplan–Meier estimation and the log-rank test was used to evaluate significant differences. Comparison between non-malignant cores and matched tumor cores were assessed using a paired t-test. Univariate and multivariate proportional hazard models (Cox regression) were used to estimate the hazard ratios for each DDR marker variable. Multivariate analysis was

performed using a forward stepwise hazard model on univariate analysis required for entry into the model. Additional clinico-pathological variables included pre-operative PSA, Gleason score (GS), surgical margin status, extra-capsular extension (ECE) and seminal vesicles involvement (SVI). A *p-value* < 0.05 was considered to be statistically significant.

3.0 Results

3.1 DDR markers validation on TMAs

In order to evaluate DDR signaling in patients' prostate cancer tissue samples, we first established a specific and quantifiable methodology to measure and quantify DDR activity in paraffin-embedded samples. We created a TMA-cell (Figure S1 A-B) consisting of cultured non-irradiated control human fibroblasts and similar cells irradiated with 10 Gy X-Ray and fixed at selected time intervals to allow DDR progression through its multiple signalling stages.

Following the immunofluorescence staining on the TMA-cell, we were able to detect a specific appearance of H2AX phosphorylation (p-H2AX) in irradiated cells correlated to the expected rapid increase in H2AX phosphorylation followed by an apparent decrease in signal intensity over time consistent with the occurrence of DSBs repair (Figure 1). When analyzing images at higher resolution, we observed the appearance of typical p-H2AX DNA damage foci, with residual foci persisting up to 24 hours after

irradiation despite the global decrease in p-H2AX (Figure 1). Using the immunofluorescence technique, we were able to simultaneously detect more than one DDR marker in a single cell (different colors for each markers). This was illustrated by the simultaneous detection of 53BP1 (red) and p-H2AX (green) showing that 53BP1 rapidly colocalizes with p-H2AX at DNA damage foci following irradiation (Figure 1).

We also detected the appearance of intense residual DNA damage foci at sites that were not repaired efficiently (persistent DDR foci associated with a senescence response ²²). This initial increase in signal is not observed using 53BP1, which is a DDR protein known to be already present in the nucleus before damage, but that relocalizes at sites of DNA damage as long as the repair is not fully completed (persistent DDR foci).

Other selected DDR antibodies were similarly validated on TMA-cell (RELA, p-21 and p-CHK2 (data not shown). Finally, we applied a software-based nuclear mask using the DAPI staining as a reference to automatically isolate individual nuclei in a TMA-cell core (Figure S1-C). Our results confirm that by choosing automated multi-color immunofluorescence image acquisition pipeline, we were able to detect DDR signalling and automatically identify substructures like nuclei in FFPE samples.

We then determined whether masking segmentation could also be applied to accurately separate epithelial and stromal tissues compartments in real tissue cores. To answer this question, we applied paraffin-validated antibodies on real tissue TMAs as

described in materials and methods. As shown in Figure 2A and 2B, we were able to validate our immunofluorescence technique, which provides a clear and a channel-independent multicolor IF signals on tissue cores (representative prostate cancer TMA-TFRI tissue core), a representative full slide prostate cancer TMA-TFRI mosaic scan is shown in figure S2. Additionally, our epithelial and nuclear IF masks were accurately and reliably detected by our software-based image segmentation analysis (Figure 2-C).

3.2 Nuclear DDR markers quantification in IF segmented images

Following successful validation of DDR markers staining and image segmentation in TMAs, we were interested in specifically quantified nuclear DDR signalling, which normally would represent the major cellular compartment of activity for the selected potential DDR biomarkers (H2AX is a nuclear histone phosphorylated *in situ*, 53BP1 is a nuclear protein that relocalizes within the nucleus following DNA damage, CHK2 is phosphorylated in the nucleus, and RELA relocalizes from the cytoplasm to the nucleus upon activation). Consistent with what we know about the DDR (Figure 3-A), our software-based quantification of nuclear DDR signal reveal that the phosphorylation of ATM targets such as p-H2AX and p-CHK2 was rapidly increased following DNA damage while 53BP1 levels remain relatively stable (as expected for a protein that is not stabilized/degraded following DNA damage but rather relocalizes to DNA damage foci). Alternatively, the p53 transcriptional target p21 was gradually increased, as we were expecting for a protein that increases in quantity following

regulation at the RNA level. Additionally, in Figure 3-B and S-3, we showed that the values acquired are based on the analysis of thousands of nuclei per data point. These results confirm and validate our software-based DDR quantification analysis.

3.3 DDR Activity quantification and correlations with clinico-pathological parameters

We next performed IF and automated image acquisition/analysis on the 300 prostate cancer patients of the TMA-*TFRI*. The final data acquired represented segmented MFI values of DDR markers p-H2AX, 53BP1, p65 and p-CHK2 for every patient's core as described in section 2.4. We performed a quality control of the data by a visual inspection. As described in section 2.2, each patient had a duplicate of its normal and tumoral cores. MFI of each set of duplicate were plotted as shown in figure 4-A. Cores that showed 2 fold differences in their MFI with its duplicate core from the same tissue section (for any DDR marker under analysis) was visually inspected by two independent collaborators in order to exclude from analysis the cores with an obvious explanation (ex: tear or spot in a core). Few cores were rejected because of discrepancies in the results (Figure 4-B). Although all R^2 were statistically significant ($p < 0.05$), they had relatively low values (0.03-0.16). These poor R^2 values can be explained by the true biological variability even between cores coming from different nearby areas from the same tissues. Indeed, even though duplicates were taken from the same patient, they are not taken from the exact same region of the tumoral or

normal tissue. After the quality control, the remaining samples were used to assess the correlation between the DDR activity and patient clinical parameters. To assess the predictive potential of each DDR activity antibody and variables, we performed Kaplan-Meier estimation based on biochemical recurrence (BCR: defined as a relapse of disease based on a PSA value $>0.3\text{ng/mL}$ following surgery) and bone metastasis as shown in figure 5. We used either the receiver operative characteristic (ROC) curves or the median calculation value of the MFI obtained by image analysis to determine the threshold value for each DDR marker.

We observed a statistically significant association between 53BP1 protein expression and bone metastasis development. Indeed, Figure 5 (E and F) shows that a weak 53BP1 signal in the stroma or epithelium of tumors is associated with better prognosis in respect to bone metastasis development ($p=0.005$). Furthermore, we found that a lower RELA in the nuclear epithelium of normal core was associated with higher biochemical recurrence free ($p=0.002$) (Figure 5C). The MFI of p-CHK2 or p-H2AX in the epithelium or stromal did not significantly predict BCR or metastasis free survival. Univariate and multivariate Cox regression analyses confirmed the association between the MFI of 53BP1 and bone metastasis free survival and included other clinico-pathological parameters such as gleason score (GS), extracapsular extension (ECE), seminal vesicle invasion (SVI) and status of surgical margins, which internally validated the analysis (Table 2). As for RELA, we found an association, in a

multivariate model including the same clinico-pathological parameters, where RELA was retained as a variable able to predict BCR.

Pearson correlations were also done between all validated DDR markers and clinico-pathological parameters such as the age of diagnosis, PSA, GS, lymph node invasion (LNI), SVI, ECE, status of surgical margins, castrate resistant prostate cancer status (CRPC) and pathological staging (pTNM) as shown in Table 3. Once again, we observed a statistically significant correlation between 53BP1 signal and development of bone metastasis as well as with SVI, CRPC and pTNM.

Using a paired T-test, we evaluated the differences in DDR markers expression within the adjacent normal and tumor cells. Our results indicated significant differences for p-CHK2, RELA, 53BP1 and p-H2AX expression within the epithelium compartment. In the stroma, RELA and pH2AX showed significant differences between the adjacent normal and tumor cells (Table 4). We also found that p-CHK2 showed increased intensity in the epithelium of the normal cores while RELA was more activated in both the epithelium and stroma of the normal cores. Alternatively, 53BP1 showed a higher signal in the epithelium of the tumoral cores. As for p-H2AX, it was more activated in the normal cores (epithelium and stroma) when compared to the tumoral cores. Overall, except for 53BP1, our results reveal that DDR activity appears higher in normal tissues surrounding the prostate cancer tissue suggesting that detected DDR activity is generally reduced in advanced prostate cancer.

4.0 Discussion

Nuclear structures termed “DNA damage foci” are hallmarks of DDR activation^{8; 22}. For example, 53BP1 is a nuclear protein that relocalizes to DNA damage foci, while H2AX is a histone that becomes phosphorylated at sites of DNA damage (named p-H2AX when phosphorylated). To preserve genome integrity, cells need to protect themselves against DSBs, which are the most lethal type of DNA damage. Once cells detect DNA breaks, the DDR is initiated which is essential to stop the proliferation of cells with genomic instability, and therefore, prevent cancer progression. DDR will lead to temporary cell cycle arrest and DNA repair, apoptosis, or senescence preventing cells with accumulated mutations to replicate and progress into cancer. Importantly, this cellular response determines how normal and cancer cells react to DNA damaging agents used for cancer therapy (radiation therapy and chemotherapy). The DDR, a central tumor suppression mechanism in mammals acts as a barrier against cancer progression. There is available data indicating that the DDR machinery is commonly activated in major types of human melanocytic nevi and precursor dysplastic and adenomatous lesions in the lung, breast, colon, urinary bladder and prostate^{4; 23; 24; 25; 26; 27}. It has been suggested that abnormal cell cycle progression via over-expression of cyclin E, Cdc25A, and E2F1 produces “DNA replication stress” that leads to activation of the DNA damage response, including ATM activation and phosphorylation of its downstream targets, p53 Ser15 (p53pSer15), H2AX, and Chk2^{23; 24}.

To refine our understanding of DDR signalling during cancer progression, we characterized this DDR activity in human prostate tissue and correlated it with clinical outcomes. In the present study, we selected prostate cancer, as it was particularly promising since preliminary data described DDR activation during prostate cancer progression ⁴ with higher DDR seen in PIN as compared to normal prostate or adenocarcinomas. However, little is known on DDR activity level from the PIN state to adenocarcinoma. Whether these levels of DDR activity will remain the same, increase or yet decrease is not much known. We found that prostate cancer cells show a decreased level of DDR as compared to normal cells in our cohort of 300 prostate cancer patients. As it has already been shown, ATM is activated in earlier stages of prostate tumorigenesis (PINs) leading to an increased level of DDR. We believe that after genetic instability, adenocarcinoma develops. The growth of tumor cells have survived the pressure of the immune system and prostatic cells have probably only stabilized their genome when becoming more aggressive, adenocarcinoma cells. These findings could be used in a clinical setting by helping patients to make a decision regarding their treatment (ie: surgery or radiotherapy).

In normal cells, an increasing level of DDR may indicate a defect in DNA repair and therefore an increased sensitivity to radiation. Indeed, cells that fail to repair will have even more difficulty to repair themselves following the DNA damage. One could also assume that a decrease in DDR activity would translate to more radio-resistance since cells would have accumulated more changes due to genetic instability and thus

accumulation of more mutations leading to more resistant to treatment. As for cancer cells, if a defect in the damage recognition exists within the cell, those cancer cells will ignore the damage and consequently would be more radio-sensitive as they would be less able to repair themselves.

One of the two distinct pathways that have evolved to eliminate DSBs is homologous recombination (HR), which requires the cells to be in the S or G2 phase of the cell cycle, when DNA replication generates the sister chromatid to direct the repair process. HR has a role to preserve the genome's integrity as well as a role in faithfully duplicating the genome by providing critical support for DNA replication and telomere maintenance. 53BP1 plays a major role in HR: it is a central component of chromatin-based DSB signalling. Important structural elements in 53BP1 include the breast cancer 1 (BRCA1) carboxy-terminal (BRCT) repeats, the tandem Tudor domains and 28 amino-terminal Ser/Thr-Gln (S/T-Q) sites, which are phosphorylated, at least in part, by ATM kinase²⁸. Loss of 53BP1 or its failure to localize to damaged chromatin significantly reduces the phosphorylation of ATM targets such as p53, CHK2 and BRCA1 and, as a consequence, leads to G2–M checkpoint defects and genomic instability. Upon entry into S phase, BRCA1 helps to switch the mode of DSB repair by excluding 53BP1–RIF1 complexes from the DSB, thus enabling extensive DSB resection and the initiation of HR²⁹. It has been demonstrated that when 53BP1 is defective, formation of the mammary tumors that normally develop in *BRCA1* mutant mice is suppressed³⁰. Mouse *BRCA1*-associated mammary tumors have significant

similarities to human *BRCA1*-associated breast cancer in regard to tumor aggressiveness, high incidence, mutations, and genetic instability. The same group has also found that inactivation of 53BP1 restored the DNA repair function that is lost when *BRCA1* is mutated. Using a strain of mice with a defective *BRCA1* gene, the team observed that the mice frequently developed mammary tumors similar to human breast cancers, but tumor formation was largely suppressed when the mice also were lacking the functional protein 53BP1. Furthermore, both *BRCA1* and 53BP1 are capable of binding to replication-associated chromosome breaks; so when both proteins are present, *BRCA1* displaces 53BP1, the HR machinery has full access to the breaks, and HR proceeds. In *BRCA1*-deficient cells, the binding of 53BP1 to the site of DNA damage interferes with the DNA repair activity of HR proteins, so an alternative pathway that is more prone to produce mutations repairs the damage. When 53BP1 is absent, *BRCA1* is not needed to displace it so HR can take place normally. Our findings showed that less 53BP1 is associated with a better prognosis. We could eventually also evaluate the presence or absence of BRCA in our cohort of patients to further explain these findings. Treatment options for localized prostate cancer in 2014 are mainly radiation therapy or surgery. Both have shown similar survival outcomes in low and intermediate risk prostate cancer patients. Contemporary radiotherapy approaches such as intensity-modulated radiation therapy (IMRT) have permitted increased delivery of radiation to the prostate while sparing adjacent organs and reducing the potential for acute and chronic toxicity. However, proctitis, cystitis, and

erectile dysfunction remain significant complications of high-dose radiotherapy. In turn, local failure after radiotherapy remains 20%–35% in intermediate and high-risk patients, leading to increased metastasis and lower survival. Hormonal therapy has a proven value when combined with localized radiotherapy in intermediate and high risk prostate cancer patients, but carries its own set of morbidities, including increased cardiovascular and thromboembolic risk. Novel agents with more attractive side effect profiles that can be combined with radiotherapy to improve local control in high-risk patients and/or permit a dose reduction in lower-risk patients would be of great value. A developing strategy to improve efficacy at lower ionizing radiation doses is the use of radiosensitizers to target recognition and repair of DNA damage ³¹. Poly ADP ribose polymerase (PARPs) are a family of enzymes that are activated by DNA damage and participate in repair of single-strand breaks by activating XRCC1 and base-excision repair, and DSB likely through influence on both the HR and NHEJ mechanisms. After a DSB, PARP are rapidly recruited and trigger poly-ADP ribosylation of PARP itself, histones, and other mediator proteins to stimulate chromatin loosening and DNA repair. It has been observed that PARP is activated by RT and chemotherapy agents, and this has provided the rationale to examine the combined effects of PARP inhibitors and genotoxic therapy in tumor models and in clinical trials ^{32; 33; 34}. A number of other mutations that decrease HR repair responses can also sensitize cells to PARP inhibitors, including defects in the inositide phosphatase PTEN, a gene commonly inactivated in prostate cancer ³⁵. Cells deficient

in DNA DSB repair have been shown to be sensitized by PARP inhibitors to DNA damaging agents³⁶. Because the DDR controls cellular responses that are absolutely essential for radiotherapy treatment outcomes, biochemical components of this signalling cascade become potential pharmaceutical targets for treatment optimization. Cancer cells, including prostate cancer cells, acquire an intrinsic capacity to tolerate DNA damage during cancer progression. This can happen through the loss of redundant DDR signalling pathways such as the p53 pathway, allowing HG-PIN to evolve into invasive carcinoma in mouse models. Because the DDR and DNA repair are absolutely essential for cell survival, cancer cells must maintain other redundant DDR pathways functional. It is thus proposed that inactivation of these remaining DDR pathways could greatly sensitize cancer cells to DNA damage^{16; 17}. Alternatively, gaining information about the initial “DDR state” of the tumor could help in predicting whether a particular cancer will respond better to DNA damaging agents during treatment. Finding new biomarkers predicting what kind of DDR individual cells/tumors mount against radiotherapy has the potential to improve treatment selection and successes. Currently, the exact regulation and outcomes of DDR signalling in cancer cells remain relatively unknown. Furthermore, because tumor cells that are *BRCAl*-deficient are driven to turn to other, less faithful DNA repair pathways and they may become resistant to chemotherapy/RT by acquiring additional mutations. Our cohort of 288 evaluated patients consisted mostly of low risk patients with only 29 patients with Gleason > 7 and 79 patients with PSA > 10 ng/mL which could explain

the low number of bone metastases (19/288) and the average follow up of 101.5 months might also explain this low number of events. Although, we did find a statistical significant relation of 53BP1 and bone metastasis free survival as well as p53 and BCR, we believe more results pertaining to biochemical control, bone metastases as well as prostate cancer survival will be obtained with longer follow-up of our cohort.

5.0 Conclusion

DDR is a complex signalling network and its failure causes genomic instability, an underlying cause of cancer. Today, the tumor's biology in individual prostate cancer patient is still not taken into consideration for clinical management of the disease. In an era of evolving personalized medicine, we confirmed that RELA (p65) and showed that DDR marker 53BP1 have prognostic value in patients with prostate adenocarcinoma. Patients expressing reduced amounts of 53BP1 have a better bone metastasis free survival ($p=0.005$) and those with reduced amounts of RELA have a better biochemical control ($p=0.002$). These findings were also correlated in univariate and multivariate cox regression analysis. Even though our follow up is quite long (101.5 months), a longer follow-up is probably needed to translate into a correlation with survival since prostate cancer patients have very good prognosis and develop metastasis leading to death many years after the initial curative treatment. Future work should focus on designing the ways to better predict responses of individual patients to DNA damaging therapies including radiation and various chemotherapeutics that are used in first line of treatment. These predictions could be based on the genetic and functional profiling of patient specific tumors. This may facilitate selection of a proper modality or combination of treatment options on an individualized basis and also optimize the dosage of such therapies according to the state of the DNA damage checkpoint and repair machineries of each individual patient.

References

1. Siegel, R., Naishadham, D. & Jemal, A. (2013). Cancer statistics, 2013. *CA Cancer J Clin* **63**, 11-30.
2. Van der Kwast, T. H. & Roobol, M. J. (2013). Defining the threshold for significant versus insignificant prostate cancer. *Nat Rev Urol* **10**, 473-82.
3. Coppe, J. P., Patil, C. K., Rodier, F., Sun, Y., Munoz, D. P., Goldstein, J., Nelson, P. S., Desprez, P. Y. & Campisi, J. (2008). Senescence-associated secretory phenotypes reveal cell-nonautonomous functions of oncogenic RAS and the p53 tumor suppressor. *PLoS Biol* **6**, 2853-68.
4. Fan, C., Quan, R., Feng, X., Gillis, A., He, L., Matsumoto, E. D., Salama, S., Cutz, J. C., Kapoor, A. & Tang, D. (2006). ATM activation is accompanied with earlier stages of prostate tumorigenesis. *Biochim Biophys Acta* **1763**, 1090-7.
5. Jackson, S. P. & Bartek, J. (2009). The DNA-damage response in human biology and disease. *Nature* **461**, 1071-8.
6. Perkins, N. D. (2012). The diverse and complex roles of NF-kappaB subunits in cancer. *Nat Rev Cancer* **12**, 121-32.
7. Gilmore, T. D. (2006). Introduction to NF-kappaB: players, pathways, perspectives. *Oncogene* **25**, 6680-4.
8. Rodier, F., Coppe, J. P., Patil, C. K., Hoeijmakers, W. A., Munoz, D. P., Raza, S. R., Freund, A., Campeau, E., Davalos, A. R. & Campisi, J. (2009). Persistent DNA damage signalling triggers senescence-associated inflammatory cytokine secretion. *Nat Cell Biol* **11**, 973-9.
9. Rodier, F. & Campisi, J. (2011). Four faces of cellular senescence. *J Cell Biol* **192**, 547-56.
10. Zhang, X. P., Liu, F., Cheng, Z. & Wang, W. (2009). Cell fate decision mediated by p53 pulses. *Proc Natl Acad Sci U S A* **106**, 12245-50.
11. Chen, Z., Trotman, L. C., Shaffer, D., Lin, H. K., Dotan, Z. A., Niki, M., Koutcher, J. A., Scher, H. I., Ludwig, T., Gerald, W., Cordon-Cardo, C. & Pandolfi, P. P. (2005).

- Crucial role of p53-dependent cellular senescence in suppression of Pten-deficient tumorigenesis. *Nature* **436**, 725-30.
12. Salmena, L., Carracedo, A. & Pandolfi, P. P. (2008). Tenets of PTEN tumor suppression. *Cell* **133**, 403-14.
 13. Meyn, R. E. (2009). Linking PTEN with genomic instability and DNA repair. *Cell Cycle* **8**, 2322-3.
 14. Meeker, A. K., Hicks, J. L., Platz, E. A., March, G. E., Bennett, C. J., Delannoy, M. J. & De Marzo, A. M. (2002). Telomere shortening is an early somatic DNA alteration in human prostate tumorigenesis. *Cancer Res* **62**, 6405-9.
 15. Di Leonardo, A., Linke, S. P., Clarkin, K. & Wahl, G. M. (1994). DNA damage triggers a prolonged p53-dependent G1 arrest and long-term induction of Cip1 in normal human fibroblasts. *Genes Dev* **8**, 2540-51.
 16. Ding, J., Miao, Z. H., Meng, L. H. & Geng, M. Y. (2006). Emerging cancer therapeutic opportunities target DNA-repair systems. *Trends Pharmacol Sci* **27**, 338-44.
 17. Zhang, J. & Powell, S. N. (2005). The role of the BRCA1 tumor suppressor in DNA double-strand break repair. *Mol Cancer Res* **3**, 531-9.
 18. Jackson, S. P. (2009). The DNA-damage response: new molecular insights and new approaches to cancer therapy. *Biochem Soc Trans* **37**, 483-94.
 19. Lessard, L., Mes-Masson, A. M., Lamarre, L., Wall, L., Lattouf, J. B. & Saad, F. (2003). NF-kappa B nuclear localization and its prognostic significance in prostate cancer. *BJU Int* **91**, 417-20.
 20. Lessard, L., Karakiewicz, P. I., Bellon-Gagnon, P., Alam-Fahmy, M., Ismail, H. A., Mes-Masson, A. M. & Saad, F. (2006). Nuclear localization of nuclear factor-kappaB p65 in primary prostate tumors is highly predictive of pelvic lymph node metastases. *Clin Cancer Res* **12**, 5741-5.
 21. Fradet, V., Lessard, L., Begin, L. R., Karakiewicz, P., Masson, A. M. & Saad, F. (2004). Nuclear factor-kappaB nuclear localization is predictive of biochemical recurrence in patients with positive margin prostate cancer. *Clin Cancer Res* **10**, 8460-4.

22. Rodier, F., Munoz, D. P., Teachenor, R., Chu, V., Le, O., Bhaumik, D., Coppe, J. P., Campeau, E., Beausejour, C. M., Kim, S. H., Davalos, A. R. & Campisi, J. (2011). DNA-SCARS: distinct nuclear structures that sustain damage-induced senescence growth arrest and inflammatory cytokine secretion. *J Cell Sci* **124**, 68-81.
23. Gorgoulis, V. G., Vassiliou, L. V., Karakaidos, P., Zacharatos, P., Kotsinas, A., Liloglou, T., Venere, M., Dittullo, R. A., Jr., Kastrinakis, N. G., Levy, B., Kletsas, D., Yoneta, A., Herlyn, M., Kittas, C. & Halazonetis, T. D. (2005). Activation of the DNA damage checkpoint and genomic instability in human precancerous lesions. *Nature* **434**, 907-13.
24. Bartkova, J., Horejsi, Z., Koed, K., Kramer, A., Tort, F., Zieger, K., Guldborg, P., Sehested, M., Nesland, J. M., Lukas, C., Orntoft, T., Lukas, J. & Bartek, J. (2005). DNA damage response as a candidate anti-cancer barrier in early human tumorigenesis. *Nature* **434**, 864-70.
25. Tort, F., Bartkova, J., Sehested, M., Orntoft, T., Lukas, J. & Bartek, J. (2006). Retinoblastoma pathway defects show differential ability to activate the constitutive DNA damage response in human tumorigenesis. *Cancer Res* **66**, 10258-63.
26. Nuciforo, P. G., Luise, C., Capra, M., Pelosi, G. & d'Adda di Fagagna, F. (2007). Complex engagement of DNA damage response pathways in human cancer and in lung tumor progression. *Carcinogenesis* **28**, 2082-8.
27. Bartkova, J., Rajpert-De Meyts, E., Skakkebaek, N. E., Lukas, J. & Bartek, J. (2007). DNA damage response in human testes and testicular germ cell tumours: biology and implications for therapy. *Int J Androl* **30**, 282-91; discussion 291.
28. Adams, M. M. & Carpenter, P. B. (2006). Tying the loose ends together in DNA double strand break repair with 53BP1. *Cell Div* **1**, 19.
29. Panier, S. & Boulton, S. J. (2014). Double-strand break repair: 53BP1 comes into focus. *Nat Rev Mol Cell Biol* **15**, 7-18.
30. Bunting, S. F., Callen, E., Wong, N., Chen, H. T., Polato, F., Gunn, A., Bothmer, A., Feldhahn, N., Fernandez-Capetillo, O., Cao, L., Xu, X., Deng, C. X., Finkel, T., Nussenzweig, M., Stark, J. M. & Nussenzweig, A. (2010). 53BP1 inhibits

homologous recombination in Brca1-deficient cells by blocking resection of DNA breaks. *Cell* **141**, 243-54.

31. Ljungman, M. (2009). Targeting the DNA damage response in cancer. *Chem Rev* **109**, 2929-50.
32. Donawho, C. K., Luo, Y., Luo, Y., Penning, T. D., Bauch, J. L., Bouska, J. J., Bontcheva-Diaz, V. D., Cox, B. F., DeWeese, T. L., Dillehay, L. E., Ferguson, D. C., Ghoreishi-Haack, N. S., Grimm, D. R., Guan, R., Han, E. K., Holley-Shanks, R. R., Hristov, B., Idler, K. B., Jarvis, K., Johnson, E. F., Kleinberg, L. R., Klinghofer, V., Lasko, L. M., Liu, X., Marsh, K. C., McGonigal, T. P., Meulbroek, J. A., Olson, A. M., Palma, J. P., Rodriguez, L. E., Shi, Y., Stavropoulos, J. A., Tsurutani, A. C., Zhu, G. D., Rosenberg, S. H., Giranda, V. L. & Frost, D. J. (2007). ABT-888, an orally active poly(ADP-ribose) polymerase inhibitor that potentiates DNA-damaging agents in preclinical tumor models. *Clin Cancer Res* **13**, 2728-37.
33. Plummer, R., Jones, C., Middleton, M., Wilson, R., Evans, J., Olsen, A., Curtin, N., Boddy, A., McHugh, P., Newell, D., Harris, A., Johnson, P., Steinfeldt, H., Dewji, R., Wang, D., Robson, L. & Calvert, H. (2008). Phase I study of the poly(ADP-ribose) polymerase inhibitor, AG014699, in combination with temozolomide in patients with advanced solid tumors. *Clin Cancer Res* **14**, 7917-23.
34. Powell, C., Mikropoulos, C., Kaye, S. B., Nutting, C. M., Bhide, S. A., Newbold, K. & Harrington, K. J. (2010). Pre-clinical and clinical evaluation of PARP inhibitors as tumour-specific radiosensitisers. *Cancer Treat Rev* **36**, 566-75.
35. Mendes-Pereira, A. M., Martin, S. A., Brough, R., McCarthy, A., Taylor, J. R., Kim, J. S., Waldman, T., Lord, C. J. & Ashworth, A. (2009). Synthetic lethal targeting of PTEN mutant cells with PARP inhibitors. *EMBO Mol Med* **1**, 315-22.
36. Loser, D. A., Shibata, A., Shibata, A. K., Woodbine, L. J., Jeggo, P. A. & Chalmers, A. J. (2010). Sensitization to radiation and alkylating agents by inhibitors of poly(ADP-ribose) polymerase is enhanced in cells deficient in DNA double-strand break repair. *Mol Cancer Ther* **9**, 1775-87.

Figure Legends

Figure 1: Detection of DDR activity and DDR foci in paraffin embedded cells using multicolor immunofluorescence

Normal human fibroblasts were left untreated or irradiated with 10 Gy X-Ray and left to recover for the indicated time periods. Cells were then fixed and embedded in paraffin to mimic tissue sections. Cores were extracted from the paraffin blocks and arrayed on a control TMA tissue micro array (TMA-cell). The TMA-cell was processed for immunofluorescence and stained. The TMA was stained for p-H2AX (green) and 53BP1 (red) and the nuclei counterstained with DAPI (blue).

Top panel: color merge; Middle panels: grayscale representation of extracted p-H2AX or 53BP1 signals (originally green and red, respectively). The bottom panel shows magnified color merge (zoomed) inset boxes that are apparent in the corresponding top panels.

Notice that the DNA damage foci detected in paraffin-embedded irradiated cells appears in yellow (arrow pointing at yellow DNA damage foci) because p-H2AX (green) and 53BP1 (red) are co-localized at damage sites in the cell). Not all foci are highlighted. 53BP1 co-localization with p-H2AX is a definitive biomarker of DSB-initiated DDR signalling.

Figure 2: Multicolor immunofluorescence and mask segmentation analysis in prostate cancer TMA core

- A-** Immunofluorescence image of one selected TMA core from prostate cancer tissue at 20-X magnification. This image is a 4-color merge, superposing the following: Epithelial mask (Ep; orange - A546 (CK18 and CK19) and Cy3 (PSA)), 53BP1 (red; CY5), p-H2AX (green; FIT-C) and nuclein (blue; DAPI)
- B-** Extraction of individual color channels from image above in color and gray scale to enhance contrast.
- C-** False color image generated following the analysis of the core in a-b using the VisioMorph and TissueMorph software. The software is used to detect and define the position of masks based on selected immunofluorescence signals. The total core is detected (purple) and superposed with the epithelial mask (light blue) and the nuclear mask (pink in the epithelial mask and cyan in the stromal area). in individual TMA cores.

Figure 3: Software-based quantification of immunofluorescence-detected DDR activity in paraffin embedded cells

Total cores from control and irradiated (10 Gy X-ray) paraffin-embedded fibroblast in TMA-cell were analyzed using automated detection of immunofluorescence signal intensity in the cell nucleus (DAPI nuclear mask). Quantifications were performed for p-H2AX, 53BP1, p21 and p-CBK2.

A- Quantified expression data for the different DDR markers is illustrated as the percentage of mean fluorescence intensity (MFI) relative to the non-irradiated control at 0 hours (Y-axis). The X-axis represents the time in hours after irradiation with 10 Gy X-Ray.

B- Immunofluorescence images used for the quantification above. The images are generated by the extraction of the individual color channels and conversion to gray scale to enhance contrast. N = Number of nucleus analyzed in the quantified signal.

Figure 4: Quality Control of DDR data on duplicate samples for prostate cancer TMA

A- The mean fluorescence intensity (MFI) of 53BP1 in total nuclear-epithelial sub-compartments defined by the epithelial and nuclear masks for each individual normal and tumoral cores was detected and quantified by the Visiomorph software. The detection is performed on each core (core1) and on the independent duplicate core (core2) associated with the same clinical sample. Reproducibility of the

stainings within the same tissue is assessed by plotting values of MFI obtained by Visiormorph for core 1 on the X axis and the value of core 2 on the Y axis.

B- Results for the quality-control analysis. Two-fold outliers values on plot presented in A were identified and cores were visually inspected and disregarded from the final analysis if they presented obvious aberrations (the results of this quality control analysis are presented for 53BP1, p-H2AX, RELA and p-CHK2). The tables summarizes the number of core used and rejected (rejected cores vary from 0.2 to 1.6% of the total).

Figure 5: Kaplan–Meier PSA recurrence-free survival and bone metastasis free curves in patients with prostate cancer for specific DDR signals

Kaplan-Meier curves were plotted for all antibodies (not all data shown) for biochemical recurrence and bone metastasis.

A- Nuclear-Epithelial pCHK2 in normal tissues.

B- Nuclear-Stromal pCHK2 in normal tissues

C- Nuclear-Epithelial p65 in normal tissues

D- Nuclear-Epithelial pCHK2 in tumoral tissues

E- Nuclear-Epithelial 53BP1 in tumoral tissues

F- Nuclear-Stromal 53BP1 in tumoral tissues

p = Significance value as indicated on bottom right corner of each graph.

N = number of patients

Figure S1

A- Schematic representation of the TMA-cell approach for irradiated cells:

- 1) Normal fibroblasts cells (BJ-u) were left untreated or irradiated with 10 Gy X-Ray and let recover for the indicated time periods.
- 2) Cells were then trypsinized to obtain formalin-fixed cell pellets in histogel.
- 3) Fixed histogel cell pellets were later embedded paraffin blocks and
- 3-4) Cylindrical cores were extracted from individual paraffin blocks using a hollow needle and deposited into a recipient TMA paraffin block in an arrayed fashion.
- 5) Slides are then sectioned for further immunofluorescence staining.
- 6) The same process can be performed but with human tissue with up to 300 cores on one slide

B- Map of the TMA-cell and representative full-core immunofluorescence images

53BP1-red; p-H2AX-green; nucleus-blue DAPI

C- Software mediated entire core detection and nucleus identification

An entire core (top panel) stained by immunofluorescence as in B is detected by automated software analysis and detected nuclei are highlighted in pink over the blue color (lower panel).

Figure S2: Multicolor immunofluorescence staining in whole prostate cancer TMA

Representative mosaic 20-X scan of an entire TMA representing 100 patients each with a normal core and a tumoral core (For a total of 200 cores, 20X magnification). This slide was stained for immunofluorescence using DAPI (blue nuclei) and CK18/CK19/PSA (orange epithelium) as well as antibodies of interest to detect DDR activity, in this case, p-H2AX (green) and 53BP1 (red).

Figure S3: Software quantification of immunofluorescence-detected DDR activity in paraffin embedded cells (magnified sections from cores in Figure 3)

Nuclear signals are easier to visualize on magnified (zoomed) sections from cores shown in figure 3 in gray scale.

Table Legends

Table 1: Terry Fox Research Institute (TFRI) TMA of prostate cancer patient cohort.

After TMA construction, patients were excluded from analysis based on pre-operative treatments (patients who had received hormonal therapy). Mortality represents the number of prostate cancer specific deaths compared to all deaths. Missing are parameters whose values were not available.

Table 2: Univariate and multivariate cox regression analysis for

A) Biochemical failure and B) Bone metastasis

Prognostic factors predicting PSA relapse and bone metastasis in prostate cancer cohort. Cox regression models and Hazard ratio are indicated. RELA and 53BP1 nuclear MFI signals were used.

Significant ($p < 0.05$) results indicated in bold.

Table 3: Pearson Correlation (2-tailed) between nuclear DDR activity and clinico-pathological parameters.

Prognostic factors predicting PSA relapse and bone metastasis in prostate cancer cohort. Pearson correlations were considered significant at a $p < 0.05$ and is indicated by bold values.

Table 4: Paired Sample T test for DDR markers between adjacent normal and tumor cells.

Paired T-test evaluating expression differences of nuclear DDR markers between adjacent normal and tumor cells (as shown by sets of patients for each individual marker and as well as for the epithelial and stromal compartment).

Figure 1: Detection of DDR activity and DDR foci in paraffin embedded cells using multicolor immunofluorescence

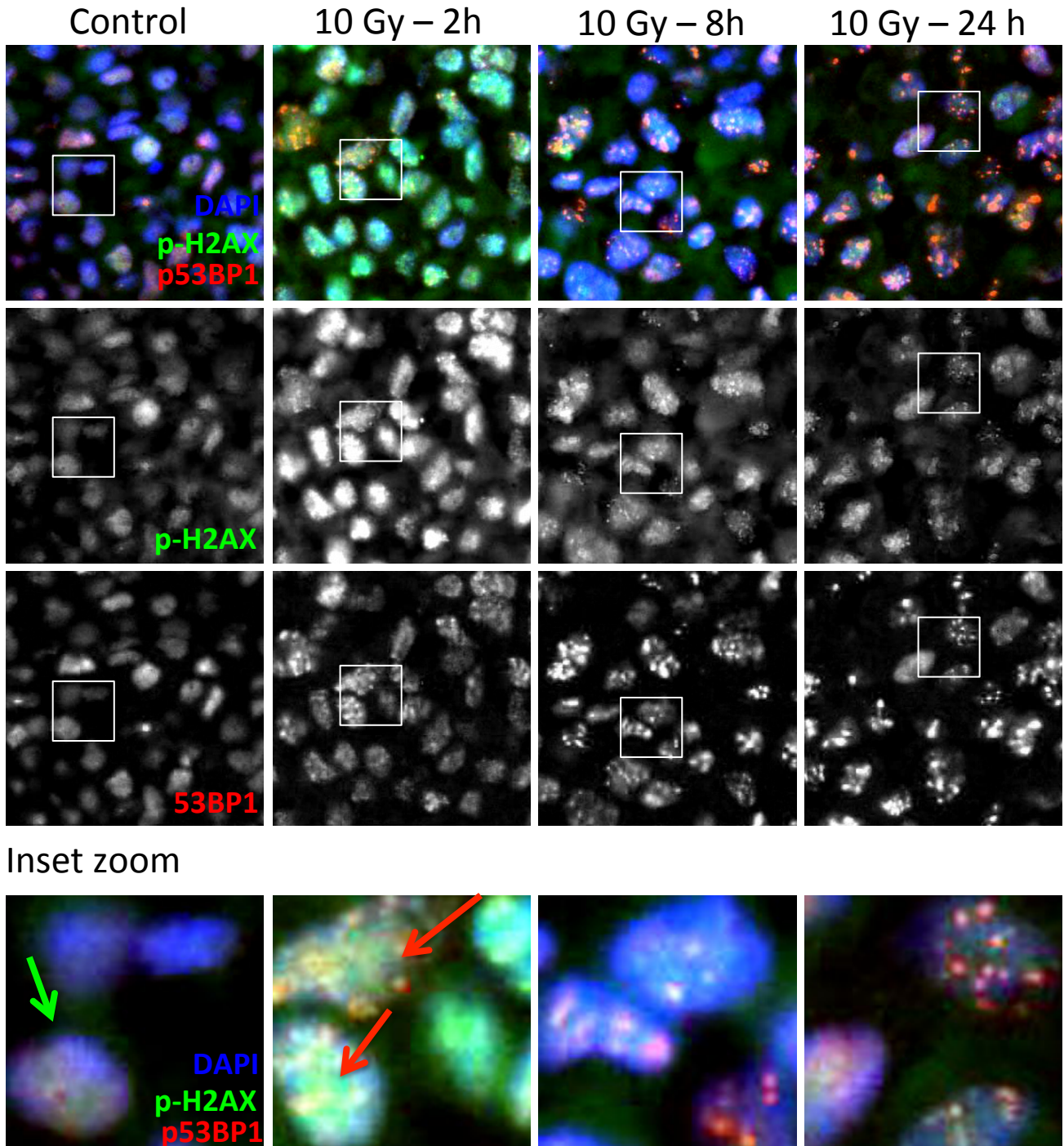
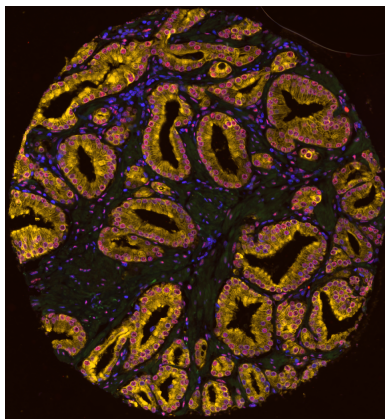


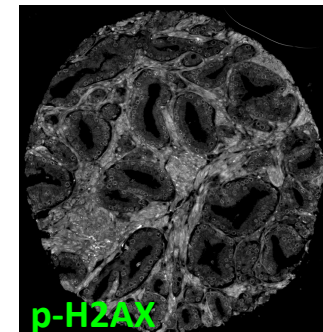
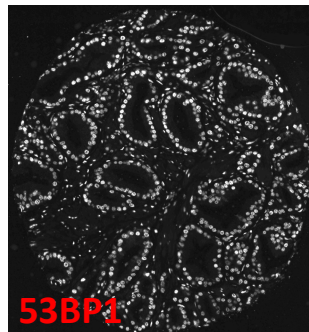
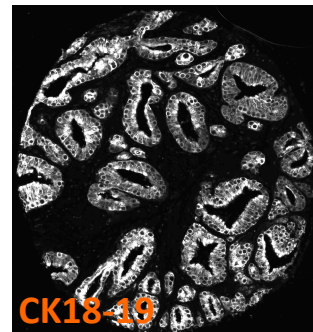
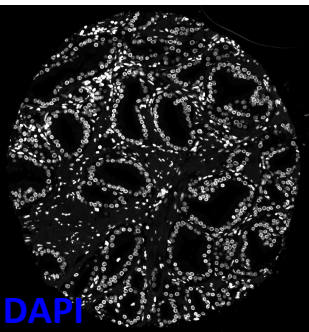
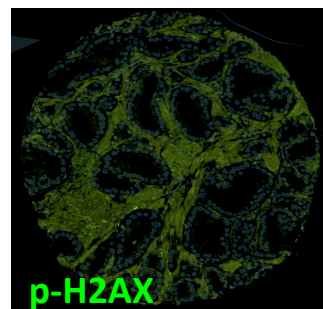
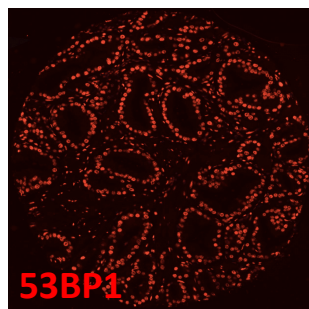
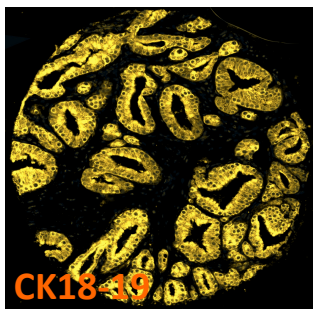
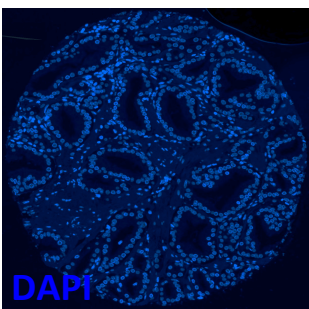
Figure 2: Multicolor immunofluorescence and mask segmentation analysis in PCa TMA core

A

MERGE OF FOUR COLOURS



B



C

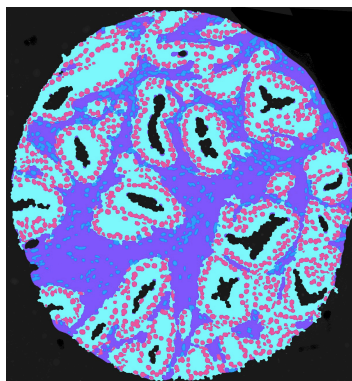


Figure 3: Software-based quantification of immunofluorescence-detected DDR activity in paraffin embedded cells

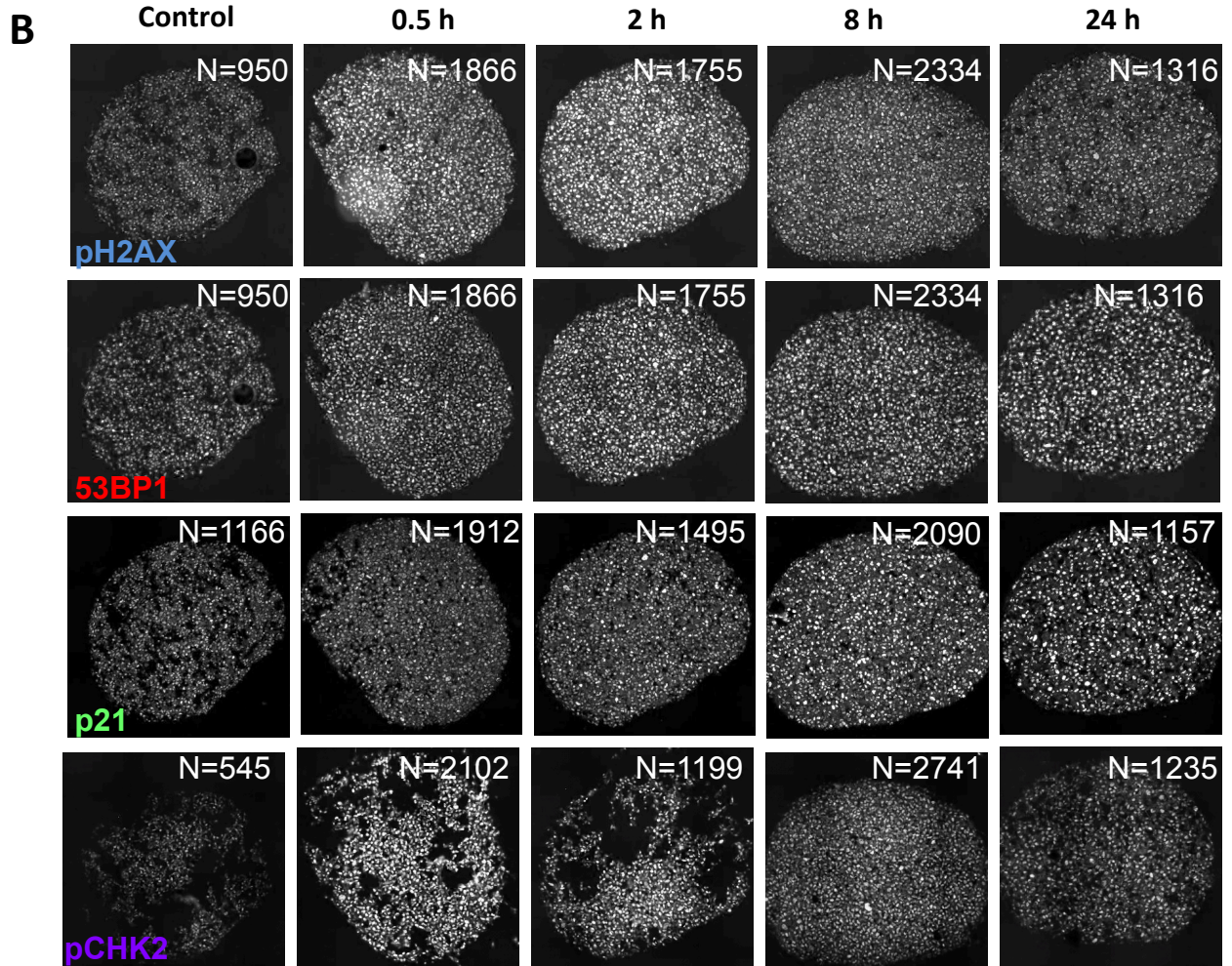
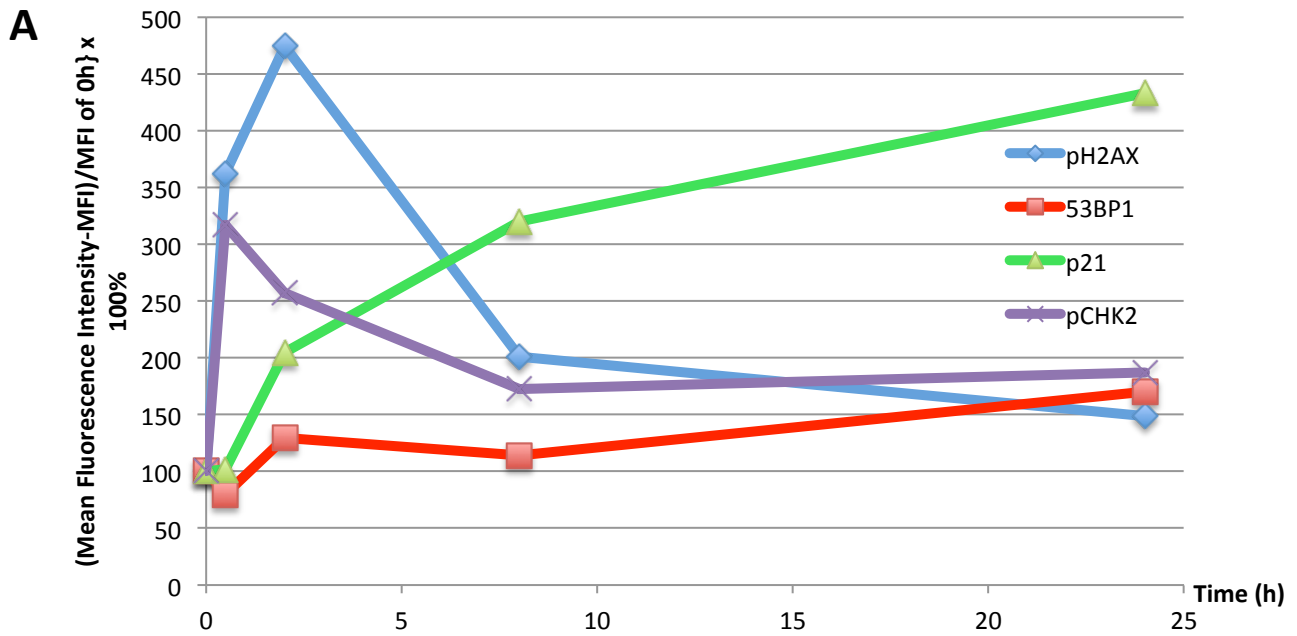
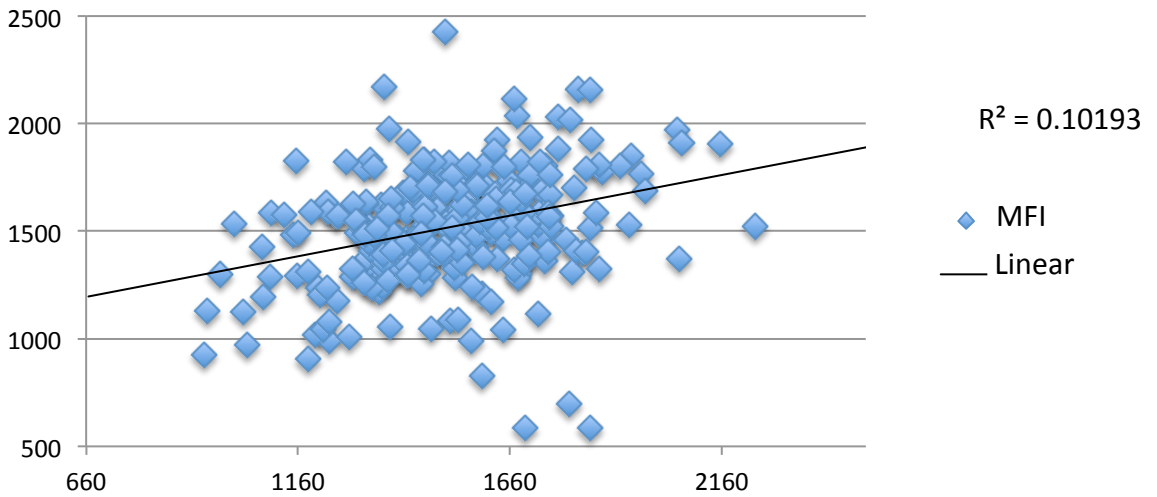
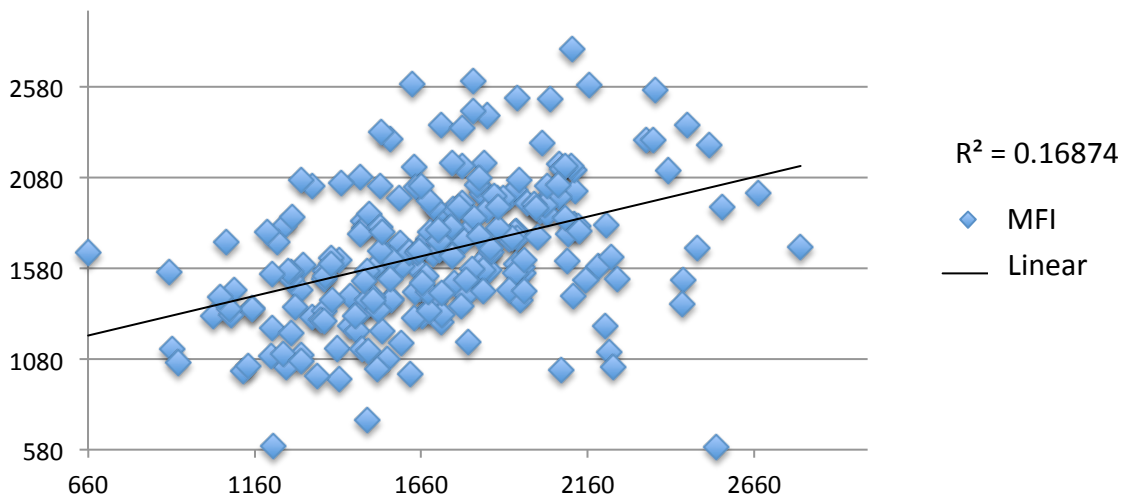


Figure 4: Quality Control of DDR data on duplicate samples for Pca TMA

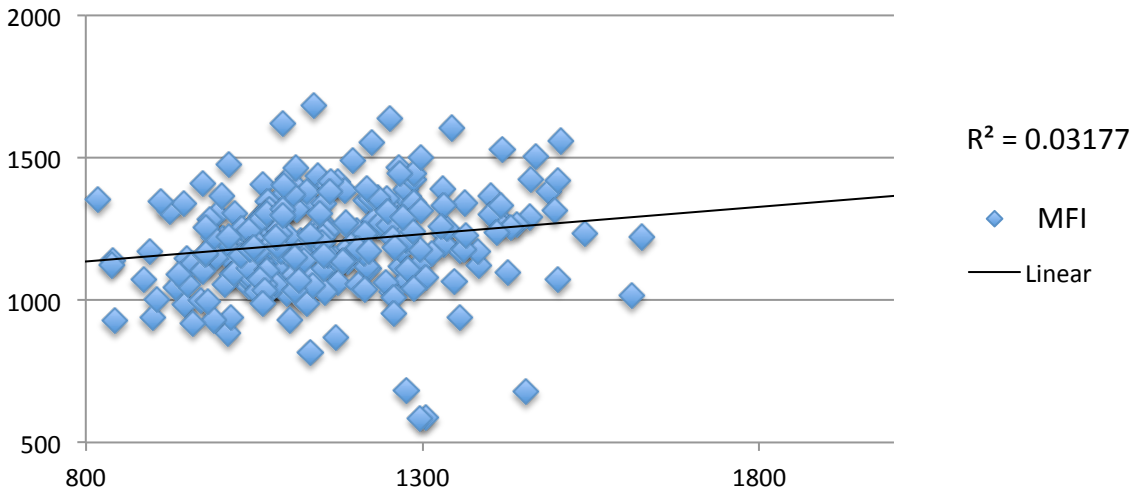
A 1) MFI of 53BP1 in total nuclear-epithelium of normal cores



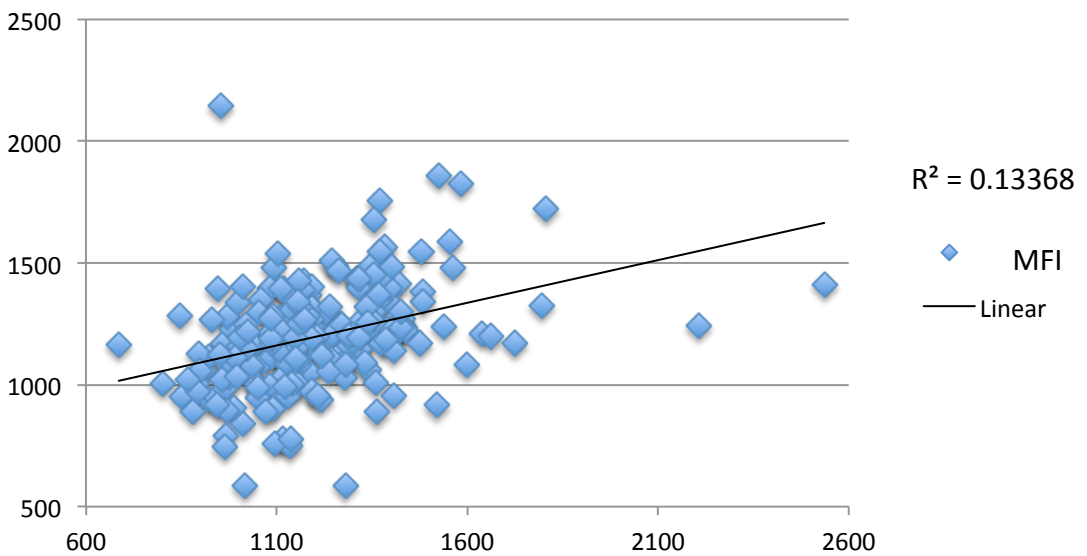
2) MFI of 53BP1 in total nuclear-epithelium of tumoral cores



3) MFI of 53BP1 in total nuclear-stroma of normal cores



4) MFI of 53BP1 in total nuclear-stroma of tumoral cores



B

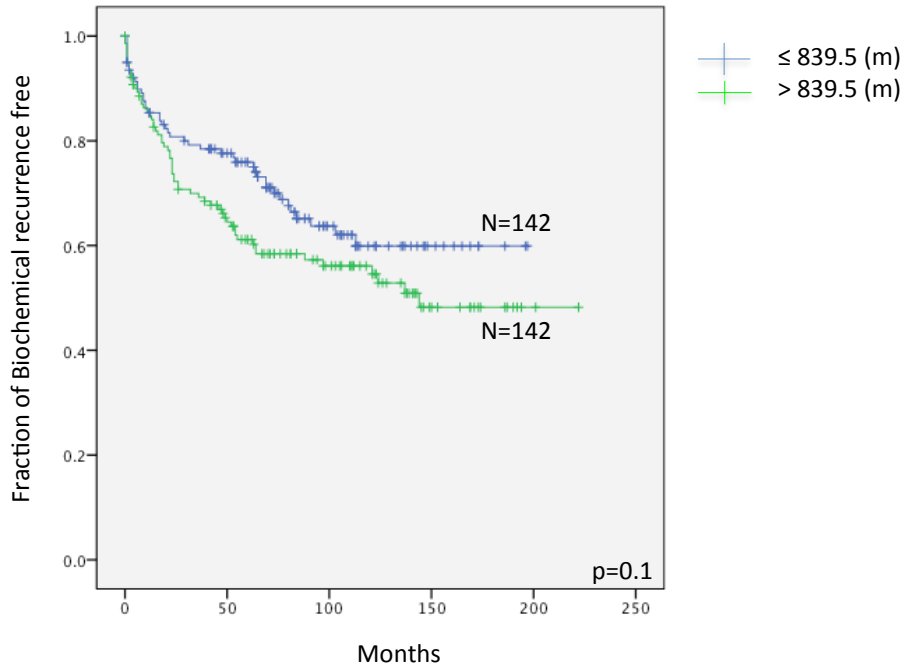
Marker	53BP1 Epithelium	53BP1 Epithelium	53BP1 Stromal	53BP1 Stromal	p-H2AX Epithelium	p-H2AX Epithelium	p-H2AX Stromal	p-H2AX Stromal
<i>Tissue status</i>	<i>Normal</i>	<i>Tumor</i>	<i>Normal</i>	<i>Tumor</i>	<i>Normal</i>	<i>Tumor</i>	<i>Normal</i>	<i>Tumor</i>
#Cores Available	586	513	586	513	586	513	586	513
#Cores Used	578	507	580	507	579	505	581	505
#Core rejected	8	6	6	6	7	8	5	8
Rejection %	1.4	1.2	1.0	1.2	1.2	1.6	0.9	1.6

Marker	p65 Epithelium	p65 Epithelium	p65 Stromal	p65 Stromal	p-CHK2 Epithelium	p-CHK2 Epithelium	p-CHK2 Stromal	p-CHK2 Stromal
<i>Tissue status</i>	<i>Normal</i>	<i>Tumor</i>	<i>Normal</i>	<i>Tumor</i>	<i>Normal</i>	<i>Tumor</i>	<i>Normal</i>	<i>Tumor</i>
#Cores Available	586	513	586	513	586	513	586	513
#Cores Used	584	512	584	512	584	512	584	512
#Core rejected	2	1	2	1	2	1	2	1
Rejection %	0.3	0.2	0.3	0.2	0.3	0.2	0.3	0.2

Figure 5: Kaplan–Meier PSA recurrence-free survival and bone metastasis free curves in patients with PCa for specific DDR signals.

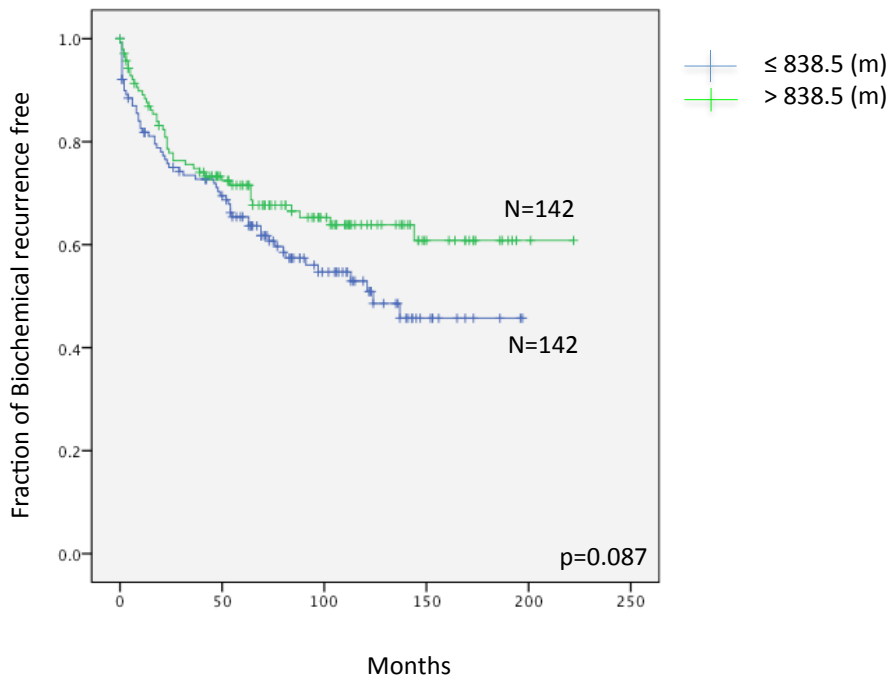
A

Correlation of Nuclear-epithelial pCHK2 in normal tissues



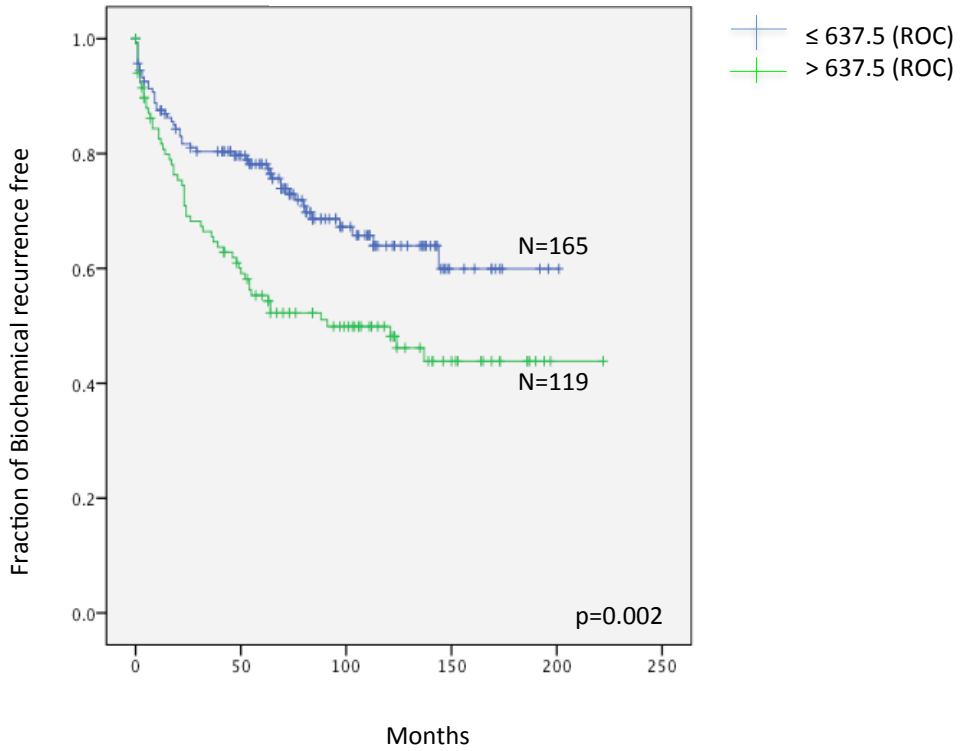
B

Correlation of Nuclear-stromal pCHK2 in normal tissues

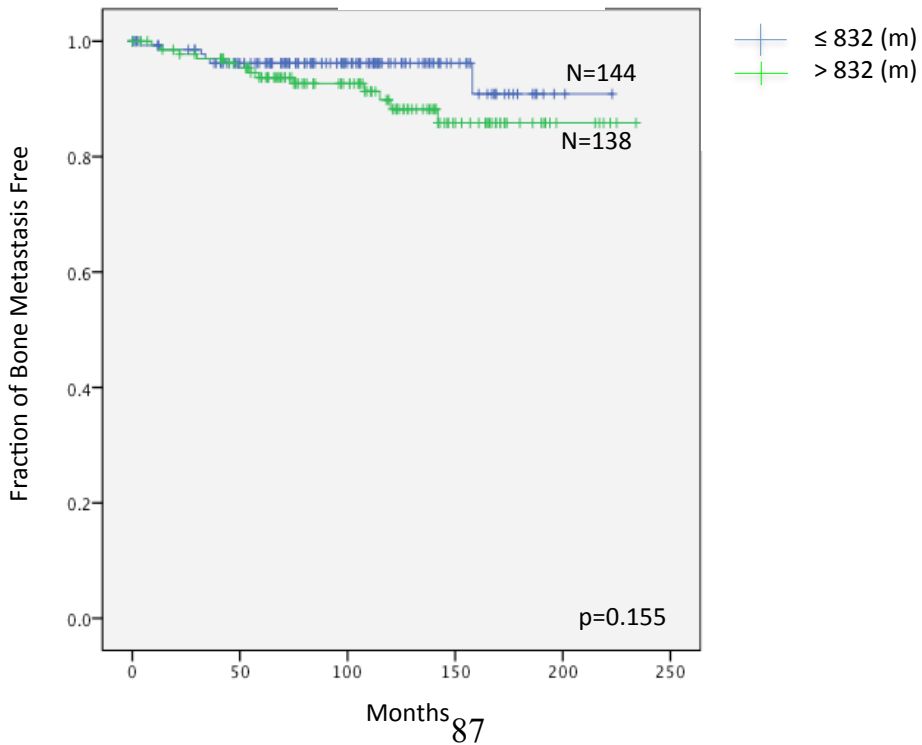


C

Correlation of Nuclear-epithelial p65 in normal tissues

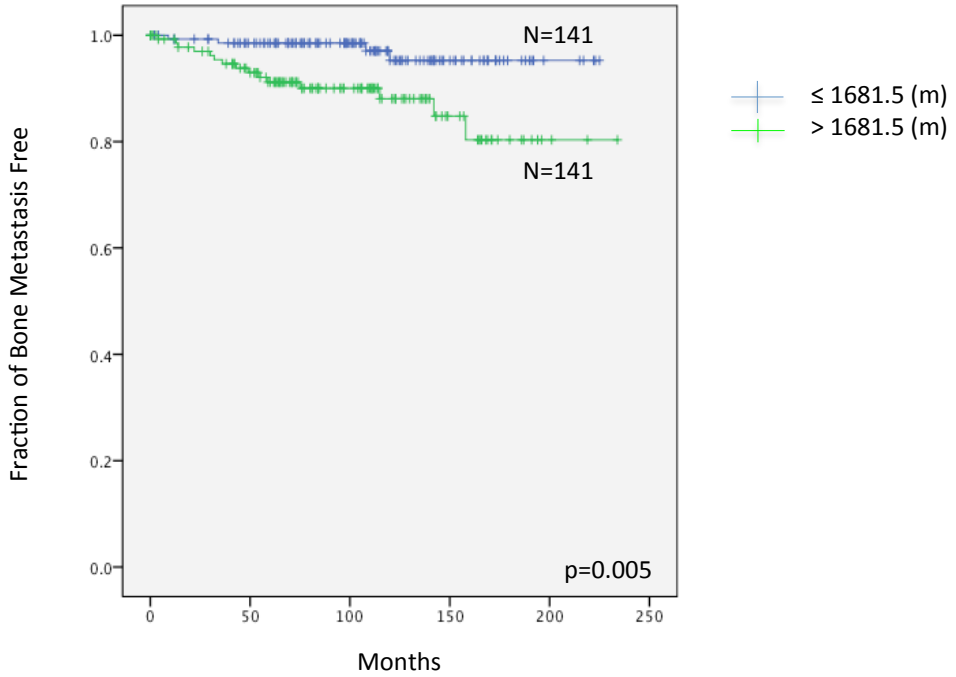
**D**

Correlation of Nuclear-epithelial pCHK2 in tumoral tissues



E

Correlation of Nuclear-epithelial 53BP1 in tumoral tissues

**F**

Correlation of Nuclear-stromal 53BP1 in tumoral tissues

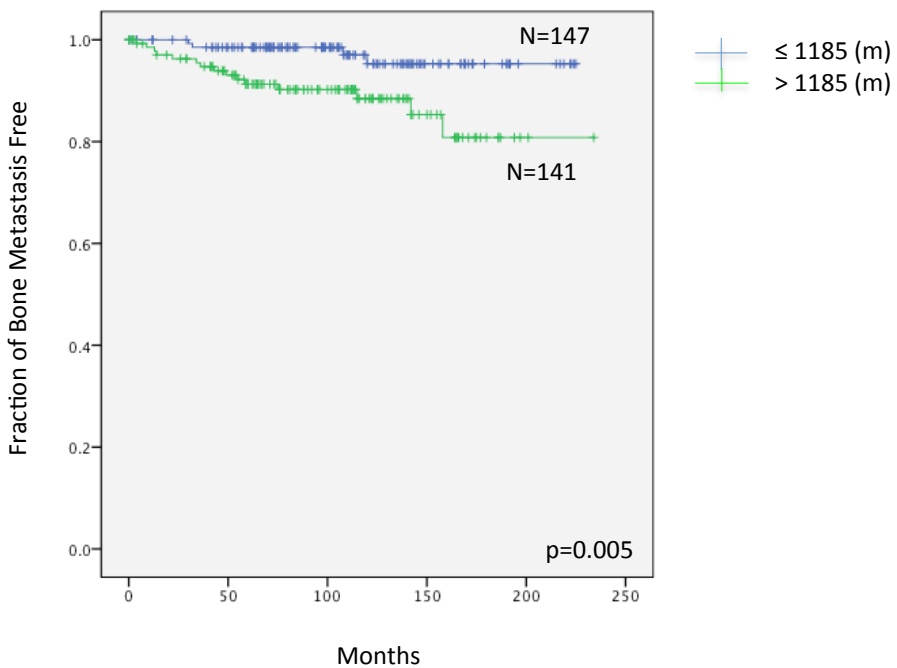
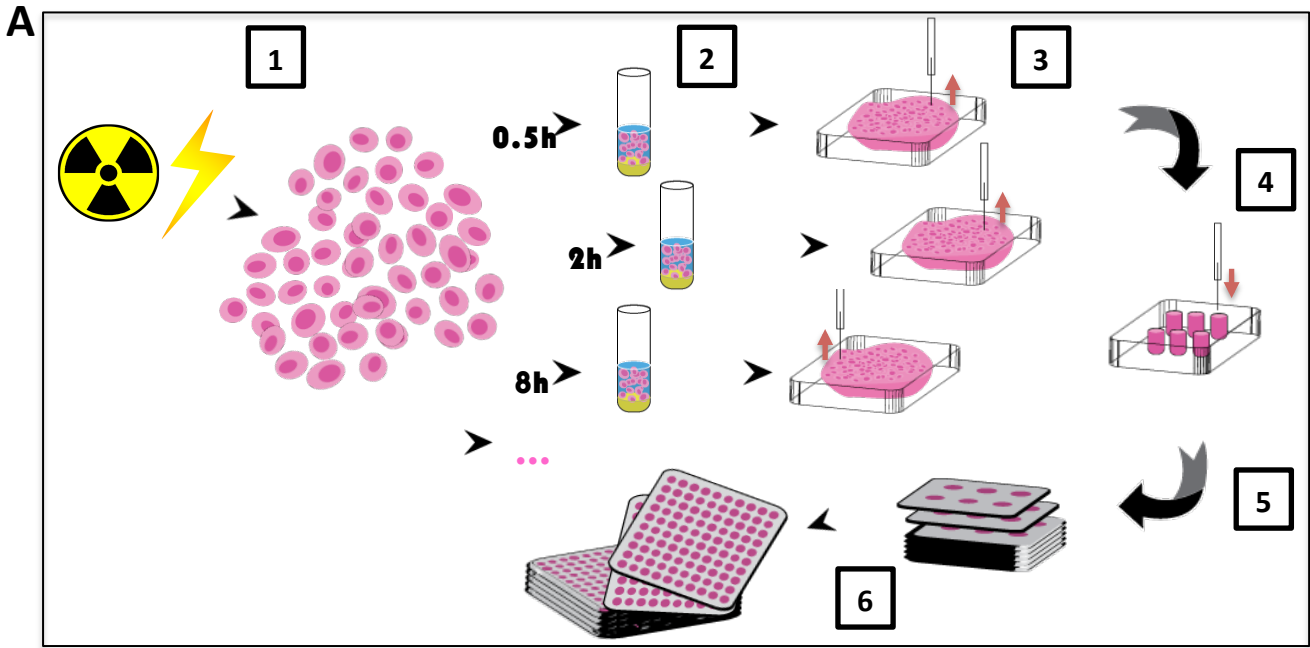
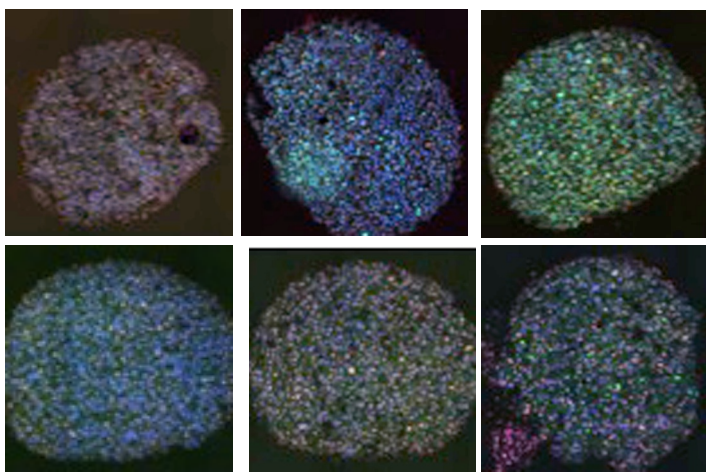


Figure S1

Schematic representation of the TMA-test approach for irradiated cells

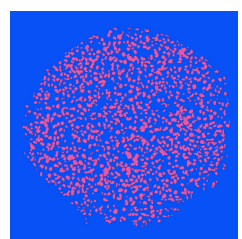
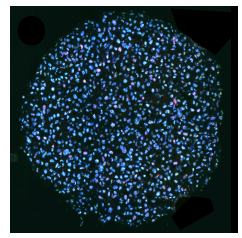


B Map of the TMA-test and representative full-core Immunofluorescence images



Ctrl	0.5 h	2 h
8 h	24 h	10 days

C Software mediated entire core detection and nucleus identification



Abbreviations: Ctrl = Control (non irradiated); 0.5h-2h-8h-24h-10 days = Timing of recovery following irradiation of 10 Gy; h= hours

Figure S2: Multicolor immunofluorescence staining in whole Pca TMA

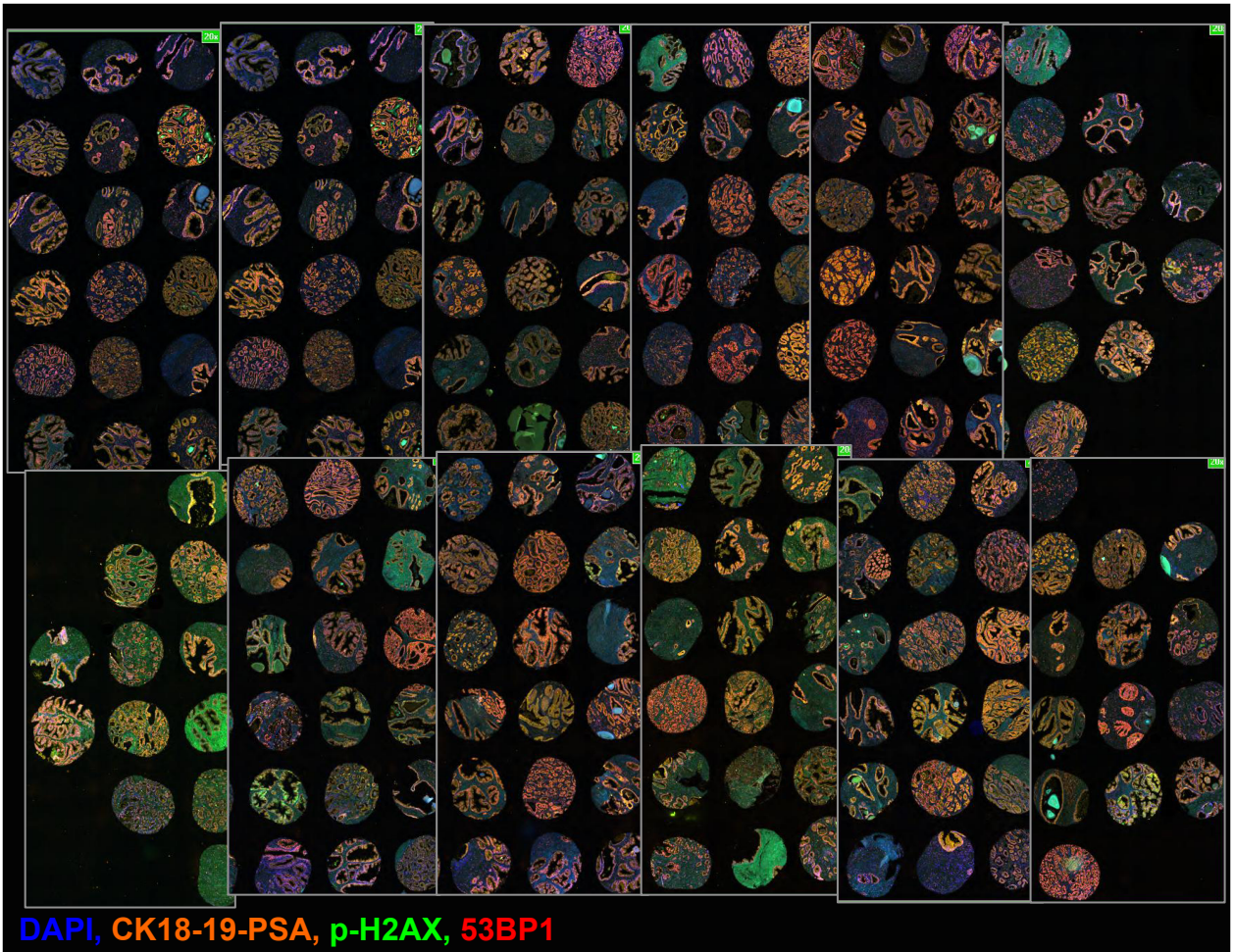


Figure S3: Software quantification of immunofluorescence-detected DDR activity in paraffin embedded cells (magnified sections from cores in Figure 3)

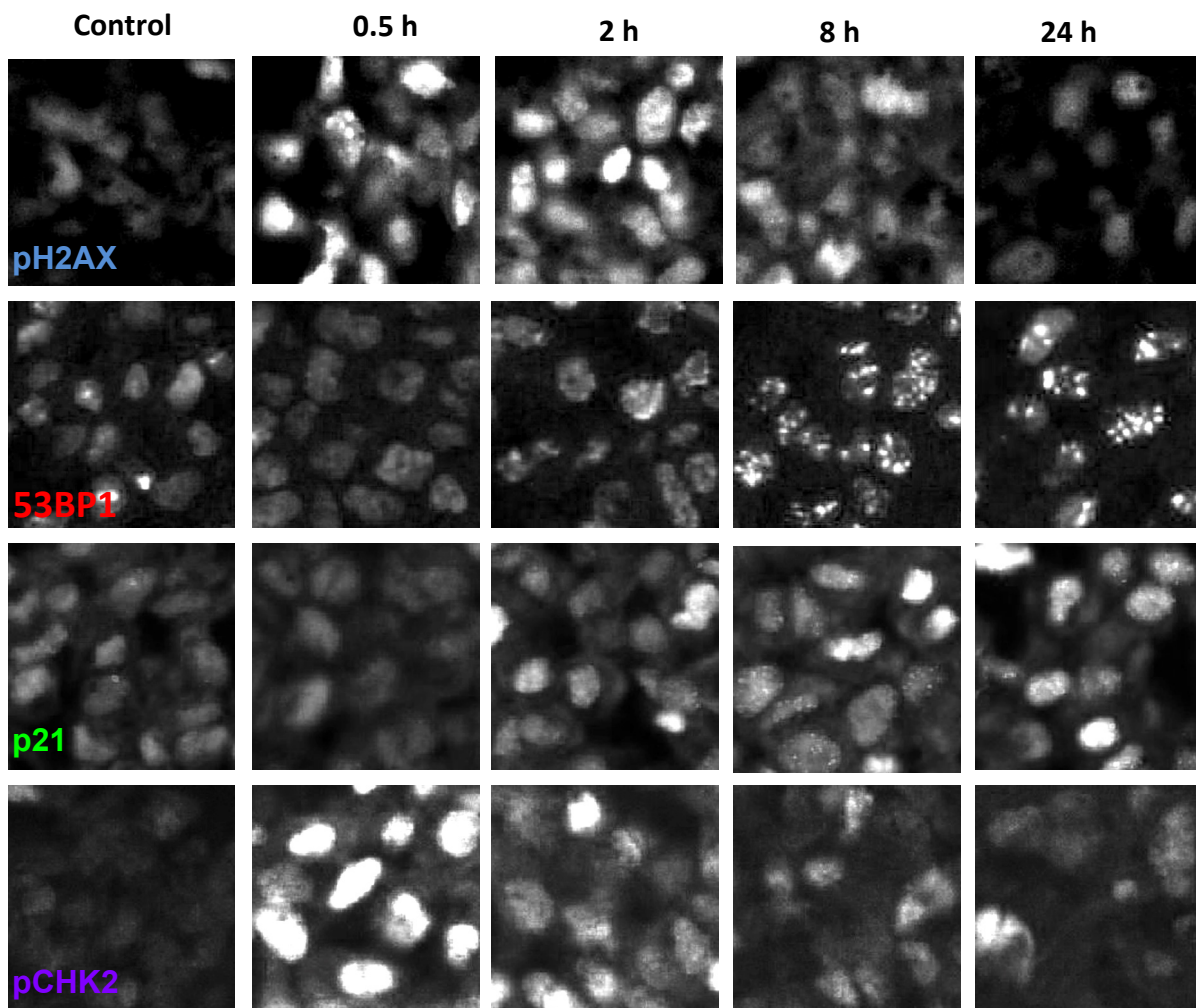


Table 1: Terry Fox TMA of prostate cancer (Pca) patient cohort

	N= 288	
Age at diagnosis	Mean	62.5 years
	Median	63 years
Follow-up	Average	101.5 months
	Median	100.5 months
Gleason Score	≤ 6	141
	7	118
	> 7	29
PSA	≤ 10 ng/mL	209
	10-20 ng/mL	65
	> 20 ng/mL	13
pT stage	2	209
	3	79
Surgical margins	Negative	180
	Positive	98
BCR	Absent	178
	Present	110
CRPC	Absent	268
	Present	20
Bone Metastasis	Absent	269
	Present	19
PCa Death	Negative	276
	Positive	12
LNI	Absent	204
	Present	11
SVI	Absent	244
	Present	34
ECE	Absent	185
	Present	84

Abbreviations: PSA = Prostatic Specific Antigen; *pT*: pathological T stage, *BCR*: Biochemical recurrence; *CRPC*: Castrate resistant prostate cancer, *Pca*: Prostate cancer, = Lymph node Invasion, *SVI* = Seminal Vesicle Invasion, *ECE* = Extracapsular extension

Table 2: Univariate and multivariate cox regression analysis for A) biochemical failure and B) Bone metastasis

A

Factor	Univariate			Multivariate		
	HR	95% CI	p	HR	95% CI	p
PSA	1.031	1.013-1.049	0.001	1.018	0.994-1.044	0.142
GS	1.837	1.528-2.208	0.000	1.431	1.161-1.764	0.001
Margins	3.256	2.21-4.797	0.000	2.116	1.31-3.417	0.002
SVI	4.872	3.134-7.576	0.000	1.682	0.967-2.925	0.066
ECE	3.891	2.643-5.728	0.000	1.833	1.088-3.089	0.023
NE_p65	1.001	1.000-1.002	0.029	1.001	1.000-1.002	0.005

B

Factor	Univariate			Multivariate (TE_53BP1)			Multivariate (TS_53BP1)		
	HR	95% CI	p	HR	95% CI	p	HR	95% CI	p
PSA	1.028	0.98-1.078	0.255	0.98	0.889-1.081	0.688	0.974	0.889-1.068	0.579
GS	2.708	1.791-4.094	0.000	2.27	1.374-3.75	0.001	2.142	1.293-3.546	0.003
Margins	2.484	0.979-6.30	0.055	0.977	0.349-2.739	0.965	0.894	0.313-2.552	0.834
SVI	10.104	4.082-25.01	0.000	2.977	0.771-11.498	0.114	3.842	1.045-14.131	0.043
ECE	4.713	1.768-12.564	0.002	1.407	0.329-6.016	0.645	1.458	0.331-6.413	0.618
TE_53BP1	1.002	1.00-1.003	0.009	1.002	1.000-1.003	0.046			
TS_53BP1	1.004	1.002-1.006	0.000				1.004	1.001-1.007	0.003

Abbreviations: PSA = Prostate Specific Antigen, GS = Gleason Score, SVI = Seminal Vesicle Invasion, ECE = Extracapsular extension, NE_p65 = Mean Fluorescent Intensity of p65 in the epithelium of normal cores, TE_53BP1 = Mean Fluorescent Intensity of 53BP1 in the epithelium of tumoral cores, TS_53BP1 = Mean Fluorescent Intensity of 53BP1 in the stroma of tumoral cores,

Table 3: Pearson Correlation (2-tailed) between DDR activity and clinico-pathological parameters.

	NE Chk2	TE Chk2	NS Chk2	TS Chk2	NE p65	TE p65	NS p65	TS p65
Age Dx	0.066	0.032	0.037	0.005	0.029	0.055	0.046	0.134
PSA	-0.041	-0.013	-0.034	0.01	-0.004	0.081	0.005	0.151
GS	-0.063	-0.181	-0.018	-0.123	-0.043	-0.153	-0.102	-0.121
LNI	0.182	0.111	-0.014	0.215	0.091	0.026	0.021	-0.005
SVI	-0.025	-0.121	-0.079	-0.089	0.011	-0.016	-0.064	0.048
ECE	-0.052	-0.066	-0.08	-0.007	0.029	-0.051	-0.023	0.036
Margins	-0.062	-0.013	-0.055	0.018	-0.052	-0.083	-0.037	0.013
CRPC	0.062	0.05	-0.006	0.065	0.037	-0.024	-0.012	0.003
pTNM	-0.018	-0.021	-0.08	0.014	0.069	-0.005	0.023	0.071
BCR	0.087	0.021	-0.094	0.036	0.14	-0.013	0.034	0.054
Bone Mets	0.092	0.057	-0.017	0.079	0.014	-0.042	-0.032	-0.046
Survival	0.071	0.004	-0.037	0.054	0.022	-0.037	-0.039	-0.032

	NE 53BP1	TE 53BP1	NS 53BP1	TS 53BP1	NE H2AX	TE H2AX	NS H2AX	TS H2AX
Age Dx	-0.031	0.021	-0.067	0.035	0.016	-0.047	0.015	0.027
PSA	-0.025	-0.061	0.032	0.05	0.025	0.007	0.056	0.087
GS	-0.032	0.036	0.115	0.025	0.019	-0.038	-0.082	-0.102
LNI	-0.014	-0.01	-0.009	0.021	0.02	-0.037	0.037	-0.09
SVI	0.055	0.17	0.125	0.067	-0.049	-0.071	-0.072	-0.036
ECE	0.076	0.107	0.046	-0.02	0.013	-0.108	0.003	-0.043
Margins	-0.026	0.041	-0.001	-0.031	-0.017	-0.058	-0.036	0.014
CRPC	-0.006	0.052	-0.027	0.186	0.002	0.071	-0.064	-0.014
pTNM	0.068	0.165	0.016	0.032	0.031	-0.096	0.045	-0.034
BCR	0.061	0.035	0.059	-0.044	0.108	0.044	0.071	0.057
Bone Mets	0.015	0.143	0.04	0.203	-0.048	0.034	-0.081	-0.079
Survival	0.045	0.14	0.05	0.188	-0.034	0.091	-0.06	-0.016

Abbreviations: Age Dx = patient's age at diagnosis, *PSA* = Prostatic specific antigen, *GS* = Gleason score, *LNI* = Lymph node invasion

SVI = seminal vesicle invasion, *ECE* = extracapsular extension, *CRPC* = castrate resistant prostate cancer, *pTNM* = pathologic stage, *BCR* = biochemical recurrence, *Bone mets* = Bone metastasis

NE = Epithelium in the normal core, *TE* = Epithelium in the tumoral core, *NS* = Stroma in the normal core, *TS* = Stroma in the tumoral core

Statistical significance ($p < 0.05$) indicated in **bold**.

Table 4: Paired Sample T test for DDR markers between adjacent normal and tumoral cells.

		Paired Differences				t	df	Sig. (2-tailed)	
		Mean MFI of total cohort	Std. Deviation	Std. Error Mean	95% Confidence Interval of the Difference				
					Lower				Upper
Pair	NE_Chk2	841.12	41.881	2.512	3.318	13.207	3.289	277	0.001
	TE_Chk2	832.85							
Pair	NS_Chk2	840.97	71.156	4.268	-10.185	6.617	-.418	277	0.676
	TS_Chk2	842.76							
Pair	NE_p65	636.62	174.633	10.474	8.202	49.438	2.752	277	0.006
	TE_p65	607.8							
Pair	NS_p65	754.54	190.399	11.419	45.894	90.854	5.988	277	0.000
	TS_p65	686.16							
Pair	NE_53BP1	1517.0	351.777	21.136	-207.735	-124.518	-7.860	276	0.000
	TE_53BP1	1683.13							
Pair	NS_53BP1	1176.87	196.041	11.779	-31.950	14.426	-.744	276	0.458
	TS_53BP1	1185.63							
Pair	NE_pH2AX	1232.54	372.367	22.414	92.915	181.164	6.114	275	0.000
	TE_pH2AX	1095.50							
Pair	NS_pH2AX	1557.98	452.697	27.249	184.857	292.143	8.753	275	0.000
	TS_pH2AX	1319.48							

Abbreviations: MFI = Mean Fluorescence Intensity, NE = Epithelium in the normal core, TE = Epithelium in the tumoral core, NS = Stroma in the normal core, TS = Stroma in the tumoral core
 Statistical significance ($p < 0.05$) indicated in **bold**.

CHAPTER 3: DISCUSSION

1.0 The DDR as a cancer barrier

In order to preserve genome integrity, cells need to protect themselves against a huge number of DNA lesions per day, particularly against DSBs, which are the most lethal type of DNA damage. Once cells detect DNA breaks, the DDR is initiated, this activation is required to stop the proliferation of cells with genomic instability, and therefore, prevent cancer progression. Other than cancer, cells defective in these mechanisms can also cause other human diseases such as neurodegenerative disorders including ataxias, Fanconi anaemia, infertility and other more diseases¹⁵¹. DDR leads to temporary cell cycle arrest and DNA repair, apoptosis, or senescence, preventing cells to replicate with accumulated mutations. The DDR is a central tumor suppression mechanism in mammals, and the loss of DDR genes such as the tumor suppressor p53 is always implicated in cancer progression. Importantly for cancer treatment, DSBs can result from ionizing radiation. Thus, the DDR determines how normal and cancer cells react to DNA damaging agents used for cancer therapy (radiation therapy and chemotherapy). We wanted to refine our understanding of DDR signalling during cancer progression or treatment and to further characterize this DDR activity in human prostate cancer.

1.1 DDR activity: a cancer barrier in prostate cancer

We elected to characterize DDR activity in human prostate cancer, which is a particularly promising model. In addition to the preliminary data describing DDR activation during prostate cancer progression¹⁰⁴, DDR activity has been detected in prostate cancer tumors following chemotherapy¹⁵⁰. Additional studies have established that a DDR-mediated barrier restrict early-stage prostate cancer progression in a mouse model (p53-mediated senescence in prostate specific PTEN-deficiency)^{106; 107}. This senescence barrier occurs at a stage equivalent to HG-PIN in humans and is consistent with the loss of the tumor suppressor PTEN relaxes PI3-K/AKT-dependant proliferation inhibition. This results in genomic instability and persistent DDR signalling¹⁰⁸. Further supporting this senescence barrier, short telomeres (known to directly trigger the DDR) have been observed in human HG-PIN¹⁰⁹. Together, these lines of evidence strongly suggest that the p53-mediated senescence barrier during HG-PIN could be partially driven by DDR signalling. Although, there is evidence of increasing DDR activity from the normal to the preneoplastic state¹⁰⁴, little is known on DDR activity during cancer progression beyond the pre-neoplastic stages. These observations suggest that during its evolution, cancer cells need to stabilize their genomes to become even more aggressive by surpassing this DDR barrier.

In our study, we found a low level of DDR activity in adenocarcinoma as compared to normal cells in our cohort of prostate cancer patients. Furthermore, within those lower

levels, patients with lowest levels could have a better prognosis. These findings can be explained by the concept of cancer immunoediting. At first, as it has already been shown, ATM is activated in earlier stages of prostate tumorigenesis (PINs) leading to an increased level of DDR. These pre-neoplastic cells are then eliminated by the immune system leading to the secretion of pro-inflammatory signals and recruitment of immune cells such as T-lymphocytes and natural killer cells resulting in the suppression of these pre-neoplastic cells. Following this process, equilibrium settles after an incomplete destruction of the tumor cells. After genetic instability, adenocarcinoma develops. The growth of tumor cells have survived the pressure of the immune system and prostatic cells have probably only stabilized their genome when becoming adenocarcinoma cells.

Moreover, a recent study has pointed out that prostate cancer progression is associated with an expansion of regulatory T cells that could down-regulate tumour immune surveillance¹⁵².

2.0 Repair Mechanisms

DDR is initiated to stop the proliferation of cells with genomic instability. DDR will lead to different cell fate including DNA repair. Two distinct pathways have evolved to eliminate DSBs: nonhomologous DNA end joining (NHEJ) and homologous recombination (HR). The HR requires that cells be in the S or G2 phase of the cell

cycle, when DNA replication generates the sister chromatid to direct the repair process. HR is a type of genetic recombination in which sequences of nucleotides are exchanged between two similar or identical molecules of DNA sequences elsewhere in the genome to serve as templates for DNA repair in order for the damaged molecule to return to their initial form, before the DSB. HR has a role in preserving the genome's integrity as well as a role in faithfully duplicating the genome by providing critical support for DNA replication and telomere maintenance. NHEJ occurs in all phases of the cell cycle, and is thus neither phase specific nor cycle specific. NHEJ is a more rapid process than HR but less accurate, with small deletions or insertions often resulting at the repaired break site. The main steps in NHEJ, after sensing the DSB, involve nucleases to remove damaged DNA, polymerases to help repair and ligases to restore the continuity of the DNA chain. The first event starts with the binding of two proteins (Ku70 and Ku80) to the DNA ends which occurs within seconds of the break. This binding serves to protect ends from degradation by exonucleases as well as to recruit DNA-PKcs. This large protein forms a physical bridge between the two ends, helping to keep them in close proximity for subsequent repair events. DNA-PKcs also phosphorylates a number of target proteins involved in checkpoints and repair. Making the choice between which pathway (HR and NHEJ) is used has been extensively studied³⁶. We will focus on the HR where the 53BP1 protein has a major role.

2.1 53BP1 and Homologous Recombination

In addition to its role in HR, 53BP1 is a central component of chromatin-based DSB signalling. 53BP1 is a large protein of 1972 amino acids that has no apparent enzymatic activity but contains interaction surfaces for numerous DSB-responsive proteins. Important structural elements in 53BP1 include the breast cancer 1 (BRCA1) carboxy-terminal (BRCT) repeats, the tandem Tudor domains and 28 amino-terminal Ser/Thr-Gln (S/T-Q) sites, which are phosphorylated, at least in part, by ATM kinase¹⁵³. Loss of 53BP1 or its failure to localize to damaged chromatin significantly reduces the phosphorylation of ATM targets such as p53, CHK2 and BRCA1 and, as a consequence, leads to G2–M checkpoint defects and genomic instability. Upon entry into S phase, BRCA1 helps to switch the mode of DSB repair by excluding 53BP1–RIF1 complexes from the DSB, thus enabling extensive DSB resection and the initiation of HR¹⁵⁴.

Although the mechanisms are not completely understood, it is known that in humans, mutations in the BRCA1 gene increase the risk of breast and ovarian cancers by impairing HR. It has been demonstrated that when 53BP1 is defective, formation of the mammary tumors that normally develop in *BRCA1* mutant mice was suppressed¹⁵⁵. Mouse *BRCA1*-associated mammary tumors have significant similarities to human *BRCA1*-associated breast cancer in regard to tumor aggressiveness, high incidence, mutations, and genetic instability. Furthermore, the team found that inactivation of

53BP1 restored the DNA repair function that is lost when *BRCA1* is mutated. The same group also discovered that both *BRCA1* and 53BP1 are capable of binding to replication-associated chromosome breaks; so when both proteins are present, *BRCA1* displaces 53BP1, the HR machinery has full access to the breaks, and HR proceeds. In *BRCA1*-deficient cells, the binding of 53BP1 to the site of DNA damage interferes with the DNA repair activity of HR proteins, so an alternative pathway that is more prone to produce mutations repairs the damage instead. When 53BP1 is absent, *BRCA1* is not needed to displace it so HR can take place normally.

Our study shows that a lower level of 53BP1 protein expression in tissue is associated with a better prognosis and it might be similarly explained by the restoration of the DNA repair. Alternatively, since this event occurs in cancer cells, it is possible that altered 53BP1 levels modulate other non-DNA repair related cell functions important for bone metastasis. To further explain these findings, our group may also evaluate the presence or absence of BRCA mutations in our cohort of patients.

3.0 Why do we need biomarkers?

Treatment options for localized prostate cancer in 2014 are mainly radiation therapy or surgery. Both have shown similar survival outcomes in low and intermediate risk prostate cancer patients. Contemporary radiotherapy approaches such as intensity-modulated radiation therapy (IMRT) have permitted increased delivery of radiation to the prostate while sparing adjacent organs, reducing the potential for acute and chronic

toxicity. However, proctitis, cystitis, and erectile dysfunction remain significant complications of high-dose radiotherapy. In turn, local failure after radiotherapy remains 20%–35% in intermediate and high-risk patients, leading to increased metastasis and lower survival. Hormonal therapy has proven value when combined with localized radiotherapy in intermediate and high risk prostate cancer patients, but carries its own set of morbidities, including increased cardiovascular and thromboembolic risk. In daily clinical setting, it is difficult for a clinician to orient a patient towards one type of treatment over another since radiotherapy and surgery both gives very good results based on the available literature. If the clinician could know, based on a biomarker, which patient will have a better response to one type of therapy (ie: radiation compared to surgery if this particular patient has a more radiosensitive tumor as compared to another patient), the patient will receive the more efficient treatment. Furthermore, the use of novel agents with more attractive side effect profiles that can be combined with radiotherapy to improve local control in high-risk patients and/or permit a dose reduction in lower-risk patients would be of great value.

3.1 DDR activity as a biomarker

The DDR is responsible for maintaining genome stability and we hypothesize that basal level of DDR in cancer prior to treatment has the potential to influence how the cancer cells will react to treatment. Current data suggest that the modified chromatin

foci at the sites of persistent DNA breaks serve to promote the tumour suppressor senescence arrest^{32;157}. Alternatively, defects in the DDR regulators and tumor suppressor pathways p53 and/or Rb are common in cancer and may allow tumor cells to maintain genomic instability and tolerate persistent DNA damage, by blocking senescent signalling while promoting cell proliferation and survival. In senescent cells or cancer cells that tolerate damage, the presence of P-H2AX and 53BP1 localization to DNA damage foci can serve as proxies for unrepaired DSBs and the DNA damage response^{158; 159}.

These DDR markers that can be accurately and quantitatively assessed could help define a strategy and novel biomarkers to predict treatment outcomes and adapt treatment strategy. For example, hormonal therapy may be used for intermediate risk cancer patient with a bad prognosis based on DDR activity. Another example is following patients presenting with PIN on their prostate biopsy under a strict surveillance protocol in order to detect prostate adenocarcinoma in early stages. Finally, these findings could help design targeted sensitization of prostate cancer cells to DNA damaging agent used in therapy including ionizing radiation.

Because the DDR controls cellular responses that are absolutely essential to radiotherapy treatment outcomes, biochemical components of this signalling cascade become potential pharmaceutical targets for treatment optimization.

Alternatively, gaining information about the initial “DDR state” of the tumor could help predict whether a particular cancer will respond well to DNA damaging agents

during treatment. Finding new biomarkers predicting what kind of DDR cells/tumors mount against radiotherapy will have the potential to improve treatment selection and success. Currently, the exact regulation and outcomes of DDR signalling in cancer cells remain relatively unknown.

Following our findings, we could try to identify if our cohort of patients are BRCA1 deficient and could eventually be more sensitive to RT. Furthermore, because tumor cells that are *BRCA1*-deficient are driven to turn to other, less faithful DNA repair pathways and they may become resistant to chemotherapy/RT by acquiring additional mutations.

4.0 DDR activity in our cohort of patients

Despite the apparent increase in the incidence of prostate cancer in the 1970-80s mostly caused by increased use of TURP for treating BPH resulting in the increased incidental detection of preclinical cases (as well as increased PSA testing), very good biochemical control and decline in mortality has been noted. Nevertheless, bone metastases are common in advanced prostate cancer, occurring in up to 75 % of patients with advanced cancer¹⁶⁰ and it is much less frequent in less advanced patients. Our cohort of 288 evaluated patients consisted mostly of low risk patients with only 29 patients with Gleason > 7 and 79 patients with PSA > 10 ng/mL which could explain the low number of bone metastases (19/288). Although the average follow up of 101.5 months is quite long, the fact that prostate cancer patients have very good prognosis

and show bone metastasis many years following their initial radical prostatectomy, might explain this low number of events. Nonetheless, we did find a statistical significant relation between two of the evaluated DDR markers and outcome (BCR and bone metastasis). This study validates a prior finding that p65 correlates with prostate cancer prognosis. In this context, our group has already address the prognostic value of the p65 subunit of Nuclear Factor κ B in prostate cancer⁵⁸. In this context the implication of NF- κ B p65 in cancer progression has been extensively studied. The frequency of p65 nuclear distribution in prostatic tumor cells has been reported to correlate with Gleason score and the presence of lymph node metastasis^{58;161}. Moreover, the presence of nuclear p65 in radical prostatectomy tissues predicts BCR in prostate cancer patients^{59; 162; 163}.

As for 53BP1, this study is, to our knowledge, the first to show a correlation with patient's prognosis. Indeed, in our cohort of patients, those expressing a lower level of 53BP1 in the nuclei of the tumor and adjacent stroma or epithelium had a lower chance of developing bone metastasis.

We suspect more results pertaining to DDR markers and biochemical control, bone metastases as well as prostate cancer survival will be obtained with longer follow-up of our cohort as the biobank continue to mature with more clinical data.

5.0 Limitations of our study

5.1 Validation study on TMA-cell and TMA-tissue

Throughout our research project, we have encountered a few challenging aspects. Firstly, our antibodies have been optimized on fibroblasts (TMA-cell) where DNA damage has been voluntarily induced by irradiation so that the DDR markers could be easily evaluated. However, DDR markers were more difficult to evaluate on human tissue (TMA-tissue and TMA-TFRI). This can be explained by the fact that blocks used were constructed from specimens obtained by the surgeon who were then placed in formalin and processed by the pathology department, processes out of our control. Furthermore, the TMA-TFRI has been built almost 5 years ago and recognition of the different epitopes may have been altered with time. This is perhaps particularly important for epitopes with sensitive modifications such as phosphorylation. In order to ensure that our methods were as reliable as possible, the TMA-cell which was built under our control and which showed an excellent recognition of investigated DDR signals, was used as a control in all our experiments.

5.2 Data quality control

Quality control on our data had to be done to validate our data. The TMA-TFRI was constructed in a manner where each patient had replicates of their tumor tissue core as

well as of normal tissue cores. For example, patient X had a core of tumoral tissue and normal tissue on two separate slides (TF-1A and TF-1B). Since those cores were taken from different areas in the tumor and normal tissue of the same patient, we had to go visually inspect each of the cores to eliminate the cores that were aberrant (damaged core, external source of artifact or unexplained cause). This quality control was performed to make sure the results obtained were due to tumor/tissue biology rather to a human factor.

5.3 Immunofluorescence technique

We mainly used IF in our experiments to detect protein expression. Although this technique has numerous advantages, it has a few limitations. IF detects more than one protein at a time and it can examine the co-localization of two antigens in the same subcellular compartment. It has therefore the capability for multiple labeling and has a higher resolution due to the fluorophores directly conjugated to the antibody. However, when IF is used on FFPE tissues, inherent autofluorescence of such specimens makes high quality immunofluorescence sometimes more difficult. Fortunately, although we did find autofluorescence in our TMA-cell, we have succeeded to optimize our antibodies and reduce this autofluorescence. Similarly, quantitative IF labeling of FFPE material, particularly that in TMA, has been achieved by the development of computer assisted fluorescence imaging systems¹⁶⁴.

Moreover, our group has optimized a method consisting of careful microscopy

practices and use of the analysis software to reliably detect protein expression of multiple markers in different compartments of FFPE human tissue.

Conclusion

DDR is a complex signalling network and its failure causes genomic instability, an underlying cause of cancer. While prostate cancer is the most frequently diagnosed cancer in Canadian men and is the third deadliest cancer in males, treatments available including surgery, different types of radiation therapy and hormonal therapy are still offered based on the patient's PSA, clinical stage and Gleason score. The tumor biology of individual patient is still not taken into consideration for clinical management of men diagnosed with prostate cancer. After creating a TMA-cell consisting of irradiated cells to induce DNA damage, we optimized 4 different antibodies that were validated on human tissue and then applied to a TMA of 300 prostate cancer patients. This was done by IF which has many advantages including the possibility to associate a fluorescent channel to an individual mask such as the nucleus, epithelium and at least two DDR markers at a time. DDR signals (fluorescent staining) obtained on the TMAs were quantified by a software which is more robust (reproducible, unbiased and versatile) than a person's visual scoring. DDR marker 53BP1 and p65 seem to have prognostic value in patients with prostate adenocarcinoma. Patients expressing reduced amounts of 53BP1 have a better bone metastasis free survival ($p=0.005$) and those with reduced amounts of p65 have a better biochemical control ($p=0.002$). These findings were also correlated in univariate and multivariate cox regression analyses. Validation of other DDR markers as they become available may also correlate with patients' outcome. Since prostate cancer

patients have very good prognosis and relapse much later than other types of cancers (ex-ovarian cancers), a longer follow-up may translate into correlation with survival.

Perspectives

The prostate TMAs used in this study consisted of samples from patients who exclusively underwent radical prostatectomy. These samples are useful to determine whether DDR activation in the original tumors correlates with treatment outcome. Upon further optimization of further DDR markers as evaluated here, our long-term objective is to broaden our views of how DDR signalling is regulated during prostate cancer progression and to provide information about potential genetic targets that could be used as predictive biomarkers. Therapy by ionizing radiation, already widely accepted as a treatment for prostate cancer, may be improved by rendering prostate cancer cells more sensitive to irradiation and protecting normal rectal and bladder cells, the organs considered at risk when treating a prostate by irradiation. We would like to construct a new TMA based on an ideal cohort for DNA damage and DDR activity evaluation. We plan to collect prospective samples of prostate cancer from all prostate risk categories (ie: NCCN low-intermediate and high risk) patients treated with external beam radiation including samples obtained following radiation treatment through biopsies. Patients who will have chosen radiation treatment will have their tissues collected at diagnosis (at the time of biopsy) where PIN samples (if existing within the specimen) will also be included, at 1 month post radiation as well as at six

months post irradiation. This would be considered ideal since ionizing radiation directly affects DDR and we would be looking at DDR markers in patients receiving DNA damage. This could help define a strategy to predict treatment outcomes and define priority targets to sensitize prostate cancer cells to DNA damaging agents including ionizing radiation. This will be done to gather prospective preliminary results of the immediate DDR response to irradiation (in prostate cancer cells), and eventually to correlate this DDR response to treatment outcomes as our biobank mature and accumulate patient's clinical outcome data.

CHAPTER 4: REFERENCES

1. Siegel, R., Naishadham, D. & Jemal, A. (2013). Cancer statistics, 2013. *CA Cancer J Clin* **63**, 11-30.
2. Bostwick, D. G., Liu, L., Brawer, M. K. & Qian, J. (2004). High-grade prostatic intraepithelial neoplasia. *Rev Urol* **6**, 171-9.
3. Kollmeier, M. A. & Zelefsky, M. J. (2012). How to select the optimal therapy for early-stage prostate cancer. *Crit Rev Oncol Hematol* **84 Suppl 1**, e6-e15.
4. Meurs, P., Galvin, R., Fanning, D. M. & Fahey, T. (2013). Prognostic value of the CAPRA clinical prediction rule: a systematic review and meta-analysis. *BJU Int* **111**, 427-36.
5. Ingram, D. G. & Kattan, M. W. (2010). Risk grouping versus risk continuum in patients with clinically localized prostate cancer: a taxometric test. *J Urol* **184**, 1937-41.
6. Shariat, S. F., Kattan, M. W., Vickers, A. J., Karakiewicz, P. I. & Scardino, P. T. (2009). Critical review of prostate cancer predictive tools. *Future Oncol* **5**, 1555-84.
7. Roach, M., 3rd, Waldman, F. & Pollack, A. (2009). Predictive models in external beam radiotherapy for clinically localized prostate cancer. *Cancer* **115**, 3112-20.
8. Rodrigues, G., Lukka, H., Warde, P., Brundage, M., Souhami, L., Crook, J., Cury, F., Catton, C., Mok, G., Martin, A. G., Vigneault, E., Morris, J., Warner, A., Maldonado, S. G. & Pickles, T. (2014). The prostate cancer risk stratification project: database construction and risk stratification outcome analysis. *J Natl Compr Canc Netw* **12**, 60-9.
9. Wilt, T. J. (2012). The Prostate Cancer Intervention Versus Observation Trial: VA/NCI/AHRQ Cooperative Studies Program #407 (PIVOT): design and baseline results of a randomized controlled trial comparing radical prostatectomy with watchful waiting for men with clinically localized prostate cancer. *J Natl Cancer Inst Monogr* **2012**, 184-90.
10. Johns, H. E. (1981). The physicist in cancer treatment and detection. *Int J Radiat Oncol Biol Phys* **7**, 801-8.

11. Radford, I. R. (1986). Evidence for a general relationship between the induced level of DNA double-strand breakage and cell-killing after X-irradiation of mammalian cells. *Int J Radiat Biol Relat Stud Phys Chem Med* **49**, 611-20.
12. Nunez, M. I., McMillan, T. J., Valenzuela, M. T., Ruiz de Almodovar, J. M. & Pedraza, V. (1996). Relationship between DNA damage, rejoining and cell killing by radiation in mammalian cells. *Radiother Oncol* **39**, 155-65.
13. Dikomey, E., Dahm-Daphi, J., Brammer, I., Martensen, R. & Kaina, B. (1998). Correlation between cellular radiosensitivity and non-repaired double-strand breaks studied in nine mammalian cell lines. *Int J Radiat Biol* **73**, 269-78.
14. Munro, T. R. (1970). The relative radiosensitivity of the nucleus and cytoplasm of Chinese hamster fibroblasts. *Radiat Res* **42**, 451-70.
15. Brenner, D. J. & Ward, J. F. (1992). Constraints on energy deposition and target size of multiply damaged sites associated with DNA double-strand breaks. *Int J Radiat Biol* **61**, 737-48.
16. Jonah, C. D. (1995). A short history of the radiation chemistry of water. *Radiat Res* **144**, 141-7.
17. Kaplan, H. S. (1979). Historic milestones in radiobiology and radiation therapy. *Semin Oncol* **6**, 479-89.
18. Boiteux, S. & Jinks-Robertson, S. (2013). DNA repair mechanisms and the bypass of DNA damage in *Saccharomyces cerevisiae*. *Genetics* **193**, 1025-64.
19. Harper, J. W. & Elledge, S. J. (2007). The DNA damage response: ten years after. *Mol Cell* **28**, 739-45.
20. Liu, Y., Prasad, R., Beard, W. A., Kedar, P. S., Hou, E. W., Shock, D. D. & Wilson, S. H. (2007). Coordination of steps in single-nucleotide base excision repair mediated by apurinic/aprimidinic endonuclease 1 and DNA polymerase beta. *J Biol Chem* **282**, 13532-41.
21. Molls, M., Stadler, P., Becker, A., Feldmann, H. J. & Dunst, J. (1998). Relevance of oxygen in radiation oncology. Mechanisms of action, correlation to low hemoglobin levels. *Strahlenther Onkol* **174 Suppl 4**, 13-6.

22. Stucki, M. & Jackson, S. P. (2006). gammaH2AX and MDC1: anchoring the DNA-damage-response machinery to broken chromosomes. *DNA Repair (Amst)* **5**, 534-43.
23. Falck, J., Coates, J. & Jackson, S. P. (2005). Conserved modes of recruitment of ATM, ATR and DNA-PKcs to sites of DNA damage. *Nature* **434**, 605-11.
24. Wilson, G. D. (2004). Radiation and the cell cycle, revisited. *Cancer Metastasis Rev* **23**, 209-25.
25. Griffiths, D. J., Barbet, N. C., McCreedy, S., Lehmann, A. R. & Carr, A. M. (1995). Fission yeast rad17: a homologue of budding yeast RAD24 that shares regions of sequence similarity with DNA polymerase accessory proteins. *EMBO J* **14**, 5812-23.
26. Maser, R. S., Monsen, K. J., Nelms, B. E. & Petrini, J. H. (1997). hMre11 and hRad50 nuclear foci are induced during the normal cellular response to DNA double-strand breaks. *Mol Cell Biol* **17**, 6087-96.
27. Abraham, R. T. (2003). Checkpoint signaling: epigenetic events sound the DNA strand-breaks alarm to the ATM protein kinase. *Bioessays* **25**, 627-30.
28. Bakkenist, C. J. & Kastan, M. B. (2003). DNA damage activates ATM through intermolecular autophosphorylation and dimer dissociation. *Nature* **421**, 499-506.
29. Kim, S. T., Lim, D. S., Canman, C. E. & Kastan, M. B. (1999). Substrate specificities and identification of putative substrates of ATM kinase family members. *J Biol Chem* **274**, 37538-43.
30. Wright, J. A., Keegan, K. S., Herendeen, D. R., Bentley, N. J., Carr, A. M., Hoekstra, M. F. & Concannon, P. (1998). Protein kinase mutants of human ATR increase sensitivity to UV and ionizing radiation and abrogate cell cycle checkpoint control. *Proc Natl Acad Sci U S A* **95**, 7445-50.
31. Matsuoka, S., Ballif, B. A., Smogorzewska, A., McDonald, E. R., 3rd, Hurov, K. E., Luo, J., Bakalarski, C. E., Zhao, Z., Solimini, N., Lerenthal, Y., Shiloh, Y., Gygi, S. P. & Elledge, S. J. (2007). ATM and ATR substrate analysis reveals extensive protein networks responsive to DNA damage. *Science* **316**, 1160-6.

32. Rodier, F., Coppe, J. P., Patil, C. K., Hoeijmakers, W. A., Munoz, D. P., Raza, S. R., Freund, A., Campeau, E., Davalos, A. R. & Campisi, J. (2009). Persistent DNA damage signalling triggers senescence-associated inflammatory cytokine secretion. *Nat Cell Biol* **11**, 973-9.
33. Rodier, F. & Campisi, J. (2011). Four faces of cellular senescence. *J Cell Biol* **192**, 547-56.
34. Zhang, X. P., Liu, F., Cheng, Z. & Wang, W. (2009). Cell fate decision mediated by p53 pulses. *Proc Natl Acad Sci U S A* **106**, 12245-50.
35. Sulli, G., Di Micco, R. & d'Adda di Fagagna, F. (2012). Crosstalk between chromatin state and DNA damage response in cellular senescence and cancer. *Nat Rev Cancer* **12**, 709-20.
36. Daley, J. M. & Sung, P. (2014). 53BP1, BRCA1, and the Choice between Recombination and End Joining at DNA Double-Strand Breaks. *Mol Cell Biol* **34**, 1380-8.
37. Morgan, D. O. (1995). Principles of CDK regulation. *Nature* **374**, 131-4.
38. Nigg, E. A. (1995). Cyclin-dependent protein kinases: key regulators of the eukaryotic cell cycle. *Bioessays* **17**, 471-80.
39. Lopez-Saez, J. F., de la Torre, C., Pincheira, J. & Gimenez-Martin, G. (1998). Cell proliferation and cancer. *Histol Histopathol* **13**, 1197-214.
40. Zetterberg, A., Larsson, O. & Wiman, K. G. (1995). What is the restriction point? *Curr Opin Cell Biol* **7**, 835-42.
41. Sinclair, W. K. (1968). Cyclic x-ray responses in mammalian cells in vitro. *Radiat Res* **33**, 620-43.
42. Terasima, T. & Tolmach, L. J. (1963). X-ray sensitivity and DNA synthesis in synchronous populations of HeLa cells. *Science* **140**, 490-2.
43. Terasima, T. & Tolmach, L. J. (1963). Variations in several responses of HeLa cells to x-irradiation during the division cycle. *Biophys J* **3**, 11-33.
44. Biade, S., Stobbe, C. C. & Chapman, J. D. (1997). The intrinsic radiosensitivity of some human tumor cells throughout their cell cycles. *Radiat Res* **147**, 416-21.

45. Zhang, Y. & Xiong, Y. (2001). A p53 amino-terminal nuclear export signal inhibited by DNA damage-induced phosphorylation. *Science* **292**, 1910-5.
46. Shieh, S. Y., Ahn, J., Tamai, K., Taya, Y. & Prives, C. (2000). The human homologs of checkpoint kinases Chk1 and Cds1 (Chk2) phosphorylate p53 at multiple DNA damage-inducible sites. *Genes Dev* **14**, 289-300.
47. Sherr, C. J. & Roberts, J. M. (1999). CDK inhibitors: positive and negative regulators of G1-phase progression. *Genes Dev* **13**, 1501-12.
48. Mailand, N., Falck, J., Lukas, C., Syljuasen, R. G., Welcker, M., Bartek, J. & Lukas, J. (2000). Rapid destruction of human Cdc25A in response to DNA damage. *Science* **288**, 1425-9.
49. Schneiderman, M. H., Schneiderman, G. S. & Rusk, C. M. (1983). A cell kinetic method for the mitotic selection of treated G2 cells. *Cell Tissue Kinet* **16**, 41-9.
50. Kaldis, P. (1999). The cdk-activating kinase (CAK): from yeast to mammals. *Cell Mol Life Sci* **55**, 284-96.
51. Falck, J., Mailand, N., Syljuasen, R. G., Bartek, J. & Lukas, J. (2001). The ATM-Chk2-Cdc25A checkpoint pathway guards against radioresistant DNA synthesis. *Nature* **410**, 842-7.
52. Takata, M., Sasaki, M. S., Sonoda, E., Morrison, C., Hashimoto, M., Utsumi, H., Yamaguchi-Iwai, Y., Shinohara, A. & Takeda, S. (1998). Homologous recombination and non-homologous end-joining pathways of DNA double-strand break repair have overlapping roles in the maintenance of chromosomal integrity in vertebrate cells. *EMBO J* **17**, 5497-508.
53. Haber, J. E. (2000). Partners and pathways repairing a double-strand break. *Trends Genet* **16**, 259-64.
54. Wang, B., Matsuoka, S., Carpenter, P. B. & Elledge, S. J. (2002). 53BP1, a mediator of the DNA damage checkpoint. *Science* **298**, 1435-8.
55. Kao, G. D., McKenna, W. G., Guenther, M. G., Muschel, R. J., Lazar, M. A. & Yen, T. J. (2003). Histone deacetylase 4 interacts with 53BP1 to mediate the DNA damage response. *J Cell Biol* **160**, 1017-27.

56. DiTullio, R. A., Jr., Mochan, T. A., Venere, M., Bartkova, J., Sehested, M., Bartek, J. & Halazonetis, T. D. (2002). 53BP1 functions in an ATM-dependent checkpoint pathway that is constitutively activated in human cancer. *Nat Cell Biol* **4**, 998-1002.
57. Lessard, L., Karakiewicz, P. I., Bellon-Gagnon, P., Alam-Fahmy, M., Ismail, H. A., Mes-Masson, A. M. & Saad, F. (2006). Nuclear localization of nuclear factor-kappaB p65 in primary prostate tumors is highly predictive of pelvic lymph node metastases. *Clin Cancer Res* **12**, 5741-5.
58. Lessard, L., Mes-Masson, A. M., Lamarre, L., Wall, L., Lattouf, J. B. & Saad, F. (2003). NF-kappa B nuclear localization and its prognostic significance in prostate cancer. *BJU Int* **91**, 417-20.
59. Gannon, P. O., Lessard, L., Stevens, L. M., Forest, V., Begin, L. R., Minner, S., Tennstedt, P., Schlomm, T., Mes-Masson, A. M. & Saad, F. (2013). Large-scale independent validation of the nuclear factor-kappa B p65 prognostic biomarker in prostate cancer. *Eur J Cancer* **49**, 2441-8.
60. Huxford, T., Huang, D. B., Malek, S. & Ghosh, G. (1998). The crystal structure of the IkappaBalpha/NF-kappaB complex reveals mechanisms of NF-kappaB inactivation. *Cell* **95**, 759-70.
61. Jacobs, M. D. & Harrison, S. C. (1998). Structure of an IkappaBalpha/NF-kappaB complex. *Cell* **95**, 749-58.
62. Hayden, M. S. & Ghosh, S. (2004). Signaling to NF-kappaB. *Genes Dev* **18**, 2195-224.
63. Yamamoto, Y. & Gaynor, R. B. (2004). IkappaB kinases: key regulators of the NF-kappaB pathway. *Trends Biochem Sci* **29**, 72-9.
64. Viatour, P., Merville, M. P., Bours, V. & Chariot, A. (2005). Phosphorylation of NF-kappaB and IkappaB proteins: implications in cancer and inflammation. *Trends Biochem Sci* **30**, 43-52.
65. Sun, Z. & Andersson, R. (2002). NF-kappaB activation and inhibition: a review. *Shock* **18**, 99-106.
66. Hoffmann, A. & Baltimore, D. (2006). Circuitry of nuclear factor kappaB signaling. *Immunol Rev* **210**, 171-86.

67. Weih, F. & Caamano, J. (2003). Regulation of secondary lymphoid organ development by the nuclear factor-kappaB signal transduction pathway. *Immunol Rev* **195**, 91-105.
68. Perkins, N. D. (2012). The diverse and complex roles of NF-kappaB subunits in cancer. *Nat Rev Cancer* **12**, 121-32.
69. Gilmore, T. D. (2006). Introduction to NF-kappaB: players, pathways, perspectives. *Oncogene* **25**, 6680-4.
70. Hoffmann, A., Natoli, G. & Ghosh, G. (2006). Transcriptional regulation via the NF-kappaB signaling module. *Oncogene* **25**, 6706-16.
71. Brach, M. A., Hass, R., Sherman, M. L., Gunji, H., Weichselbaum, R. & Kufe, D. (1991). Ionizing radiation induces expression and binding activity of the nuclear factor kappa B. *J Clin Invest* **88**, 691-5.
72. Criswell, T., Leskov, K., Miyamoto, S., Luo, G. & Boothman, D. A. (2003). Transcription factors activated in mammalian cells after clinically relevant doses of ionizing radiation. *Oncogene* **22**, 5813-27.
73. Wang, C. Y., Mayo, M. W., Korneluk, R. G., Goeddel, D. V. & Baldwin, A. S., Jr. (1998). NF-kappaB antiapoptosis: induction of TRAF1 and TRAF2 and c-IAP1 and c-IAP2 to suppress caspase-8 activation. *Science* **281**, 1680-3.
74. Bours, V., Bentires-Alj, M., Hellin, A. C., Viatour, P., Robe, P., Delhalle, S., Benoit, V. & Merville, M. P. (2000). Nuclear factor-kappa B, cancer, and apoptosis. *Biochem Pharmacol* **60**, 1085-9.
75. Pahl, H. L. (1999). Activators and target genes of Rel/NF-kappaB transcription factors. *Oncogene* **18**, 6853-66.
76. Barkett, M. & Gilmore, T. D. (1999). Control of apoptosis by Rel/NF-kappaB transcription factors. *Oncogene* **18**, 6910-24.
77. Hoesel, B. & Schmid, J. A. (2013). The complexity of NF-kappaB signaling in inflammation and cancer. *Mol Cancer* **12**, 86.
78. Lawrence, T. (2009). The nuclear factor NF-kappaB pathway in inflammation. *Cold Spring Harb Perspect Biol* **1**, a001651.

79. Tabruyn, S. P. & Griffioen, A. W. (2007). A new role for NF-kappaB in angiogenesis inhibition. *Cell Death Differ* **14**, 1393-7.
80. Sethi, G., Sung, B. & Aggarwal, B. B. (2008). Nuclear factor-kappaB activation: from bench to bedside. *Exp Biol Med (Maywood)* **233**, 21-31.
81. Karin, M. (2006). NF-kappaB and cancer: mechanisms and targets. *Mol Carcinog* **45**, 355-61.
82. Wang, W., Abbruzzese, J. L., Evans, D. B., Larry, L., Cleary, K. R. & Chiao, P. J. (1999). The nuclear factor-kappa B RelA transcription factor is constitutively activated in human pancreatic adenocarcinoma cells. *Clin Cancer Res* **5**, 119-27.
83. Sovak, M. A., Bellas, R. E., Kim, D. W., Zanieski, G. J., Rogers, A. E., Traish, A. M. & Sonenshein, G. E. (1997). Aberrant nuclear factor-kappaB/Rel expression and the pathogenesis of breast cancer. *J Clin Invest* **100**, 2952-60.
84. Pallares, J., Martinez-Guitarte, J. L., Dolcet, X., Llobet, D., Rue, M., Palacios, J., Prat, J. & Matias-Guiu, X. (2004). Abnormalities in the NF-kappaB family and related proteins in endometrial carcinoma. *J Pathol* **204**, 569-77.
85. Oya, M., Takayanagi, A., Horiguchi, A., Mizuno, R., Ohtsubo, M., Marumo, K., Shimizu, N. & Murai, M. (2003). Increased nuclear factor-kappa B activation is related to the tumor development of renal cell carcinoma. *Carcinogenesis* **24**, 377-84.
86. Huang, S., DeGuzman, A., Bucana, C. D. & Fidler, I. J. (2000). Nuclear factor-kappaB activity correlates with growth, angiogenesis, and metastasis of human melanoma cells in nude mice. *Clin Cancer Res* **6**, 2573-81.
87. Baldwin, A. S. (2001). Control of oncogenesis and cancer therapy resistance by the transcription factor NF-kappaB. *J Clin Invest* **107**, 241-6.
88. Ahmed, K., Gerber, D. A. & Cochet, C. (2002). Joining the cell survival squad: an emerging role for protein kinase CK2. *Trends Cell Biol* **12**, 226-30.
89. Litchfield, D. W. (2003). Protein kinase CK2: structure, regulation and role in cellular decisions of life and death. *Biochem J* **369**, 1-15.

90. Kato, T., Jr., Delhase, M., Hoffmann, A. & Karin, M. (2003). CK2 Is a C-Terminal I κ B Kinase Responsible for NF- κ B Activation during the UV Response. *Mol Cell* **12**, 829-39.
91. Wu, Z. H. & Miyamoto, S. (2008). Induction of a pro-apoptotic ATM-NF- κ B pathway and its repression by ATR in response to replication stress. *EMBO J* **27**, 1963-73.
92. Huang, J., Teng, L., Liu, T., Li, L., Chen, D., Li, F., Xu, L. G., Zhai, Z. & Shu, H. B. (2003). Identification of a novel serine/threonine kinase that inhibits TNF-induced NF- κ B activation and p53-induced transcription. *Biochem Biophys Res Commun* **309**, 774-8.
93. Li, M., Shillinglaw, W., Henzel, W. J. & Beg, A. A. (2001). The RelA(p65) subunit of NF- κ B is essential for inhibiting double-stranded RNA-induced cytotoxicity. *J Biol Chem* **276**, 1185-94.
94. Piret, B., Schoonbroodt, S. & Piette, J. (1999). The ATM protein is required for sustained activation of NF- κ B following DNA damage. *Oncogene* **18**, 2261-71.
95. Wu, Z. H., Shi, Y., Tibbetts, R. S. & Miyamoto, S. (2006). Molecular linkage between the kinase ATM and NF- κ B signaling in response to genotoxic stimuli. *Science* **311**, 1141-6.
96. Wu, Z. H. & Miyamoto, S. (2007). Many faces of NF- κ B signaling induced by genotoxic stress. *J Mol Med (Berl)* **85**, 1187-202.
97. Habraken, Y. & Piette, J. (2006). NF- κ B activation by double-strand breaks. *Biochem Pharmacol* **72**, 1132-41.
98. Veuger, S. J. & Durkacz, B. W. (2011). Persistence of unrepaired DNA double strand breaks caused by inhibition of ATM does not lead to radio-sensitisation in the absence of NF- κ B activation. *DNA Repair (Amst)* **10**, 235-44.
99. Stein, B., Rahmsdorf, H. J., Steffen, A., Litfin, M. & Herrlich, P. (1989). UV-induced DNA damage is an intermediate step in UV-induced expression of human immunodeficiency virus type 1, collagenase, c-fos, and metallothionein. *Mol Cell Biol* **9**, 5169-81.

100. Tsuchiya, Y., Asano, T., Nakayama, K., Kato, T., Jr., Karin, M. & Kamata, H. (2010). Nuclear IKKbeta is an adaptor protein for I kappa Balpha ubiquitination and degradation in UV-induced NF-kappaB activation. *Mol Cell* **39**, 570-82.
101. Devary, Y., Rosette, C., DiDonato, J. A. & Karin, M. (1993). NF-kappa B activation by ultraviolet light not dependent on a nuclear signal. *Science* **261**, 1442-5.
102. Bender, K., Gottlicher, M., Whiteside, S., Rahmsdorf, H. J. & Herrlich, P. (1998). Sequential DNA damage-independent and -dependent activation of NF-kappaB by UV. *EMBO J* **17**, 5170-81.
103. Janssens, S. & Tschopp, J. (2006). Signals from within: the DNA-damage-induced NF-kappaB response. *Cell Death Differ* **13**, 773-84.
104. Fan, C., Quan, R., Feng, X., Gillis, A., He, L., Matsumoto, E. D., Salama, S., Cutz, J. C., Kapoor, A. & Tang, D. (2006). ATM activation is accompanied with earlier stages of prostate tumorigenesis. *Biochim Biophys Acta* **1763**, 1090-7.
105. Bartkova, J., Horejsi, Z., Koed, K., Kramer, A., Tort, F., Zieger, K., Guldborg, P., Sehested, M., Nesland, J. M., Lukas, C., Orntoft, T., Lukas, J. & Bartek, J. (2005). DNA damage response as a candidate anti-cancer barrier in early human tumorigenesis. *Nature* **434**, 864-70.
106. Chen, Z., Trotman, L. C., Shaffer, D., Lin, H. K., Dotan, Z. A., Niki, M., Koutcher, J. A., Scher, H. I., Ludwig, T., Gerald, W., Cordon-Cardo, C. & Pandolfi, P. P. (2005). Crucial role of p53-dependent cellular senescence in suppression of Pten-deficient tumorigenesis. *Nature* **436**, 725-30.
107. Salmena, L., Carracedo, A. & Pandolfi, P. P. (2008). Tenets of PTEN tumor suppression. *Cell* **133**, 403-14.
108. Meyn, R. E. (2009). Linking PTEN with genomic instability and DNA repair. *Cell Cycle* **8**, 2322-3.
109. Meeker, A. K., Hicks, J. L., Platz, E. A., March, G. E., Bennett, C. J., Delannoy, M. J. & De Marzo, A. M. (2002). Telomere shortening is an early somatic DNA alteration in human prostate tumorigenesis. *Cancer Res* **62**, 6405-9.

110. Di Leonardo, A., Linke, S. P., Clarkin, K. & Wahl, G. M. (1994). DNA damage triggers a prolonged p53-dependent G1 arrest and long-term induction of Cip1 in normal human fibroblasts. *Genes Dev* **8**, 2540-51.
111. Ding, J., Miao, Z. H., Meng, L. H. & Geng, M. Y. (2006). Emerging cancer therapeutic opportunities target DNA-repair systems. *Trends Pharmacol Sci* **27**, 338-44.
112. Vernier, M., Bourdeau, V., Gaumont-Leclerc, M. F., Moiseeva, O., Begin, V., Saad, F., Mes-Masson, A. M. & Ferbeyre, G. (2011). Regulation of E2Fs and senescence by PML nuclear bodies. *Genes Dev* **25**, 41-50.
113. Kakizuka, A., Miller, W. H., Jr., Umesono, K., Warrell, R. P., Jr., Frankel, S. R., Murty, V. V., Dmitrovsky, E. & Evans, R. M. (1991). Chromosomal translocation t(15;17) in human acute promyelocytic leukemia fuses RAR alpha with a novel putative transcription factor, PML. *Cell* **66**, 663-74.
114. Gurrieri, C., Capodici, P., Bernardi, R., Scaglioni, P. P., Nafa, K., Rush, L. J., Verbel, D. A., Cordon-Cardo, C. & Pandolfi, P. P. (2004). Loss of the tumor suppressor PML in human cancers of multiple histologic origins. *J Natl Cancer Inst* **96**, 269-79.
115. Bartkova, J., Rezaei, N., Liontos, M., Karakaidos, P., Kletsas, D., Issaeva, N., Vassiliou, L. V., Kolettas, E., Niforou, K., Zoumpourlis, V. C., Takaoka, M., Nakagawa, H., Tort, F., Fugger, K., Johansson, F., Sehested, M., Andersen, C. L., Dyrskjot, L., Orntoft, T., Lukas, J., Kittas, C., Helleday, T., Halazonetis, T. D., Bartek, J. & Gorgoulis, V. G. (2006). Oncogene-induced senescence is part of the tumorigenesis barrier imposed by DNA damage checkpoints. *Nature* **444**, 633-7.
116. Di Micco, R., Fumagalli, M., Cicalese, A., Piccinin, S., Gasparini, P., Luise, C., Schurra, C., Garre, M., Nuciforo, P. G., Bensimon, A., Maestro, R., Pelicci, P. G. & d'Adda di Fagagna, F. (2006). Oncogene-induced senescence is a DNA damage response triggered by DNA hyper-replication. *Nature* **444**, 638-42.
117. Mallette, F. A., Gaumont-Leclerc, M. F. & Ferbeyre, G. (2007). The DNA damage signaling pathway is a critical mediator of oncogene-induced senescence. *Genes Dev* **21**, 43-8.
118. Choi, J., Shendrik, I., Peacocke, M., Peehl, D., Buttyan, R., Ikeguchi, E. F., Katz, A. E. & Benson, M. C. (2000). Expression of senescence-associated beta-galactosidase in

- enlarged prostates from men with benign prostatic hyperplasia. *Urology* **56**, 160-6.
119. Davis, J. N., Wojno, K. J., Daignault, S., Hofer, M. D., Kuefer, R., Rubin, M. A. & Day, M. L. (2006). Elevated E2F1 inhibits transcription of the androgen receptor in metastatic hormone-resistant prostate cancer. *Cancer Res* **66**, 11897-906.
120. Dyson, N. (1998). The regulation of E2F by pRB-family proteins. *Genes Dev* **12**, 2245-62.
121. Muller, H., Bracken, A. P., Vernell, R., Moroni, M. C., Christians, F., Grassilli, E., Prosperini, E., Vigo, E., Oliner, J. D. & Helin, K. (2001). E2Fs regulate the expression of genes involved in differentiation, development, proliferation, and apoptosis. *Genes Dev* **15**, 267-85.
122. Chicas, A., Wang, X., Zhang, C., McCurrach, M., Zhao, Z., Mert, O., Dickins, R. A., Narita, M., Zhang, M. & Lowe, S. W. (2010). Dissecting the unique role of the retinoblastoma tumor suppressor during cellular senescence. *Cancer Cell* **17**, 376-87.
123. Stanbrough, M., Bubley, G. J., Ross, K., Golub, T. R., Rubin, M. A., Penning, T. M., Febbo, P. G. & Balk, S. P. (2006). Increased expression of genes converting adrenal androgens to testosterone in androgen-independent prostate cancer. *Cancer Res* **66**, 2815-25.
124. Schayek, H., Haugk, K., Sun, S., True, L. D., Plymate, S. R. & Werner, H. (2009). Tumor suppressor BRCA1 is expressed in prostate cancer and controls insulin-like growth factor I receptor (IGF-IR) gene transcription in an androgen receptor-dependent manner. *Clin Cancer Res* **15**, 1558-65.
125. Fiorentino, M., Judson, G., Penney, K., Flavin, R., Stark, J., Fiore, C., Fall, K., Martin, N., Ma, J., Sinnott, J., Giovannucci, E., Stampfer, M., Sesso, H. D., Kantoff, P. W., Finn, S., Loda, M. & Mucci, L. (2010). Immunohistochemical expression of BRCA1 and lethal prostate cancer. *Cancer Res* **70**, 3136-9.
126. Zhang, J. & Powell, S. N. (2005). The role of the BRCA1 tumor suppressor in DNA double-strand break repair. *Mol Cancer Res* **3**, 531-9.

127. Srigley, J. R., Amin, M., Boccon-Gibod, L., Egevad, L., Epstein, J. I., Humphrey, P. A., Mikuz, G., Newling, D., Nilsson, S., Sakr, W., Wheeler, T. M. & Montironi, R. (2005). Prognostic and predictive factors in prostate cancer: historical perspectives and recent international consensus initiatives. *Scand J Urol Nephrol Suppl*, 8-19.
128. Grignon, D. J., Caplan, R., Sarkar, F. H., Lawton, C. A., Hammond, E. H., Pilepich, M. V., Forman, J. D., Mesic, J., Fu, K. K., Abrams, R. A., Pajak, T. F., Shipley, W. U. & Cox, J. D. (1997). p53 status and prognosis of locally advanced prostatic adenocarcinoma: a study based on RTOG 8610. *J Natl Cancer Inst* **89**, 158-65.
129. Che, M., DeSilvio, M., Pollack, A., Grignon, D. J., Venkatesan, V. M., Hanks, G. E. & Sandler, H. M. (2007). Prognostic value of abnormal p53 expression in locally advanced prostate cancer treated with androgen deprivation and radiotherapy: a study based on RTOG 9202. *Int J Radiat Oncol Biol Phys* **69**, 1117-23.
130. Pollack, A., Grignon, D. J., Heydon, K. H., Hammond, E. H., Lawton, C. A., Mesic, J. B., Fu, K. K., Porter, A. T., Abrams, R. A. & Shipley, W. U. (2003). Prostate cancer DNA ploidy and response to salvage hormone therapy after radiotherapy with or without short-term total androgen blockade: an analysis of RTOG 8610. *J Clin Oncol* **21**, 1238-48.
131. Chakravarti, A., Heydon, K., Wu, C. L., Hammond, E., Pollack, A., Roach, M., Wolkov, H., Okunieff, P., Cox, J., Fontanesi, J., Abrams, R., Pilepich, M. & Shipley, W. (2003). Loss of p16 expression is of prognostic significance in locally advanced prostate cancer: an analysis from the Radiation Therapy Oncology Group protocol 86-10. *J Clin Oncol* **21**, 3328-34.
132. Chakravarti, A., DeSilvio, M., Zhang, M., Grignon, D., Rosenthal, S., Asbell, S. O., Hanks, G., Sandler, H. M., Khor, L. Y., Pollack, A. & Shipley, W. (2007). Prognostic value of p16 in locally advanced prostate cancer: a study based on Radiation Therapy Oncology Group Protocol 9202. *J Clin Oncol* **25**, 3082-9.
133. Pollack, A., DeSilvio, M., Khor, L. Y., Li, R., Al-Saleem, T. I., Hammond, M. E., Venkatesan, V., Lawton, C. A., Roach, M., 3rd, Shipley, W. U., Hanks, G. E. & Sandler, H. M. (2004). Ki-67 staining is a strong predictor of distant metastasis and mortality for men with prostate cancer treated with radiotherapy plus androgen

- deprivation: Radiation Therapy Oncology Group Trial 92-02. *J Clin Oncol* **22**, 2133-40.
134. Li, R., Heydon, K., Hammond, M. E., Grignon, D. J., Roach, M., 3rd, Wolkov, H. B., Sandler, H. M., Shipley, W. U. & Pollack, A. (2004). Ki-67 staining index predicts distant metastasis and survival in locally advanced prostate cancer treated with radiotherapy: an analysis of patients in radiation therapy oncology group protocol 86-10. *Clin Cancer Res* **10**, 4118-24.
135. Khor, L. Y., Desilvio, M., Al-Saleem, T., Hammond, M. E., Grignon, D. J., Sause, W., Pilepich, M., Okunieff, P., Sandler, H. & Pollack, A. (2005). MDM2 as a predictor of prostate carcinoma outcome: an analysis of Radiation Therapy Oncology Group Protocol 8610. *Cancer* **104**, 962-7.
136. Khor, L. Y., Desilvio, M., Li, R., McDonnell, T. J., Hammond, M. E., Sause, W. T., Pilepich, M. V., Okunieff, P., Sandler, H. M. & Pollack, A. (2006). Bcl-2 and bax expression and prostate cancer outcome in men treated with radiotherapy in Radiation Therapy Oncology Group protocol 86-10. *Int J Radiat Oncol Biol Phys* **66**, 25-30.
137. Khor, L. Y., Moughan, J., Al-Saleem, T., Hammond, E. H., Venkatesan, V., Rosenthal, S. A., Ritter, M. A., Sandler, H. M., Hanks, G. E., Shipley, W. U. & Pollack, A. (2007). Bcl-2 and Bax expression predict prostate cancer outcome in men treated with androgen deprivation and radiotherapy on radiation therapy oncology group protocol 92-02. *Clin Cancer Res* **13**, 3585-90.
138. Abdel-Wahab, M., Berkey, B. A., Krishan, A., O'Brien, T., Hammond, E., Roach, M., 3rd, Lawton, C., Pilepich, M., Markoe, A. & Pollack, A. (2006). Influence of number of CAG repeats on local control in the RTOG 86-10 protocol. *Am J Clin Oncol* **29**, 14-20.
139. Khor, L. Y., Bae, K., Pollack, A., Hammond, M. E., Grignon, D. J., Venkatesan, V. M., Rosenthal, S. A., Ritter, M. A., Sandler, H. M., Hanks, G. E., Shipley, W. U. & Dicker, A. P. (2007). COX-2 expression predicts prostate-cancer outcome: analysis of data from the RTOG 92-02 trial. *Lancet Oncol* **8**, 912-20.

140. Torres-Roca, J. F., DeSilvio, M., Mora, L. B., Khor, L. Y., Hammond, E., Ahmad, N., Jove, R., Forman, J., Lee, R. J., Sandler, H. & Pollack, A. (2007). Activated STAT3 as a correlate of distant metastasis in prostate cancer: a secondary analysis of Radiation Therapy Oncology Group 86-10. *Urology* **69**, 505-9.
141. Roach, M., 3rd, De Silvio, M., Rebbick, T., Grignon, D., Rotman, M., Wolkov, H., Fisher, B., Hanks, G., Shipley, W. U., Pollack, A., Sandler, H. & Watkins-Bruner, D. (2007). Racial differences in CYP3A4 genotype and survival among men treated on Radiation Therapy Oncology Group (RTOG) 9202: a phase III randomized trial. *Int J Radiat Oncol Biol Phys* **69**, 79-87.
142. Khor, L. Y., Bae, K., Al-Saleem, T., Hammond, E. H., Grignon, D. J., Sause, W. T., Pilepich, M. V., Okunieff, P. P., Sandler, H. M. & Pollack, A. (2008). Protein kinase A RI-alpha predicts for prostate cancer outcome: analysis of radiation therapy oncology group trial 86-10. *Int J Radiat Oncol Biol Phys* **71**, 1309-15.
143. Kononen, J., Bubendorf, L., Kallioniemi, A., Barlund, M., Schraml, P., Leighton, S., Torhorst, J., Mihatsch, M. J., Sauter, G. & Kallioniemi, O. P. (1998). Tissue microarrays for high-throughput molecular profiling of tumor specimens. *Nat Med* **4**, 844-7.
144. Sauter, G., Simon, R. & Hillan, K. (2003). Tissue microarrays in drug discovery. *Nat Rev Drug Discov* **2**, 962-72.
145. Camp, R. L., Charette, L. A. & Rimm, D. L. (2000). Validation of tissue microarray technology in breast carcinoma. *Lab Invest* **80**, 1943-9.
146. Nazarian, R. M., Prieto, V. G., Elder, D. E. & Duncan, L. M. (2010). Melanoma biomarker expression in melanocytic tumor progression: a tissue microarray study. *J Cutan Pathol* **37 Suppl 1**, 41-7.
147. Becker, D., Mihm, M. C., Hewitt, S. M., Sondak, V. K., Fountain, J. W. & Thurin, M. (2006). Markers and tissue resources for melanoma: meeting report. *Cancer Res* **66**, 10652-7.
148. Assadian, S., El-Assaad, W., Wang, X. Q., Gannon, P. O., Barres, V., Latour, M., Mes-Masson, A. M., Saad, F., Sado, Y., Dostie, J. & Teodoro, J. G. (2012). p53 inhibits angiogenesis by inducing the production of Arresten. *Cancer Res* **72**, 1270-9.

149. Watson, P. H., Nussbeck, S. Y., Carter, C., O'Donoghue, S., Cheah, S., Matzke, L. A., Barnes, R. O., Bartlett, J., Carpenter, J., Grizzle, W. E., Johnston, R. N., Mes-Masson, A. M., Murphy, L., Sexton, K., Shepherd, L., Simeon-Dubach, D., Zeps, N. & Schacter, B. (2014). A framework for biobank sustainability. *Biopreserv Biobank* **12**, 60-8.
150. Coppe, J. P., Patil, C. K., Rodier, F., Sun, Y., Munoz, D. P., Goldstein, J., Nelson, P. S., Desprez, P. Y. & Campisi, J. (2008). Senescence-associated secretory phenotypes reveal cell-nonautonomous functions of oncogenic RAS and the p53 tumor suppressor. *PLoS Biol* **6**, 2853-68.
151. Jackson, S. P. & Bartek, J. (2009). The DNA-damage response in human biology and disease. *Nature* **461**, 1071-8.
152. Brusa, D., Carletto, S., Cucchiara, G., Gontero, P., Greco, A., Simone, M., Ferrando, U., Tizzani, A. & Matera, L. (2011). Prostatectomy restores the maturation competence of blood dendritic cell precursors and reverses the abnormal expansion of regulatory T lymphocytes. *Prostate* **71**, 344-52.
153. Adams, M. M. & Carpenter, P. B. (2006). Tying the loose ends together in DNA double strand break repair with 53BP1. *Cell Div* **1**, 19.
154. Panier, S. & Boulton, S. J. (2014). Double-strand break repair: 53BP1 comes into focus. *Nat Rev Mol Cell Biol* **15**, 7-18.
155. Bunting, S. F., Callen, E., Wong, N., Chen, H. T., Polato, F., Gunn, A., Bothmer, A., Feldhahn, N., Fernandez-Capetillo, O., Cao, L., Xu, X., Deng, C. X., Finkel, T., Nussenzweig, M., Stark, J. M. & Nussenzweig, A. (2010). 53BP1 inhibits homologous recombination in Brca1-deficient cells by blocking resection of DNA breaks. *Cell* **141**, 243-54.
156. Ljungman, M. (2009). Targeting the DNA damage response in cancer. *Chem Rev* **109**, 2929-50.
157. Rodier, F., Munoz, D. P., Teachenor, R., Chu, V., Le, O., Bhaumik, D., Coppe, J. P., Campeau, E., Beausejour, C. M., Kim, S. H., Davalos, A. R. & Campisi, J. (2011). DNA-SCARS: distinct nuclear structures that sustain damage-induced senescence growth arrest and inflammatory cytokine secretion. *J Cell Sci* **124**, 68-81.

158. Bonner, W. M., Redon, C. E., Dickey, J. S., Nakamura, A. J., Sedelnikova, O. A., Solier, S. & Pommier, Y. (2008). GammaH2AX and cancer. *Nat Rev Cancer* **8**, 957-67.
159. Huyen, Y., Zgheib, O., Ditullio, R. A., Jr., Gorgoulis, V. G., Zacharatos, P., Petty, T. J., Sheston, E. A., Mellert, H. S., Stavridi, E. S. & Halazonetis, T. D. (2004). Methylated lysine 79 of histone H3 targets 53BP1 to DNA double-strand breaks. *Nature* **432**, 406-11.
160. Coleman, R. E. (2001). Metastatic bone disease: clinical features, pathophysiology and treatment strategies. *Cancer Treat Rev* **27**, 165-76.
161. Fradet, V., Lessard, L., Begin, L. R., Karakiewicz, P., Masson, A. M. & Saad, F. (2004). Nuclear factor-kappaB nuclear localization is predictive of biochemical recurrence in patients with positive margin prostate cancer. *Clin Cancer Res* **10**, 8460-4.
162. Domingo-Domenech, J., Mellado, B., Ferrer, B., Truan, D., Codony-Servat, J., Sauleda, S., Alcover, J., Campo, E., Gascon, P., Rovira, A., Ross, J. S., Fernandez, P. L. & Albanell, J. (2005). Activation of nuclear factor-kappaB in human prostate carcinogenesis and association to biochemical relapse. *Br J Cancer* **93**, 1285-94.
163. Lessard, L., Mes-Masson, A. M. & Saad, F. (2006). [NFkappaB : a new marker kappable of predicting prostate cancer outcome]. *Bull Cancer* **93**, 891-9.
164. Giltneane, J. M. & Rimm, D. L. (2004). Technology insight: Identification of biomarkers with tissue microarray technology. *Nat Clin Pract Oncol* **1**, 104-11.

